Detection of *Salmonella* Typhimurium on Environmental Surfaces Using Magnetoelastic/magnetostrictive (ME) Biosensors.

by

Yuzhe Liu

A dissertation submitted to the Graduate Faculty of
Auburn University
in partial fulfillment of the
requirements for the Degree of
Doctor of Philosophy

Auburn, Alabama
May. 2 2020

Keywords: magnetoelastic biosensor, planar coil, membrane filter, swab, gelatin

Approved by

Dr. Zhongyang Cheng, Chair, Professor of Material Engineering
Dr. Tung-shi Huang, Professor of Poultry Science Department
Dr. Pengyu Chen, Assistant Professor of Mechanical Engineering
Dr. Siyuan Dai, Assistant Professor of Material Engineering

Abstract

Food products can be contaminated by *Salmonella* anywhere along the food supply chain, so that serious foodborne illnesses, hospitalizations, and even death are caused. The conflict between the fast food-supply requirement and the long-time sample preparing process of the conventional *Salmonella* detection method cannot be settled. A wireless *Salmonella* sensing technique based on magnetoelastic/magnetostrictive (ME) biosensors was developed to provide a low-cost, portable, label-free, on-site detection to ensure the safety of our food. In this dissertation, utilizing the newly developed planar spiral coil, fast detections of *Salmonella* Typhimurium on sample surfaces were demonstrated. At first, a methodology for the rapid and sensitive detection of *Salmonella* on plastic food processing plates using ME biosensors was developed. With the application of the microfabricated planar spiral coil and 1 mm long ME sensors, real-time and *in-situ* detection of *S.* Typhimurium on plastic surface without sample preparation and/or enrichment in the testing process was achieved with a sensitivity lower than 150 CFU/mm^2. Based on this direct surface measurement method, a new approach to monitor the *Salmonella* in a large volume of water using a membrane filter was also developed. By passing the *Salmonella* suspension through a membrane filter, almost all target cells were isolated on the filter surface. With this method, a detection of bacteria in liquid was transformed into a surface detection. The concentration efficiency of bacteria on the membrane filter was almost 100%, and the limit of detection of this measurement system was found at 54 CFU. Furthermore, swabs and gelatin are also employed and compared as

new large-scale surface sampling technologies. Widely used in hospitals, labs, and food supply chains, the swab is an essential sampling tool for microorganisms. However, for the surface detection, it only covers a small area. Gelatin is a translucent, colorless, flavorless food additive that was derived from collagen obtained from various animal body parts. Gelatin solution was directly sprayed onto a surface of interest to form a solid film that could be peeled off from the surface and removed the bacterial cells from the surface. Therefore, the gelatin can be used to cover a large area. The gelatin film with target bacterial cells was then dissolved in water so that the technologies for detecting bacterial cells in water could be used to detect the bacteria cells. It was experimentally demonstrated both swabs and gelatin are great candidates for bacteria sampling from sample surfaces. In this research, the detection methods by using the ME sensing system was demonstrated.

Acknowledgments

At first, I want to express my deep gratitude to my supervisors and committee members. I want to thank Dr. Bryan Chin, for giving me a chance to do my Ph.D. research in Auburn and providing invaluable guidance throughout this research. In the past five years, he not only introduced magnetoelastic sensor as a fascinating topic to me but also continuously helped me with detailed ideas and research. I also want to thank Dr. Zhongyang Cheng, for being my supervisor after Dr. Chin's retirement. Dr. Cheng spared no effort to help me through all the difficulties smoothly, and finally made sure that I could meet the goal of graduation. I want to thank Dr. Tung-shi Huang, Dr. Pengyu Chen, and Dr. Siyuan Dai for being my Ph.D. committee members and giving valuable ideas and suggestions. I would also like to than Dr. Yucheng Feng for serving as my university reader.

My sincere thanks also goes to my family, especially my wife and my parents, for offering me endless mental support all the time and help me succeed through tough times.

I would like to thank my friends and colleagues in Auburn, including but not limited to Songtao Du, Shin Horikawa, I-Hsuan Chen, Lang Zhou, Jianguo Xi, Jun Chen, Jiajia Hu, Feng'en Wang, Xingxing Zhang, Liangxi Li, Yuzhe Sun, Jiacheng Liu, for offering me help on both research and life. I also would like to thank Steven Moore, Cheryl Rhodes, Steve Best, and Mike Crumpler for their help on orders, experiments, and programs.

Thank you for everyone that has helped me during this time of my life. Without your help, I would have struggled to complete this doctoral program.

Table of Contents

List of Tables

List of Illustrations

List of Abbreviations

CFU	Colony Forming Unit
CDC	Centers for Disease Control and Prevention
FDA	Food and Drug Administration
PCR	Polymerase Chain Reaction
ELISA	Enzyme-linked Immunosorbent Assay
SPR	Surface Plasmon Resonance
ME	Magnetoelastic/magnetostrictive
E. coli	*Escherichia coli*
S. aureus	*Staphylococcus aureus*
AW	Acoustic Wave
PVDF	Polyvinylidene Fluoride
CSFV	Classical Swine Fever Virus
PEG	Polyethylene Glycol
GO	Graphene Oxide
AuNP	Gold Nanoparticles
BSA	Bovine Serum Albumin
SEM	Scanning Electron Microscopy
ISO	International Organization of Standardization
ASTM	American Society for Testing and Materials
NASA	National Aeronautics and Space Administration
Q-tip	Cotton Swabs

EPA	Environmental Protection Agency
LOD	Limit of Detection
CVT	Copan Venturi Tran-system
PE	Polyethylene
TBS	Tris-Buffered Saline
PBS	Phosphate Buffered Saline
UHMW-PE	Ultra-high-molecular-weight Polyethylene
FSMA	Food Safety Modernization Act

Chapter 1. Introduction

1.1 Importance of pathogen detection for food safety

In the 21st century, food safety problems are still a major public health concern [1]. Food products can be contaminated with bacteria, spores, viruses, and other pathogens at any point in the farm-to-table continuum causing foodborne illnesses. Every year, 48 million foodborne illnesses and 3000 deaths were reported by the Centers for Disease Control and Prevention (CDC) in the U.S. [2]. Among all these cases, *Salmonella* causes 1.2 million foodborne illnesses which lead to 19 thousand hospitalizations, and 450 deaths [3]. Considering the local public health conditions, people who live in developing countries are threatened by pathogenic foodborne illnesses [4].

Salmonella, a genus of motile Enterobacteriaceae, is one of the primary pathogens for humans. It causes Salmonellosis, such as food poisoning, enteric inflammation, fever or even death [5], [6]. *Salmonella* has two species - *Salmonella enterica* and *Salmonella bongori* and it further divides into more than 2600 serotypes [5], [7]. It widely exists among warm-blood animals, such as humans, pigs, and chickens, and it can spread through the whole food supply chain. Usually, humans get Salmonellosis through eating or drinking eggs, meat, and milk, which are contaminated by *Salmonella* or even polluted vegetables. In most of these cases, Salmonellosis only causes weak symptoms for adults, and patients can recover themselves

without hospitalization. However, in some individual cases, such as when children and seniors are poisoned under an outbreak of *Salmonella*, severe dehydration caused by the disease can lead to death [1], [5].

Table 1.1 summarized the food related *Salmonella* outbreak investigations selected by CDC in the past two years (2018/2019). According to the investigation records, *Salmonella* contaminations frequently originate from fresh cut fruits or vegetables, ground or cut meat products, eggshell, etc. [2] Since cutting and washing are common processes in the processing of these foods, *Salmonella* is likely to be spread by food preparation surfaces and wash water. According to the guidance from U.S. Food and Drug Administration (FDA) [7], all producers and food processors who manufacture, process, pack or hold foods should strictly have the *Salmonella* tests. A fast, *in-situ Salmonella* measurement method is required for the detection: 1) on food preparation surfaces, such as: plastic chopping board, stainless steel food processing stage, etc.; 2) in water or other liquid. A suitable sampling method is also needed for large scale sampling from targeted surfaces with different materials or different roughness.

Table 1. 1 Investigations of food safety related *Salmonella* Outbreaks by CDC in 2018 / 2019

Year	Source	Bacteria Strain	Cases	States	Hospitalizations	Investigation Date	Ref.
2019	Cut Fruit	*Salmonella* Javiana	165	14	73	18-Feb-20	[28]
	Ground Beef	*Salmonella* Dublin	13	8	9	30-Dec-19	[27]
	Papayas	*Salmonella* Uganda	81	9	27	12-Sep-19	[26]
	Kawaran Brand Tahini	*Salmonella* Concord	15	8	2	22-May-19	[22]
	Frozen Raw Tuna	*Salmonella* Newport	15	8	2	22-May-19	[25]
	Pre-Cut Melon	*Salmonella* Carrau	137	10	38	24-May-19	[24]
	Butterball Brand Ground Turkey	*Salmonella* Schwarzengrund	7	3	1	7-May-19	[23]
2018	Tahini Produced by Achdut Ltd.	*Salmonella* Concord	8	4	0	27-Feb-19	[22]
	Salmonella Agbeni Infections		7	5	0	14-Jan-19	[21]
	Raw Chicken Products	*Salmonella* Infantis	129	32	25	21-Feb-19	[20]
	Ground Beef	*Salmonella* Newport	403	30	117	22-Mar-19	[19]
	Gravel Ridge Farms Shell Eggs	*Salmonella* Enteritidis	44	11	12	25-Oct-18	[13]
	Chicken	*Salmonella I 4,[5]],12:i:-*	25	6	11	7-Dec-18	[18]
	Raw Turkey Products	*Salmonella Infections*	358	42	133	30-Apr-19	[17]
	Hy-vee Spring Pasta Salad	*Salmonella* Sandiego	101	10	25	5-Sep-18	[16]
	Kellogg’ s Honey Smacks	*Salmonella* Mbandaka	136	36	34	26-Sep-18	[15]
	Pre-Cut Melon	*Salmonella* Adelaide	77	9	36	26-Jul-18	[14]
	Shell Eggs	*Salmonella* Braenderup	45	10	11	14-Jun-18	[13]
	Dried Coconut	*Salmonella* Typhimurium	14	8	3	18-May-18	[12]
	Chicken Salad	*Salmonella* Typhimurium	265	8	94	21-Feb-18	[11]
	Kratom	*Salmonella* I 4,[5],12:b:-	199	41	50	24-May-18	[10]
	Raw Sprouts	*Salmonella* Montevideo	10	3	0	28-Feb-18	[9]
	Frozen Shredded Coconut	*Salmonella* I 4,[5],12:b:-	27	9	6	15-Feb-18	[8]

1.2 Current methods for pathogenic bacteria detection

The polymerase chain reaction (PCR) method, which is currently considered as the golden standard for microbial detection [29], amplifies small quantities of genetic material to determine the presence of bacteria [30]. It can offer very high sensitivity for pathogen detection while it requires a rigorous sample preparation, complex reactive components with limited shelf life, precise temperature regulation, complicated detection process and trained personnel. A schematic of the PCR thermal cycle which illustrates the processes of denaturation (30 s at 95 °C for double-stranded DNA separation), annealing (20-40 s at 50-65 °C for primers to form hydrogen bonds with single-stranded DNA), and elongation (several minutes at 70 °C for DNA synthesizing) is shown in the Fig. 1.1. Normally totals for 20-40 cycles are needed for the measurements to get enough DNA copies. The recent advances in PCR technologies, such as the real-time PCR [30], digital PCR [31], and microfluidic PCR [32], could provide better performance in terms of assay time, reagent volume, and cost. However, these PCR variants additionally require the use of reporter dyes and/or fluorescent-labeled probes, resulting in an increase in the total assay cost and complexity.

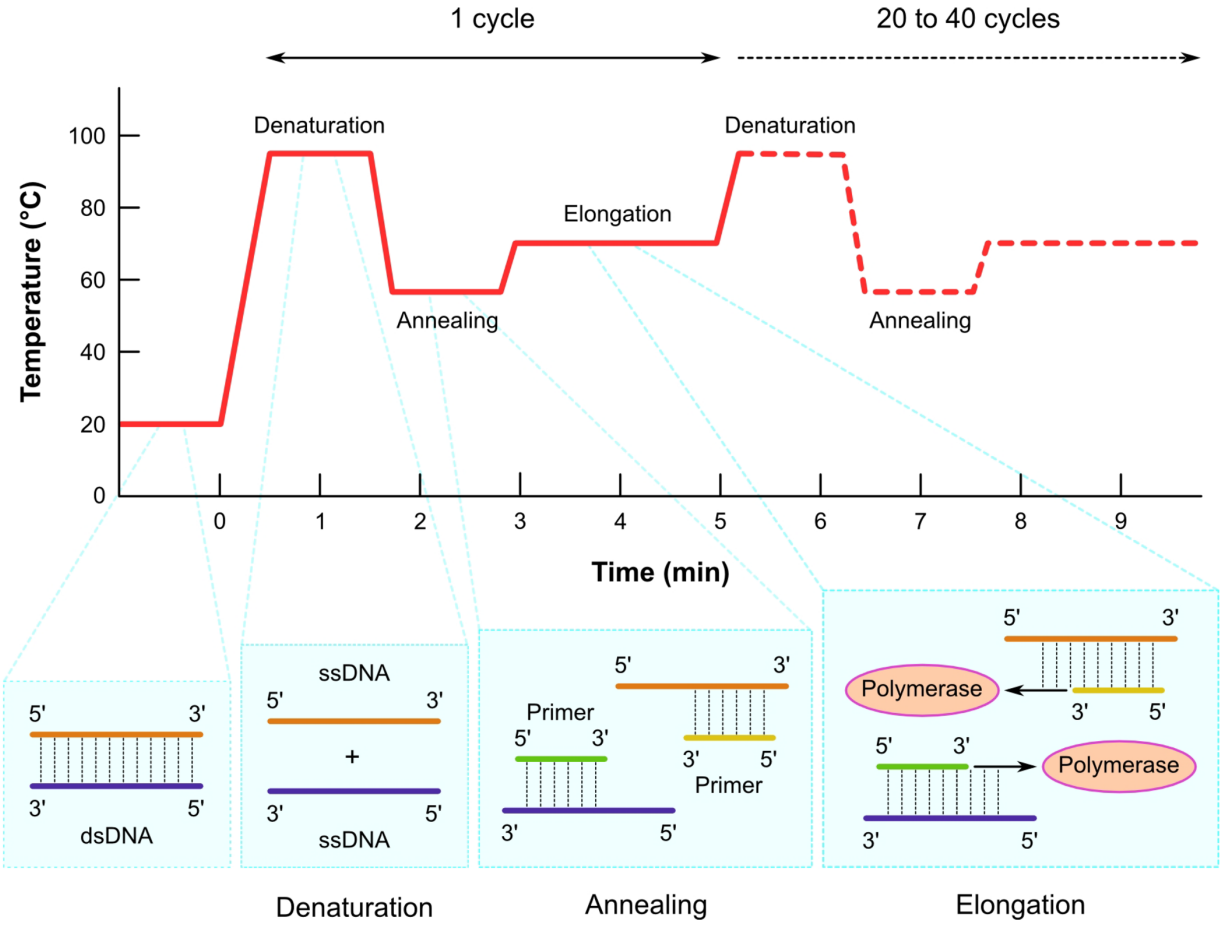

Figure 1. 1 Schematic illustration of the PCR cycle. [33]

As an alternative, the enzyme-linked immunosorbent assay (ELISA) has been developed and widely used for the detections of food safety [34]. The ELISA is an immunological technique that employs two kinds of antibodies with an enzyme. After a target antigen is captured by a primary antibody immobilized on an ELISA plate and linked to the enzyme by a secondary antibody, optical signals can be generated through biochemical reactions between the enzyme and a chromogenic substrate that is subsequently added [35]. Although the ELISA can reduce assay time and cost, it still takes hours of assays. The relatively lower sensitivity (10^4-10^6 Colony Forming Unit (CFU)/mL, compared with 10^3 CFU/mL for PCR) makes the ELISA difficult to become a real alternative [36].

Current methods for pathogenic bacteria detections normally ask for a pre-enrichment process so that the target bacteria can grow into a detectable population. As shown in Table 1.2, a normal assay time for traditional PCR takes 24-48 h prior to detection [36], [37]. Even for more advanced real-time PCR, it still takes 10 h for the incubation. This process leads to an advantage of these technologies that even if the number of target pathogens is minimal, a colony with defined population can be derived slowly. However, the disadvantage also comes from this process that it takes time, and it is costly due to specialized trained labor.

Table 1. 2 Comparison between PCR, ELISA and biosensors on *Salmonella* measurements

Detection method		Concept	Advantages	Limitations	LOD (CFU/mL)	Reference
Nucleic acid-based	Traditional PCR	Measure the amount of the final PCR product at the end of the PCR cycles	• High sensitivity • High specificity • Automated • Reliable results	• Long assay time (24-48 h) • non-quantitative	10^3	[37]
	Real-time PCR	Measure the accumulating of PCR products during the cycles	• High sensitivity • High specificity • Rapid cycling • Reproducible • Real-time detection	• High cost • Long assay time (10 h) • Complex sample preparation • Requires trained personnel.	5×10^3	[37]
Immunological based	ELISA	Measure the optical signal from the interaction between antibody & antigen	• High specificity • Automated	• Low sensitivity • False negative results • Limited quantitate ability	10^4-10^6	[36]
Biosensor-based	Optical	Measure the optical signal from the interaction between biorecognition element & sample targets	• High sensitivity • Real-time monitoring • Small size	• High cost	10^4	[38], [39]
	Electro-chemical	Measure the electric signal from the electro-chemical reaction	• High throughput • Automated • Label-free	• Low specificity • Low sensitivity	10^5	[40]
	Acoustic wave based	Measure the mass change from the signal of a piezoelectric crystal	• Cost effective • Easy to operate • Label-free detection • Real-time detection	• Low specificity • Low sensitivity • Long incubation time of bacteria	10^5	[41]

A biosensor is a device for detecting an analyte by using a combination of biological elements and physicochemical detection elements. It normally consists of three parts: 1. Biological recognize probe (biological materials such as antibodies, phages, nucleic acids, etc.); 2. Sensor platform (operated by optical, electrochemical, acoustic wave based, etc.); 3.

Readout systems which analysis signals and process data. An advantage of biosensor system is non-pathogen-labeling which makes the detection process fast. Rapid detection method using biosensors provide various advantages according to their detection methods (optical / electrochemical / mass-based). Their characteristics and limit of detections (LOD) are also summarized in Table 1.2.

Optical biosensors are based on detecting optical index changes according to the reaction between biological probes and target pathogens [38]. As the most widely used optical biosensor, a surface plasmon resonance (SPR) biosensor measures resonances produced by electromagnetic radiation in the electron cloud of a gold thin film. When target pathogens were absorbed onto the metal surface, this interaction changed the wavelength of the electron resonance [38]. Compard with other biosensors, SPR is successful on its real-time, continuous measurements with high sensitivity and specificity. For the detection of DNA samples, LOD of SPR test systems can be 2-6 nM [42], and can even reach 20 fM with the aid of an enzymatically amplification [43]. However, a detection of *Salmonella* in milk using SPR was demonstrated by Mazumdar et al., and the LOD was found at 1.25×10^5 cells/ml [44]. By the analysis of Liu et al., combined with antibody functionalized magnetic nanoparticles, the sensitivity of SPR on *Salmonella* increased by 4 orders of magnitude to be 14 cfu/mL [39]. SPR's relatively lower sensitivity in bacteria detection (without the application of amplifiers) is because compared with DNA and protein molecules, bacteria has much larger size, lower concentration, and fewer binding sites. What's more, the widespread use of SPR is also limited by the expense of sensor chips and instruments and the meticulously designed experiments [45].

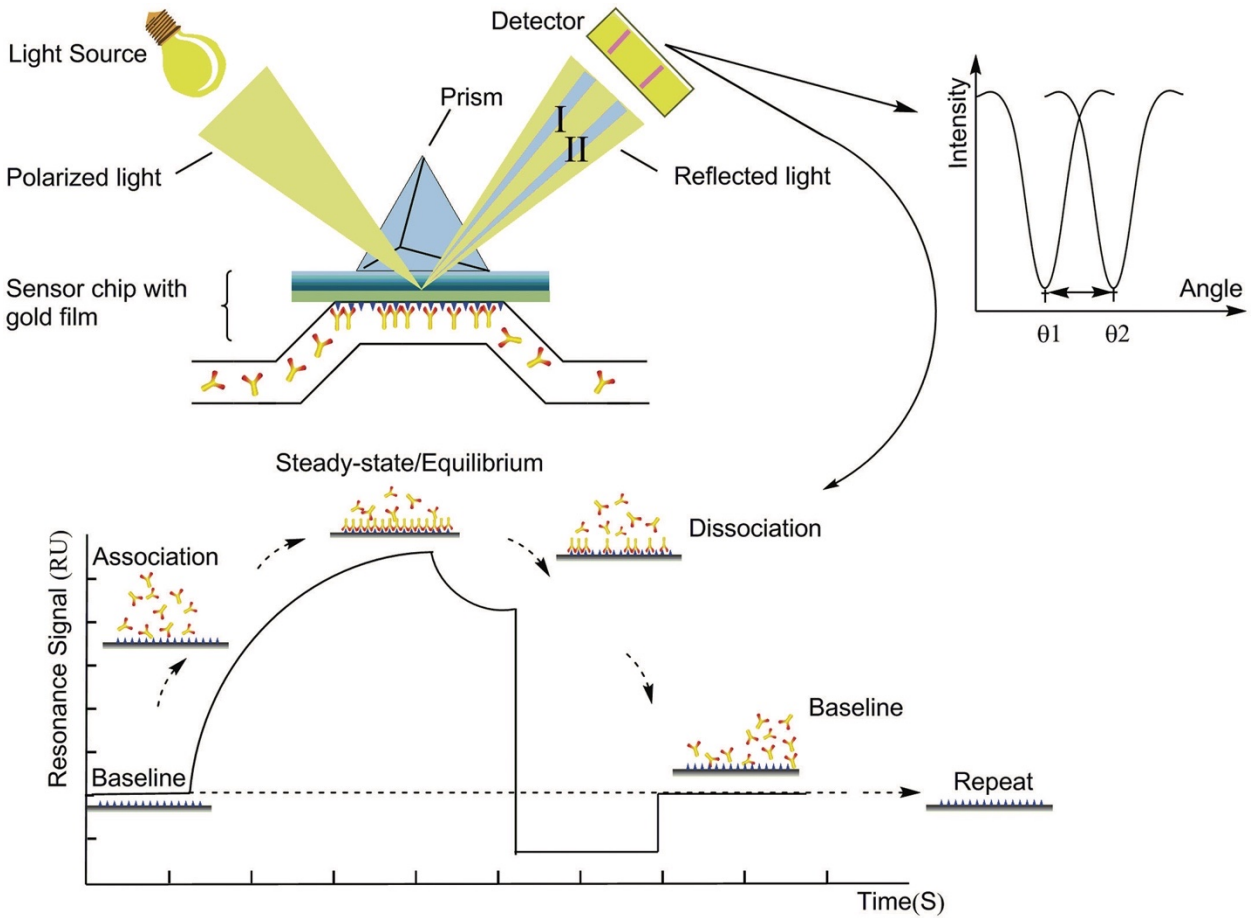

Figure 1. 2 Schematic illustration of SPR. SPR detects the change in refractive index that is caused by the combination of biomolecules and antibodies near the gold layer on the sensor chip surface, which in turn causes the SPR angle to change (from I to II in the figure). [46]

Electrochemical biosensors are biosensors that detect current, voltage, or impedance changes caused by antigen-bioreceptor interactions (Fig. 1.3). Glucose, uric acid and cholesterol are the most commonly antigens measured by electrochemical biosensors. Utilizing a microfabricated organic electrochemical transistor, Wang et al. performed a highly sensitive (LOD: 1 nM) and rapid detection of dopamine [47]. Zhou et al. combined the optical (SPR) and electrochemical biosensors into one *in-situ* monitoring system [48]. Through cross-validation of the three simultaneously generated signals (SPR, fluorescence, and electrochemistry), they have performed highly reliable monitoring of the dynamic changes of

the components involved in the interface binding. In the test of pathogens, electrochemical biosensors have the advantages of high throughput, easy miniaturization and automation, but at the same time, because they are easily interfered by other factors in the environment, poor selectivity often affects people's choices for it [40].

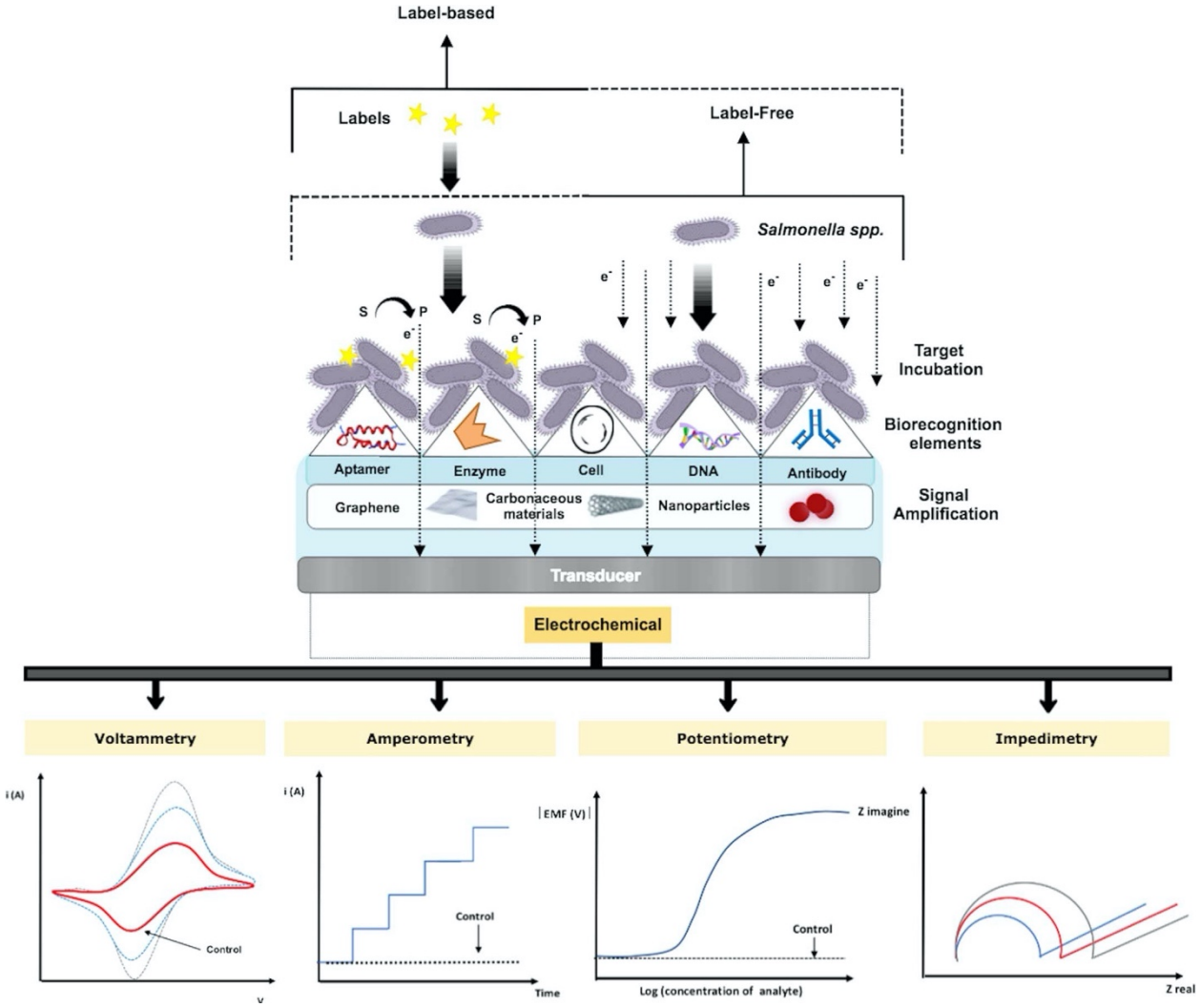

Figure 1. 3 Schematic illustration of electrochemical biosensors detecting *Salmonella* using biological probes (transducer, amplification layers, bioreceptor), with different detection modes (label-based or label-free) and electrochemical transducing techniques (voltammetry, amperometry, potentiometry and impedimetry). [49]

Acoustic wave based biosensors are detecting mass changes caused by target pathogens. According to the actuating/sensing mechanism, acoustic wave based sensors can be separated into three types: magnetostrictive sensors, silicon-based microcantilevers, and piezoelectric microcantilevers. Among them, the piezoelectric microcantilevers and magnetostrictive sensors are active, while the silicon-based one is inactive. Although silicon-based can be extremely miniaturized to achieve a good detection limit, its passive nature makes it necessary to be equipped with a large readout system [50]. For active sensors, the piezoelectric microcantilevers can minimize the readout system, but it needs a wire connected to the sensors to make detection [51]. The ME sensor can have a similar size readout system with a piezoelectric sensor, and it does not have to have a wire connected. Therefore, the ME sensor has some unique advantages.

1.3 Magnetoelastic/magnetostrictive (ME) sensor in the recent decade

1.3.1 Fundamental of ME sensor platforms

In the presence of an AC magnetic field, the ME platform undergoes a corresponding oscillating shape change that gives rise to mechanical vibrations. This mechanical vibration consequently causes the emission of a magnetic flux from the platform that can be wirelessly detected by an electromagnetic coil. When the magnetostrictive material forms a strip, in which the length (L) is larger than the width (W) and much larger than the thickness (t), the shape change would be mainly longitudinal (oscillating along the length direction) (Fig. 1.4). This vibration, which happens in the core of the solenoid coil detector would generate a magnetic flux, so the signal can be detected by the detection coil wirelessly.

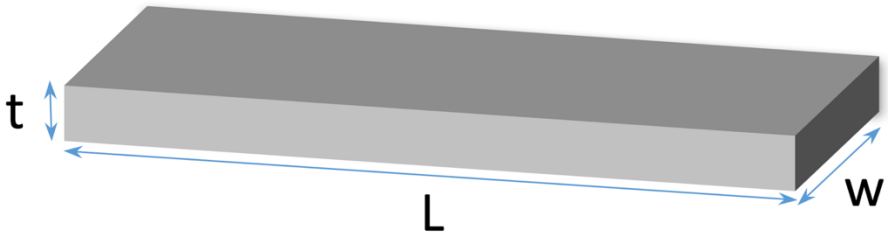

Figure 1. 4 Schematic illustration of an ME platform with the dimension of t×L×W.

For ME platforms whose L>W>>t (as shown in Fig. 1.4), the ME platform vibrates longitudinally in its first order mode with a resonant frequency (f). In this case, the resonant frequency of an ME resonator can be calculated as:

$$f = \frac{1}{2L}u \tag{1}$$

where f is the resonant frequency, L is the length of the ME platform, u is the acoustic wave velocity of the ME material. The acoustic wave velocity is dependent on the elastic properties of the ME material:

$$u = \sqrt{\frac{E}{\rho(1-\vartheta)}} \tag{2}$$

where E is the Young's modulus of elasticity, ρ is the density, and ϑ is the Poisson's ratio of the ME material. By the research of Ong [52], once a mass of Δm is loaded on to the resonator, the resonant frequency changes for the reason that the density of the resonator increases by a factor of $1 + \Delta m \,/\, M$. In this case, the mass-loaded resonant frequency (f_m) can be calculated as:

$$f_m = \sqrt{\frac{1}{\left(1 + {\Delta m}/{M}\right)}} f_i \tag{3}$$

From the equation, the shift of resonant frequency Δf caused by the mass loading can be easily calculated as $\Delta f = f_m - f_i$, where f_i is the initial resonant frequency before mass loading. It is obvious that Δf would be smaller than 0.

According to the basic theories above, the sensitivity of an ME platform is defined as the change of resonant frequency (Δf) based on the amount of mass (Δm) loaded onto the sensor surface. The mass sensitivity (S_m) is a critical parameter which describes the ability of an ME sensor to detect its target. When the mass attachment on the ME sensor is uniform, S_m is calculated by the following equation [53]:

$$S_m = -\frac{\Delta f}{\Delta m} = \frac{f_0}{2m} \ (\Delta m \ll m) \tag{4}$$

where m and f_0 are the mass and fundamental-mode resonant frequency of the ME platform. For ununiform mass attachment, Zhang et al. discussed the influence of the mass sensitivity (S_m) due to the position of mass loading and the resonance modes theoretically [54], [55]. It was found that, under the 1st resonance mode, S_m demonstrates a larger value on the two ends of ME sensor and it goes down to 0 when the mass loaded on the center of the sensor. A total of 5 resonance modes were also compared and found that all had a response to the viscosity change by Cheng et al. [56] The 1st resonance peak showed a better resolution while the higher resonance modes showed larger frequency shifts.

The most common ME sensors were fabricated into rectangular metallic glass platforms by microelectronic dicing or laser cutting a Metglas 2826MB strip [57]. For years, the development of the ME sensor structure was based on reducing the size, since the sensitivity of this rectangular sensor is exponentially related with its size. The problems such as edge effect, hard-to-handle, and low signal intensity come out with the decrease of sensor size.

Other solutions are required for the improvement of sensitivity of ME sensors. To perform an *in-vivo* and *in-situ* monitoring of blood viscosity, an integrated rectangular sensor array with three difference sizes was fabricated by Green et al. [58]

In addition to the commonly used rectangular sensors, the use of new geometries for better detection is also a development path. Tang et al. used a microelectronic fabrication method to build a hexagonal sensor [59]. This sensor has a size 100 times smaller than commercial sensing tags and a signal 75 times stronger than similar size normal sensors. According to Pacella et al. [60], by a geometrical modification from rectangular to triangular, the sensitivity of sensors can be improved by 3 - 11 times. It was found that by applying samples to the tip of the triangular sensor, the sensitivity can be even higher. A detector disc assembled by multiple triangular sensors was designed and fabricated for multiple target detections in the same time [60]. Based on the triangular structure, an arched triangle (Fig. 1.5) with a sensitivity of 435% higher than a similar size rectangular sensor was designed, while the improvement of the triangular sensor is only 270% [61].

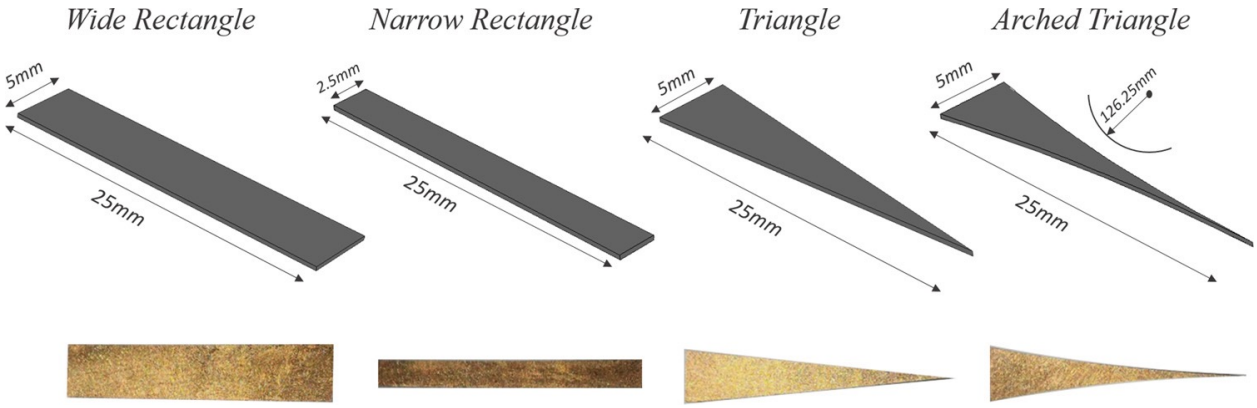

Figure 1. 5 Scheme (upper) & Top view (lower) of the rectangular, triangular and arched triangular shape ME sensors [61].

Due to the size effect, the physical properties of thin films are often better than bulky materials. In Kittmann's research [62], a thin layer of amorphous metal was coated on the

interdigital electrode, and the so-called love magnetic field is measured by the magnetoelastic coupling of surface acoustic waves. Not only single layer thin film metallic glass was used, multiple-layer thin film, with a composition of $Fe_{32}Co_{44}Hf_{12}N_{12}/Ti_{50}N_{50}$, was fabricated and applied for the detection of stress [63].

Like thin films, microfilaments can also take advantage of their size effects to obtain special characteristics and applications. FeSiB microwires with very high magnetostriction under certain DC bias magnetic field were synthesized and utilized for the detection of liquid viscosity [64]. Based on the capability of fluid pressure detection, ME microwires were applied as sensors for the cardiovascular local diagnosis [65]. By synthesizing and analyzing the ME microwires ($Fe_{73}Si_{11}B_{13}Nb_3$), Herrero-Gomez found a key feature of such microwires can perform magnetoelastic resonance without the application of a DC magnetic field. This is different from regular ribbon-based ME sensors [66]. With the principle of magnetoelasticity, small oscillations can be detected. Therefore, a new type of sensor for non-invasive pulse wave detection was demonstrated by using $Co_{68.18}Fe_{4.32}Si_{12.5}B_{15}$ microwires [67]. A similar pulse wave tester was fabricated using a novel nanocrystalline $Fe_{73.5}Cu_1Nb_3Si_{13.5}B_9$ (FINEMET) microwire with enhanced soft magnetic properties to achieve a higher sensitivity than $Co_{68.18}Fe_{4.32}Si_{12.5}B_{15}$ [68].

1.3.2 ME platform materials

As a well commercialized magnetostrictive material, Metglas 2826MB is most commonly used for ME sensor fabrication. This material with a saturation magnetostriction (λ_s) of 12 ppm is normally produced as rolls of ribbons with a composition of $Fe_{40}Ni_{38}Mo_4B_{18}$ [69]. The alloy exhibits high permeability, low resistivity, high mechanical tensile strength,

and most importantly, high magnetostriction coefficient. It has been widely used for the detection of bacterial [70], inert gas [71], mechanic properties [72], etc.

Metallic glass alloys with compositions different from the Metglas 2826 alloy are also used for ME sensors for their good magnetostriction properties. For example, CoFe thin films ($Co_{68}Fe_{32}$) [73] and FeNiMoB thin films [74] were fabricated as MEMS for the stress reconfiguration. Its magnetostrictive properties are further analyzed under magnetic field and pressure [75]. FeCo based ribbon ($Fe_{74.4}Co_{21.6}Si_{0.5}B_{3.3}Mn_{0.1}C_{0.1}$) [76] was also analyzed by clamping it on both ends and exciting with a $Pb(Zr,Ti)O_3$ (PZT) element. FeCo based alloys (for example, $Fe_{59}Co_{16}Si_{15}B_{10}$ [77]) and FeNiMoB based alloys are composite with Polyvinylidene fluoride (PVDF) to form bilayer or three-layer sandwich like structures for various sensing applications [78]. $Fe_{83}Ga_{17}$ (Galfenol) is also a good candidate for ME sensing applications, such as microwires [79] and thin films [80]. $Fe_{80}Al_{20}$ was produced into whisker sensors which just like the Metglas2826 sensors, the influence of film thickness has been analyzed by Na et al. [81]

Cobalt ferrite ($CoFe_2O_4$), which has a spinel crystal structure, has been chosen to be a candidate of ME materials with high magnetostriction parameters at low magnetic fields [82], [83]. It is one magnetostrictive material with a maximum magnetostriction strain (λ_{max}) of 500-600 ppm with a single crystal structure. Just like other ceramic materials, sintered polycrystalline cobalt ferrite with a basic λ_{max} at 150 ppm is studied for its much lower cost and more practical usage. By optimizing the sintering method, either liquid-phase [82] or low-temperature (1100 °C, comparing with 1450 °C) [84], it can reach higher magnetostriction properties. By doping a small amount of Mg to substitute Fe, it can achieve a 140% higher λ_{max} and a better strain sensitivity without affecting the magnetostriction

coefficient [83]. A similar doping effect was also reported by Monaji. By doping Zr into $CoFe_2O_4$, the material can achieve a larger saturation magnetization (Ms), and the piezomagnetic coefficient $d\lambda/dH$ increases 300% [85].

To use the properties brought by heterostructures, the composites are formed between ME materials and polymers, glasses, and crystalline. With the great piezoelectric property, inexpensive processing price, and other chemical properties, PVDF has been widely used for tactile sensors, strain gauges, and audio transducers. The high cross-correlation coupling between ME materials and PVDF can cause ME coupling and help with the application of new sensors and actuators [78].

Based on ME microwire sensing materials, glass-coated ME microwire with a composition of FeSiBCr was fabricated and studied by Klein et al. [86]. The stress dependence of FeNbSiB microwire with a glass coating was also analyzed by Sabol et al. and found that this dependency could be adjusted by the frequency of the excitation field. At low frequencies, the switching field is weakly dependent on mechanical stress, and increasing the frequency results in an increase in the stress dependence of the switching field. The slope of stress dependence is almost linear [87].

ME sensor / zeolite film composites utilize the magnetic properties of ME materials and the porosity and ion exchange properties of zeolites, enabling many novel detection practices. For example, in the work of Baimpos et al., the ME sensor was used to combine four different zeolite membranes, FAU, LTA, MFI and b-oriented MFI, to measure benzene, n-hexane, n-hexane, o-p-xylene and the six volatile substances of ethyl acetate [88]. Further using electron beam lithography, a zeolite film having a micron pattern is prepared on the surface of the ME sensor and forms a microsensor. Thus, the sensor of this ME sensor and zeolite composite

can have a shorter response time [89]. By coating hard clay slurries on the surface of ME strip, ME sensor can also be used for the analysis of drying behavior of ceramic particles [90].

1.3.3 ME sensors used for pathogen detection

For pathogen detection, Metglas 2826MB, the most representative ME material, is often coated with Cr/Au layers to become biocompatible [91].This way, antigen recognizers, such as antibodies, aptamers, or phages, can bond on the gold surfaces of ME sensors better to form biological probes of biosensors.

As a promising antigen recognizer, antibody is frequently used for specific binder in biosensors. In a research of classical swine fever virus (CSFV) detection, the ME sensor was immobilized with anti-CSFV IgG so that CSFV would be physically absorbed to cause a mass and resonant frequency change [92]. Based on this detection, whose detection limit was 0.6 μg/mL, Guo and coworkers used E2 glycoprotein which was targeting the E2 antibody of swine fever virus for the measurement [93]. With the help of biocatalytic precipitant as an amplifier, the detection limit of this research was boosted into 2.466 ng/mL. Menti et al. added a layer of protein G on the surface of ME sensor to keep the antibody oriented for the detection of *S. aureus*. According to the results, comparing with non-oriented or random antibody coating, this specific-oriented antibody sensor provided the highest *S. aureus* capture rate [94].

Other than antibodies, aptamer-based ME biosensors are also tested for the determination of pathogenic bacteria. An aptamer refers to a single-stranded DNA or peptide chain that specifically binds to a target molecule. By applying an aptamer specific to *S. aureus*, ME sensors were able to detect 5 – 10 CFU/mL in around 6 min [95]. A silicon alkoxide precursors based hybrid film consists of tetraethoxysilane and methacrylate was coated on ME platforms for the detection of bacteria (*E. coli* and *S. aureus*) in milk [96].

A phage, or a bacteriophage, is a virus that specifically hosts bacteria. Considering that antibodies are fragile and expensive, phage is considered as an alternative to antibodies because its ability to survive in a wider environmental conditions (Table 1.3) [97]. By adjusting the protein on the phage surface, E2 phage was developed as a specific bio-molecular recognizer for *Salmonella* [98], [99]. By applying E2 phage on gold coated Metglas 2826MB platforms as probes, *Salmonella* was detected on the surfaces of egg shells with a LOD at 160 CFU/mm^2 [100]. Not only on sample surface, *Salmonella* was also tested by ME sensors with phage in spinach leave broth [101] and in chicken meat [102]. Zhang et al. applied both antibodies (polyclonal antibody anti-*E. coli* and monoclonal antibodies anti-*Listeria monocytogenes*) and phage (E2) on ME sensor's gold layer for the detection of bacteria in water flow and found the LOD at around 100 CFU/mL [91].

Table 1. 3 Longevity of a landscape phage and monoclonal antibody at various temperatures. [103]

Temperature	Landscape phage	Antibody
Room temp.	> 6 months	> 6 months
37 °C	950 days (half-life)	107 days (half-life)
50 °C	5 weeks (half-life)	5 weeks
63 °C	6 weeks	24 h
76 °C	2.4 days	No binding activity

1.3.4 Other Applications of ME sensors

In addition to being studied as a biosensor, ME platforms are also used for the measurement of mechanical properties, such as force [104], stress [105], strain [106], and

pressure [65]. ME force sensor can be separated as: 1. Strip based unidimensional system. 2. Frame, array [107], or block [108] based two or three dimensional system [109]. For example: an ME strip was used as a tensile force sensor on a wound repair site by connecting to suture threads [110]. And another ME sensor was installed in the lower limb prosthesis for long-term and real-time force mapping, which can monitor the interface force distribution of the human prosthesis, thereby better guiding postoperative cooperation [111]. An ME strain sensor is normally made based on ΔE effect as the transduction mechanism which says the applied strain on ME materials would cause a change of stiffness. A remote strain sensor was fabricated by combining two magnetostrictive strips, one for the transducer and the other for the resonator, plus a bias-magnet to form a sensing system [112]. Also in another strain sensor with similar structure, a polycrystalline $(Fe_{0.8}Al_{0.2})_{98}B_2$ alloy was used as the transducer and Metglas2826MB3 was the resonator [106]. A bulk amorphous ME strain sensor can be attached to a bone for detecting bone plate strain and used to determine the healing state of a patient's fracture [113]. Because the sensor is wirelessly connected, it eliminates the need for battery and disassembly in the body. It can be used in the clinical practice of fracture healing and can also be used in the design of fracture treatment and rehabilitation equipment. Stress is also monitored by ME sensors. Due to an analysis, the resonant frequency changes of ME sensors, which were caused by magnetostrictive strain, show a strong dependence on uniaxial stresses [76]. By wrapping the ME detection coil around the three steel truss structures to form a triangular closed magnetic circuit and using the truss structures themselves as bulk ME elements, the stress of the whole structure was measured [114].

To solve the health problems caused by the toxic heavy metals, such as Pb^{2+}, Cd^{2+}, Cu^{2+}, etc., ME sensors were also designed to composite with some other materials so that the heavy

metals ions could be targeted and combined with the sensors. For the sensing of mercury ion (Hg^{2+}) in liquid, an ME sensor platform was covered with graphene oxide (GO) as the absorbent and an aptamer as the specific probe. Unlike other ME sensor would try to bind the target heavy metal ion, the mechanism of this detection was to have the specific aptamer reacting with Hg^{2+} ions and bind the part without Hg^{2+} ion on GO surface to cause the resonant frequency change. To enlarge the signal, gold nanoparticles (AuNP) were used as a signal amplifier [115]. This signal amplification method was also applied on the detection of other heavy metal ions [116] and biomass [117]. ME sensors with a bovine serum albumin (BSA) coating would have a reaction between heavy metal ions (Pb^{2+} and Cd^{2+}). In this research, a gold-coated ME sensor platform was fully cleaned and modified by thiol and then immobilized with BSA. Due to the adherence of the BSA precipitate induced by heavy metal ions, there was a mass increase on the ME sensor so that a resonant frequency change could be seen [118]. By another article from the same group, Metglas 2826MB raw material was used for a direct detection of Pb^{2+} ion [119]. The authors claimed that the replacement reaction between Pb^{2+} and Fe or Ni elements in the metallic glass would cause mass increase and resonant frequency decrease.

1.3.5 Development of the interrogation unit

As illustrated in Fig. 1.6, an ME sensing system normally consists of a DC magnetic field, a detection coil, a network analyzer or impedance analyzer, and an ME sensor. The DC magnetic field, which was normally provided by one magnet [79] or a magnet array [70], is set to provide the bias magnetic field. A typical coil detector is a solenoid coil that holds the ME sensor in the center for detection [79]. When connected with a network analyzer or impedance analyzer, the solenoid coil is able to generate a varying magnetic field as a driving

coil and accept the ME sensor resulting field as a signal-pickup coil at the same time. An ME sensor is often an ME resonator platform which was functionalized by phage [57], antibody [120], etc. for various applications.

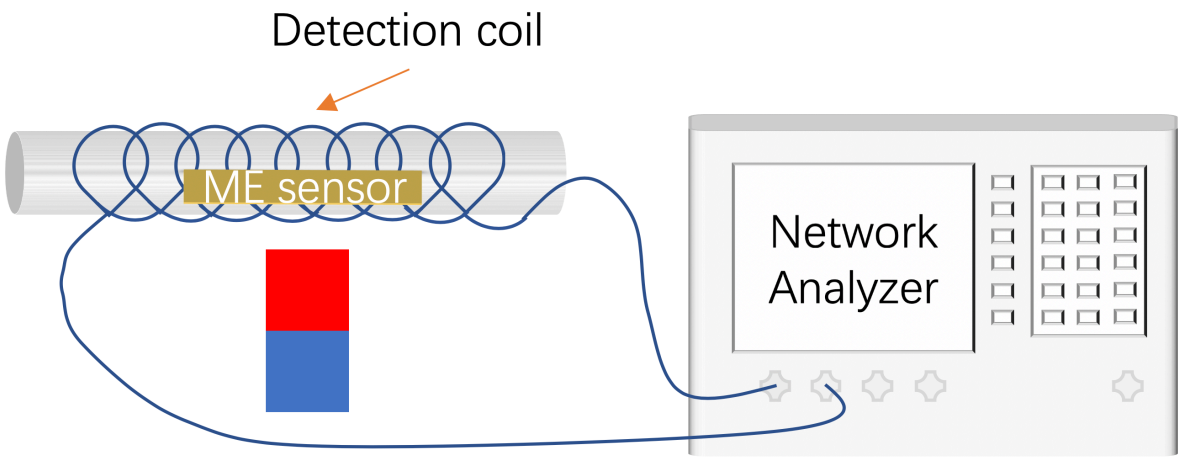

Figure 1. 6 Schematic illustration of a conventional ME sensing system.

Once measured by a network analyzer, the reflection coefficient, S_{11}, which describes the comparison results between the incident signal and the reflected signal, is a concept from telecommunications. The relation between the reflection coefficient (S_{11}, as shown in Fig 1.7), the internal impedance of the network analyzer, Z_s, and the load impedance, Z_{ab}, is written as: [121]

$$S_{11} = \frac{Z_{ab} - Z_s}{Z_{ab} + Z_s} \tag{5}$$

For the same ME sensor, a larger S_{11} value normally means a more significant signal, which can be optimized by adjusting the pulse current [122].

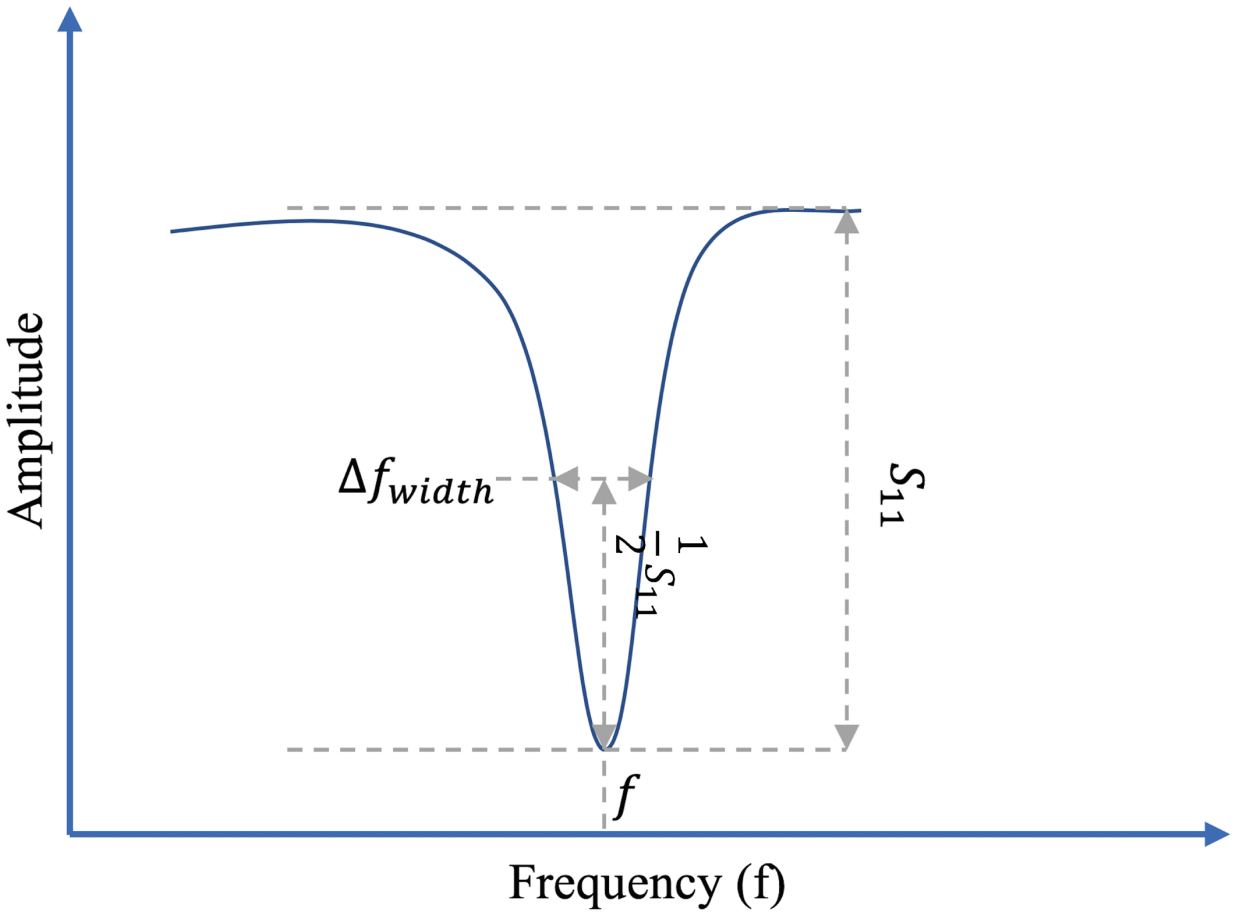

Figure 1. 7 A typical signal from network analyzer

The Q-value, so called quality merit factor, is defined as the ratio of the energy stored in the resonant structure to the total energy loss per oscillation cycle. A common understanding is that this parameter is used to demonstrate the sharpness of the formant. The larger the Q-value, the sharper the formant, which means a more accurate measurement of ME sensor. For easy calculation, Q-value of ME sensors are normally experimentally determined as:

$$Q = {}^{f}/_{\Delta f_{width}} \tag{6}$$

where Q is the Q-value, f is the resonant frequency of ME sensor, and Δf_{width} is the width of the resonant peak at its half height. The value of f and Δf_{width} can also be found and

determined in Fig. 1.7. According to experiments, the Q-value of a ME-based microcantilever in the air and liquid was around 200 and 30, respectively, which is much larger than the value of [123], [124]. In Chen et al.'s research, the decrease in the Q-value was used to represent the increase in liquid viscosity caused by an increase in shear force at the solid-liquid interface [125].

The typical solenoid coil detector generates a varying magnetic field as a driving coil and accepts the ME sensor resulting field as a signal-pickup coil for the ME sensing system. As discussed above, solenoid ME sensor coil detectors were used for Pb^{2+} sensing [119], bacteria detection [91], force demonstration [110], etc. With this kind of structure, the sample can be placed at the center of the coil and get detected wirelessly. Since there is no physical connection between the coil detector and sensor, the sensor is able to attach onto bones to achieve *in-situ* strain monitoring without hurting the patient [113]. Under a continuous periodic measurement, this solenoid coil can also keep a real-time recording of the reaction between Pb^{2+} and the sensor in hours [119]. Cheng et al. even tried to detect multiple parameters of human blood by adjusting the setup of sensors in the solenoid coils to change the resonance modes [56].

With the increase of application needs and accuracy requirements, the solenoid detectors have been developed to some new forms. Considering the influence of the earth's magnetic field to the DC bias and AC signal magnetic fields, a four-layer coil system (as-coil, pickup-coil, h-coil, and ac-coil) was designed to reduce the influence of the earth's magnetic field by 77% [126]. By hybrid with bacterial phages, the ME sensor has also been developed for the detection of pathogenic bacteria on food surfaces [70], [127]. To perform the detection on sample surfaces *in-situ* and real-time, a new cuboid solenoid coil which can provide a proper

AC magnetic field was designed to move sensor detection from inside (Fig. 1.8a) to outside (Fig. 1.8b) [70].

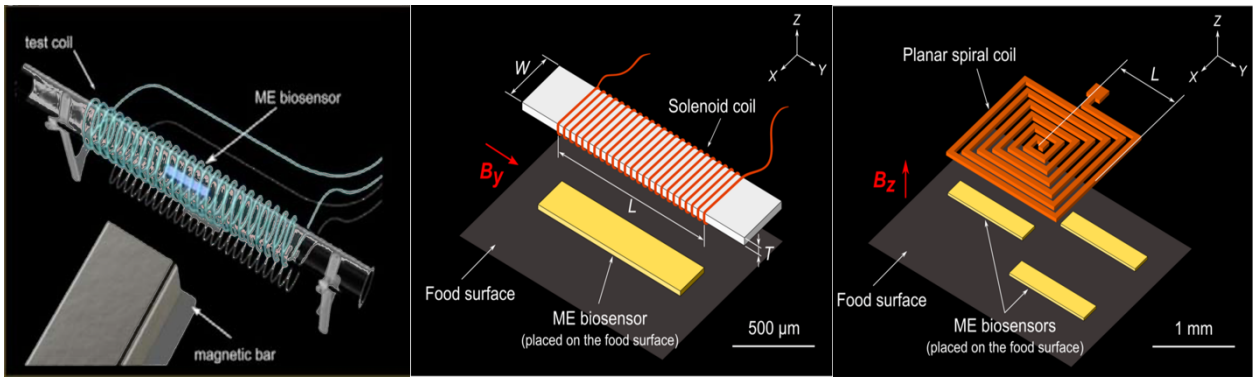

Figure 1. 8 a. sensor detected inside solenoid coil [70]; b. sensor detected outside solenoid coil [128]; c. sensor detected under planar spiral coil [128].

To further improve signal amplitude and detection distance, a microfabricated planar spiral coil has been designed to produce a much higher magnetic flux change [70]. According to Horikawa et al. [129], sensors were placed under different positions of the coil by the application of a XYZ-axis translation system and the signals show as large as a 150Hz change of resonant frequency.

1.4 Sampling technologies for pathogens

1.4.1 Current sampling methods for pathogenic bacteria

With a newly designed planar spiral coil [128], more sensing methods were developed for quicker and more efficient detection in a larger area, more volume, or a lower population. Based on the basic theory, the smaller an ME sensor is, the more sensitivity it would provide. However, a smaller sensor size also means smaller sensor coverage in the direct surface sensing. Once assisted by an appropriate sampling method, pathogens can be efficiently

collected from a large surface area thousands of times larger than the area covered by ME sensors.

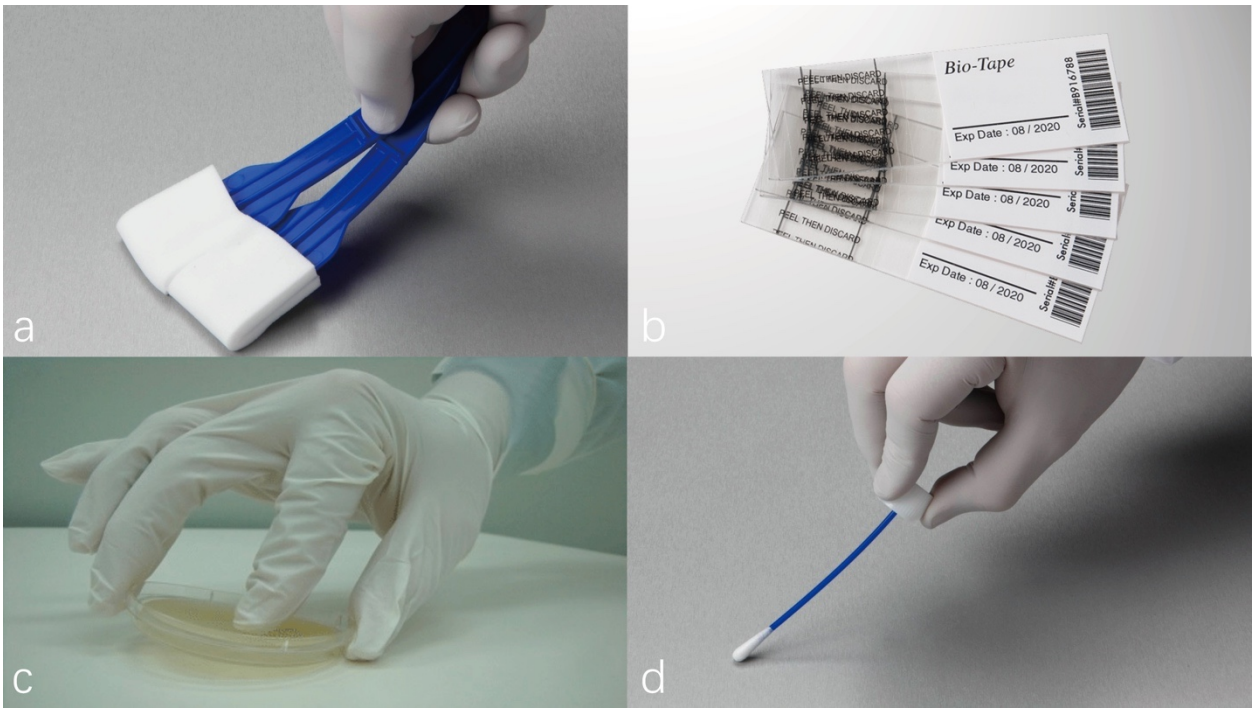

Figure 1. 9 a. scrubbing [130], b. adhesive taps [131], c. contact plate sampling [132], d. swabbing [130].

There are several different kinds of microbial sampling methods that are commonly used to determine the existence of pathogens and evaluate the effectiveness of cleansing. As shown in Fig. 1.9, these include scrubbing methods [133], adhesive tape sampling [134], contact plate sampling [135], [136], and swab sampling [137].

The scrubbing method (Fig. 1.9a) using sterile sponges is suggested only for the sampling of a large surface area (>100 cm^2) by a standard, International Organization of Standardization (ISO) 18593:2004 [138]. The efficiency of this method was only as high as traditional cotton swabs [139] and the duplicability was poor due to the varying force applied

during the sampling process [133]. In other research, wipes were claimed as a better alternative to swabs due to its narrower confidence interval [140].

Adhesive tapes (Fig. 1.9b) were designed for pathogen collection from surfaces, while the limitation of this method was a flawlessly flat sample surface needed [141],[134]. Otherwise, the adhesive layer of the tape would not be able to contact target pathogens within the flaws. An adhesive sheet was invented as an improvement of adhesive tape because it could be used for direct counting of bacteria [142].

In contact plate sampling (Fig. 1.9c) [135], [136], a culture plate was held face down and pressed onto the targeted detection area for a certain time so that the microorganisms had an opportunity to be immobilized on the culture medium. Then the contaminated culture plate was covered and incubated for later observation. In other research [143], it was found that Rodac plates were more sensitive to gram-positive cocci, while the swabs were more efficient for the capture of gram-negative bacteria. The primary disadvantage of contact plate sampling was similar to that of the adhesive tape technique; both methods were only suitable for use on a smooth, firm surface.

Table 1. 4 Comparison between sampling methods

	Scrubbing	Swabbing	Adhesive tape	Contact plate
Area	>100 cm^2	small	<10 cm^2	30-50 cm^2
Surface type	Any	Any	Smooth	Smooth/firm
Efficiency	High	High	Mild	Low
Sample agents	Bacteria, viruses, fungi, toxins		Bacteria, fungi	

Swabbing (Fig. 1.9d) is a widely used surface sampling technique which is regulated by ISO [138], American Society for Testing and Materials (ASTM) [144], and CDC [145]. Based

on these recommendations, swabs are used in hospitals not only for pathogen sampling [146], but also for first aid or cleaning [147]. For food safety area, it is frequently used as a recommended sampling tool in the food supply chain, mainly for surfaces used in food preparation [148]. National Aeronautics and Space Administration (NASA) also recommends its use as a microbiological detection tool on spacecraft [149] and even Mars [150].

Cotton remains the most commonly used fiber material for applicators, but rayon [148], foam [151], polyester [152], nylon [153], and other synthetic fibers have also been used to compose the tips for various purposes. In addition to the expansion of tip materials, the handles of swabs have evolved from wood to plastic, paper, or aluminum. The construction of the tips underwent a revolution from wrapped heads to flocked ones with a better release rate of absorbed pathogens [153], [154]. Besides the new design of swabs themselves, assistant wetting agents, such as Tween 20 [155] and Tween 80 [156], are utilized in the sampling and transportation system to improve the recovery rates of pathogens and sensitivity of measurements.

1.4.2 Development of swabbing as a sampling technology

1.4.2.1 Construction fibers and structures of swab tips

With the same structure as it was invented, cotton swabs (Q-tip) which consist of a cotton bud on a wood or plastic rod, are the most common swabs in the markets. Even though the applications of them have been evolved to cosmetic usage or painting, the main functions are still medical applications such as cleaning, sampling and first aid. As the complexity of the sampling environments continues to increase, as alternatives of conventional cotton swabs, rayon [148], polyester [152], foam [151], nylon [153], and other synthetic fibers have begun to be used for a variety of purposes.

For characteristics of absorbance, softness, low cost, and safety, cotton swabs are still widely used in almost every area from basic patient care to crime scene investigation. The Q-tip, a ubiquitous cotton swab brand in the U.S., was established by Leo Gerstenzang [157], the swab inventor. SEM images of a Q-tip used for pesticide screening were taken by Gong et al. [158] In these images, the cotton fibers of a blank Q-tip swab were rough and twisted, at around 10-20 μm in diameter. According to Scherer et al. [159], a cotton swab was moistened with PBS solution and then moved across the virus particles contaminated area. After the virus particles were released into a clean PBS solution, the recovery rates were tested by real-time PCR. Based on their tests of four contaminated environmental surfaces (stainless steel, ceramic plate, polyethylene, wood), the recovery rates vary between 26 and 52% (norovirus) and between 10 and 58% (rotavirus).

Rayon, the first invented synthetic fiber [160], has properties similar to cotton fibers. It is also commonly used for diagnostic specimen collection and patient care because of its softness and cost efficiency. In 2007, Brown et al. evaluated the sampling validity of rayon swabs for bacillus spores from nonporous surfaces [148]. In their research, sterile rayon swabs wetted by de-ionized water were used to pick up the spores from stainless steel and painted wallboard surface. After extraction and calculation, the researchers found that the recovery rate of spores were 41.4% from stainless steel surfaces and 40.5% from painted wallboard surfaces. In this paper, it was also mentioned that when using a low population of target pathogens, the swabs would show a decrease in efficiency. When researchers compared traditional wound swabs and flocked swabs, rayon was a more commonly used material in traditional ones [153], [154], [161], [162]. This demonstrates that the rayon-tipped swabs are a type of widely used traditional swab.

A polyester swab is a synthetic spun fiber with excellent collection and release properties validated for use in microbiology, rapid test diagnostics, and PCR analysis. Crawford et al. examined the performance of polyester swabs for rapid screening of pesticides present on the surfaces of fruits and vegetables [163]. The results showed that cotton swabs and polyester swabs were able to detect pesticide from fruits at a LOD of 3 ppm, which is 10 to 100 times more accurately than the U.S. Environmental Protection Agency (EPA) standard.

Foam and sponge swabs do not have long fibers wound around the tips of handles, but they are made by wrapping the material, a small piece of polyurethane or sponge, around the heads of sticks to form the swabs. In a comparison between macrofoam swab with cotton, rayon, and polyester ones [164], the macrofoam one has the highest recovery rate in all the tested circumstances. For the optimal procedure in this research, which includes a pre-moistened swab with vortexing, the recovery rates of the swabs were 43.6% for macrofoam, 41.7% for cotton, 9.9% for polyester and 11.5% for rayon (Table 1.5). The foam performs better due to its unique honeycomb structure. Suggested by Laboratory Response Network (LRN), the protocol of swabbing using macrofoam swabs was studied by Hodges et al. [165], [166]. The detection of *Bacillus* spores was performed using macrofoam and contact plate methods [167], for different environmental surfaces. The LOD for swabbing was superior to the contact plates, ranging from 2-500 per coupon.

Each swab fiber material has its own advantages which makes it suitable for specific applications. The characteristics of the materials are determined by its structures. The power of microscopy technology allows for detailed studies of different structures of swab tip materials. Rose's work [164], clearly shows the SEM images of cotton, macrofoam, rayon, and polyester swabs. In those images, polyester, rayon, and cotton appeared to have fibers

similar in size and density, though polyester had more spaces closed due to irregularly shaped fibers. The macrofoam has a honeycomb-like structure which is more regular than the other three materials. The comparison results of recovery rates of pathogens using swabs with various fiber tips were listed below in Table 1.5.

Table 1. 5 Recovery rates of pathogens using swabs with various fiber tips.

Pathogens	Recovery rates			
	Cotton	Rayon	Polyester	Macro-foam
norovirus GII.4-positive [168]	29.2±17.1	18.8±6.9	16.6±2.3	43.5±21
Bacillusanthracis Spore [164]	41.7±14.6	11.5±7.9	9.9±3.8	43.6±11
E. Coli [169]	21.82±3.9	12.21±4.4	14.03±3.19	N/A
S. Aureus [169]	7.59±1.94	3.06±1.52	6.19±2.54	N/A

*The highest recovery rates of certain pathogens from each paper were used.

In the last decade, a new swab fabrication method, flocking, was developed. In traditional wrapped swab manufacturing, differences in swabs were due to the type of fiber wound to create the swab head. The foam and sponge swabs, although each with different microstructures, were also made by wrapping the materials directly to the stick. The flocking method introduced a more ordered structure. The applicator was no longer wrapped and tangled but coated with short nylon fibers arranged vertically [170]. This improvement was promising for an increase in target pathogen collection efficiency, and it was quickly accepted as an improved sample collection tool.

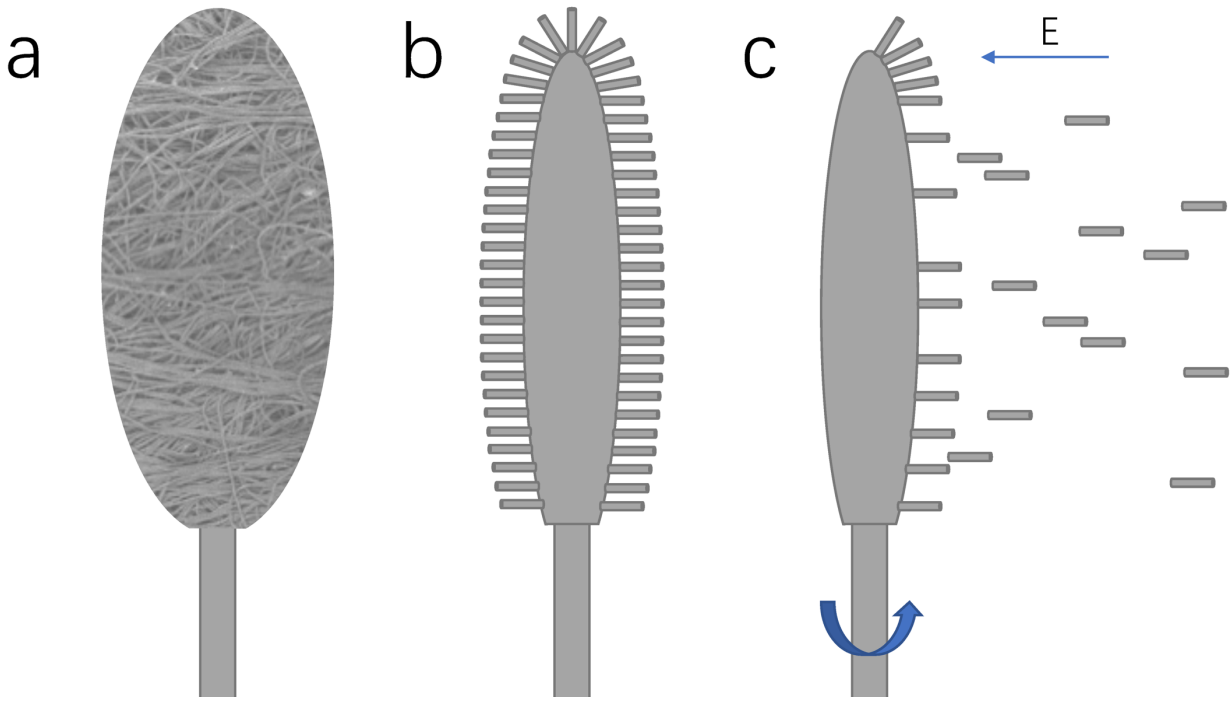

Figure 1. 10 Schematic illustration of a. traditional wrapped swab; b. flocked swab; c. manufacturing of flocked swabs.

The manufacturing process of flocked swabs, flocking, is described in detail by Copan's patent [171] and Dalmaso's paper [170]. As shown in Fig. 1.10c, short nylon fibers were sprayed onto an adhesive layer at the head of the swab stick. An electrostatic field was applied to induce the fibers to collect in one direction as an array. As a result, a perpendicular arrangement of swab head fibers with a stable, anchored structure could be formed. A heating process or a radio-frequency treatment was applied to dry the water-based adhesive layer for the bonding between fibers and swab stick could be firm.

Properties of materials are determined by structure. Differences in performance between traditionally wrapped swabs in pathogen recovery are due to structural differences between the fiber types. Short fibers integrated on the handle structure [171] allow the flocked swabs to form a more open structure with no internal absorbent core to disperse and entrap specimens.

To demonstrate advantage of flocked swabs, Probst et al. [150] compared the capture/recovery of bacteria between a flocked swab (*Copan FLOQSwab*) and a traditional cotton swab by SEM imaging. With a higher capacity and quicker elution of *B. atrophaeus* spores, flocked swabs improved both the speed and sensitivity of pathogen diagnostic tests for a significantly higher efficiency in environmental surface sampling [150]. Between rayon and nylon flocked swabs, nylon proved a better material for detection of *S. aureus* [172]. Other works have compared flocked swabs (ESwab [162], FLOQSwab [172], [173] with traditional swabs confirmed that flocked swabs have a higher sensitivity than traditional ones, and that the flocked structure was superior in pathogen collection and detection. In a comparison between flocked (HydraFlock and one Copan product) swabs and traditional (rayon and macrofoam) swabs, the HydraFlock was found to have the highest water and protein absorption and the top bacterial recovery rate [174].

1.4.2.2 Assistant wetting agents

For increased sensitivity in pathogen detection using swab sampling, some assistant wetting agents including surfactants and transportation systems have been employed. Surfactants, such as Tween 20 [164] and Tween 80 [165] are widely used to enhance detection of pathogens from environmental surfaces because of their ability to isolate and release the target pathogens without killing them. Suitable surfactants have been used as releasing agents to increase pathogen collection from the environmental surfaces and transportation systems protect pathogen strains during transportation and storage.

Tween 80 at different concentrations, 0.01% [148], 0.02% [150], 0.04%[140] have been applied in experimental processes for pathogen recovery improvement. In these works, Tween 80 was diluted with a PBS solution as a sterile buffer and used to extract microorganisms

collected by swabbing. In Buttner et al.'s research [175], a 0.05% Tween 20 solution was used to suspend B. *atrophaeus* before swab tests. The high recovery rate, 73.5±3.0%, was hypothesized to be influenced by the low coherence between spores and the sample surface. By comparing 11 different solutions in a series of experiments to identify the best for swab wetting. Moore and Griffith showed that the high recovery rate of pathogens in the diluent was mainly influenced by the pick-up and release rates [169]. Although their performance varied, all the surfactants significantly improved the two processes, mitigated the damage to bacterial cells during dry swabbing, and maximized elution.

Although surfactants are useful for removing pathogens from most surfaces, D'aoust et al. suggested the performance of eight commonly used surfactants didn't contribute to the recovery of *Salmonella* from fatty food [155]. Even though surfactants used in this study may not help with pathogen pick-up from fatty or oily areas, no toxic effect on the pathogens was observed. In addition to surfactants, other wetting agents such as DI water, sterile saline, and sterile PBS were suggested.

1.4.3 Concentration technology of pathogens using membrane filter

In the process of food production, transportation, or consuming, in addition to various food surfaces and food-contact surfaces, the source of bacteria may also be tap water, wash water, milk, and other liquids [176], [177]. In the previous studies on ME sensors, the measurement of samples in liquids often stayed in the ME sensor directly in liquid and measured with a solenoid detection coil for a long time to obtain enough data [93]. In some cases, in order to allow the sensor to have sufficient opportunity to contact with the target pathogen, the sensor needs to have 1 h of rotation in the measured liquid [101]. Therefore, a

method that can greatly concentrate or amplify bacterial population in liquid is needed for a more efficient and sensitive detection.

Membrane filtration offers this concentration/amplification strategy a possibility of low-cost implementation. Membrane filtration is a process that allows most solvents, small molecules, and a small number of large solutes to pass through a membrane with a specific designed pore size under pressure, so that small particles in the solution could be separated. A variety of materials are used to make up membrane filters, including PVDF [176], cellulose acetate [178], cellulose nitrate [179], nylon [177], polycarbonate [180], polypropylene [181], Teflon [182], etc. Most membrane filters are composed of very fine fibers interwoven with each other to form a dense and complex network and form pores of a certain size [177], [178]. Polycarbonate membrane filters are unique in that their material properties allow them to form a series of cylindrical holes that penetrate the entire membrane filter and form an array [180]. In contrast, membrane filters made of polycarbonate materials have a smaller pore-surface area , while most other membrane filters have larger filter surfaces and therefore can achieve greater flow rates [183]. Because of the uniformly distributed through-holes on the polycarbonate materials of the membrane filter, it presents a very good filtration effect on relatively small and uniform bacteria cells. It can effectively keep bacteria on the surface of the membrane filter instead on being stuck in the complex network [180].

Because of its smaller pore size and surface application of the filtration, membrane filters tend to have slower flow rates and can often become clogged. To perform a rapid filter job and avoid clogging, a laboratory membrane filtration system for cells often consists of a membrane filter with a pore size much smaller than the cell size, a suitable funnel, a flask, and a pump which was used to create vacuum or negative pressure. Compared with the

traditional measurement in liquid, using the membrane filtration method, the small amount of target particles contained in a large number of solutions can be highly concentrated to a point in a short time. Therefore, the measurement time could be greatly reduced, and the measurement accuracy could also be improved.

1.5 Objectives

The long-term goal of this project is to figure out fast detection methods of *Salmonella* using ME biosensors and to use the capability of ME sensors for real food safety detection. A fast, *in-situ Salmonella* measurement method is required for the detection: 1) on food preparation surfaces, such as: plastic chopping board, stainless steel food processing stage, etc.; 2) in water or other liquids. A suitable sampling method is also needed for large scale sampling from targeted surfaces with different materials or different roughness. To achieve this overall goal, the specific objectives are established as follows:

1. To make the detections of *Salmonella* Typhimurium on a plastic board which was used to simulate a food preparing surface.

Previously, detections of *Salmonella* Typhimurium were performed on egg shells with a solenoid coil detection system [100], on tomato skins with a cuboid solenoid coil detection system [70]. Considering the *Salmonella* contaminations most likely originate from fresh cut fruits or vegetables, ground or cut meat products, etc. [2], the monitoring on food preparing surface, for example plastic board in this research, is necessary. The newly designed planar spiral coil was used for the measurement of *Salmonella* on sample surfaces for the first time.

2. To make the detections of *Salmonella* Typhimurium in liquid by using a membrane filter to transfer *Salmonella* cell from liquid to surface.

The direct detection of *Salmonella* in liquid using an ME sensor could reach a very high sensitivity at around 100 CFU/mL. However, it still could not meet the requirement of the Food Safety Modernization Act (FSMA). According to hypothesis, with the application of a suitable membrane filter, bacteria from liquid could be concentrated on the filter surfaces. Using the surface detection ability of ME sensor implemented in Objective 1, *Salmonella* can be transferred from liquid to surface for rapid detection. Because the membrane filter allows high throughput of water to pass through, even if the density of bacteria in water is very low, a sufficient amount of bacteria for measurement can still accumulate on the filter surface.

3. To develop a large-scale sampling method to compensate for the small detection coverage caused by the size of a single sensor.

In objective 1, the direct detection of *Salmonella* on food processing surfaces was performed with 1 mm long ME sensors. Here comes the dilemma that a smaller ME sensor will have a higher sensitivity but also cover a smaller surface area. It is hypothesized that by applying a suitable large-scale sampling method, *Salmonella* from various kinds of food processing surfaces could be accumulated and recovered into a liquid media. The most used surface sampling method, swabbing, and the common food additive, gelatin, will be compared for *Salmonella* sampling from surfaces. By combining the surface detection capability of the planar spiral coil, the ability of membrane filter to concentrate *Salmonella* onto surface, and the large-scale collection capability of the sampling method, it can achieve a *Salmonella* detection with a wider range and higher sensitivity.

Chapter 2. ME Sensor for Direct Detection of *Salmonella* Typhimurium on Surface of Plastic Food Processing Plates

2.1 Introduction

Salmonella, one of the leading foodborne pathogens of human concern, causes one in six people in the U.S. to get Salmonellosis every year, and further leads to food poisoning, enteric inflammation, fever, and even death [5], [6]. According to the CDC's investigations about *Salmonella* in recent year [2], contaminations most likely originate from fresh cut fruits or vegetables, ground or cut meat products, etc. In order to prevent cross-infection and expansion of contamination between these pre-cut foods, the monitoring on food preparing surface, for example plastic board in this research, is necessary.

For the detection of *Salmonella*, the lab measurement methods, such as PCR [184], [185] and ELISA [35], have great features on their ultra-high sensitivity. To achieve this sensitivity, the complicated pre-enrichment processes and sample preparations make these lab-only test time-consuming and expensive. For biosensor based rapid detection methods, to perform a highly sensitive detection, costly gold thin film for SPR sensors [48] or microfabricated transistor for electrochemical sensors [47] are needed. Based on this situation, new technology is needed to make *Salmonella* field analysis and real-time detection easier, low-cost, portable, and label-free.

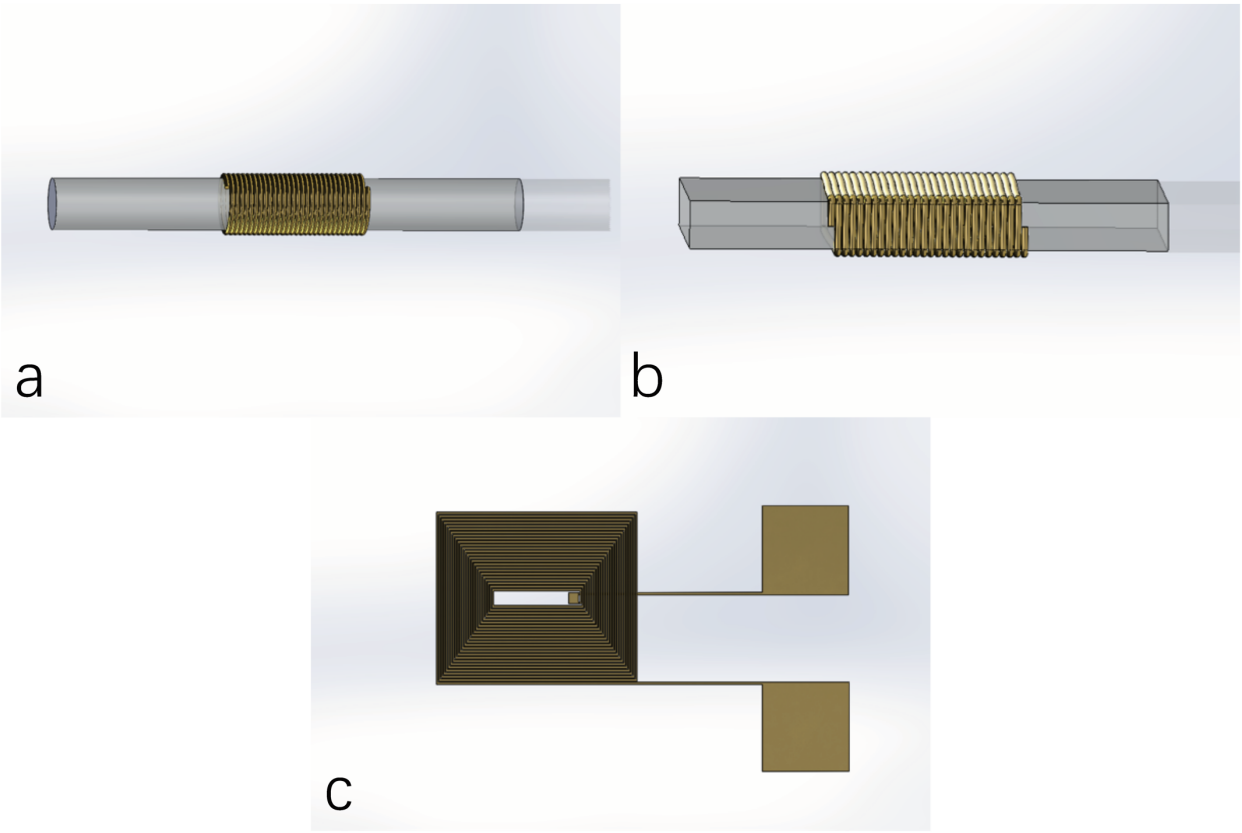

Figure 2. 1 a, solenoid coil detector with sensors measured inside; b, solenoid coil with sensors measured outside; c, planar spiral coil detector.

With the development of detection technique in the last decade, the design and fabrication method of the detection coil in the wireless sensing system has been developed over several generations. By using a solenoid coil detector (Fig. 2.1a), detections of *Salmonella* Typhimurium were performed on egg shells with a LOD at 160 CFU/mm^2 [100]. Utilizing a peristaltic pump to flow *Salmonella* suspension with different density of bacteria, *Salmonella* in liquid was also tested in this system with a LOD at round 100 CFU/mL[91]. A cuboid solenoid coil [186] was designed with the ability to provide a proper AC magnetic field to move sensor detection from inside the coil (Fig. 2.1a) to outside (Fig. 2.1b) and used for the *Salmonella* detection on tomato skins [70]. The LOD of the detection using cuboid

solenoid coil was lower than 1.5×10^3 CFU/mm^2. Later, a planar spiral coil (Fig. 2.1c) has been used to provide a higher magnetic flux change, signal amplitude, and detection distance than previous technologies [70], [128]. In this research, this newly designed planar spiral coil was microfabricated and used for the *Salmonella* detection on a food preparing surface, a food-grade polyethylene (PE) board. A measurement system which could measure both measurement sensors (coated with E2 phage and SuperBlock) and control sensors (without E2 phage, coated with SuperBlock only) simultaneous was built.

2.2 Materials and methods

2.2.1 Planar spiral coil fabrication

Micro-electronic fabrication methods, including photolithography, electroplating, and sputtering thin film deposition, were employed for the fabrication of the planar spiral coil detector. The micro-fabrication process is shown in Fig. 2.2. A transparent glass wafer was used as the substrate of the structure (Fig. 2.2a). Before the sputtering of 10 nm of Ti thin film and 200 nm Cu thin film (Fig. 2.2b), Ar plasma was applied for the surface cleansing for 10 min. The pattern described above was used for the photolithography process (Fig. 2.2c) for the preparation of copper plating (Fig. 2.2d). After coating with a 10 μm Cu layer, the unwanted part of photoresist/Cu/Ti was etched by acetone (Fig. 2.2e), the copper etchant (HAc:H_2O_2:H2O=1:1:20), and Buffered Oxide Etch (BOE, mixture of NH_4F, HF, and H_2O) (Fig. 2.2f). The first layer pattern packaging (Fig. 2.2g) was followed by the alignment and the fabrication of a second layer, repeating the processes (Fig. 2.2h-m). The performance of the planar spiral coil, which was determined by the coil's self-resistance, self-inductance, and self-capacitance, was controlled by the geometry of the coil. After the fabrication was complete, a thin layer of SU-8 photoresist was used to "package the device", making the

whole device resistant to physical damage, oxidization, and contamination. A picture (Fig. 2.3) of as-fabricated planar spiral detection coil was taken by a microscope. The two shinny strips placed on the coil are the 1mm size ME platforms used in this research.

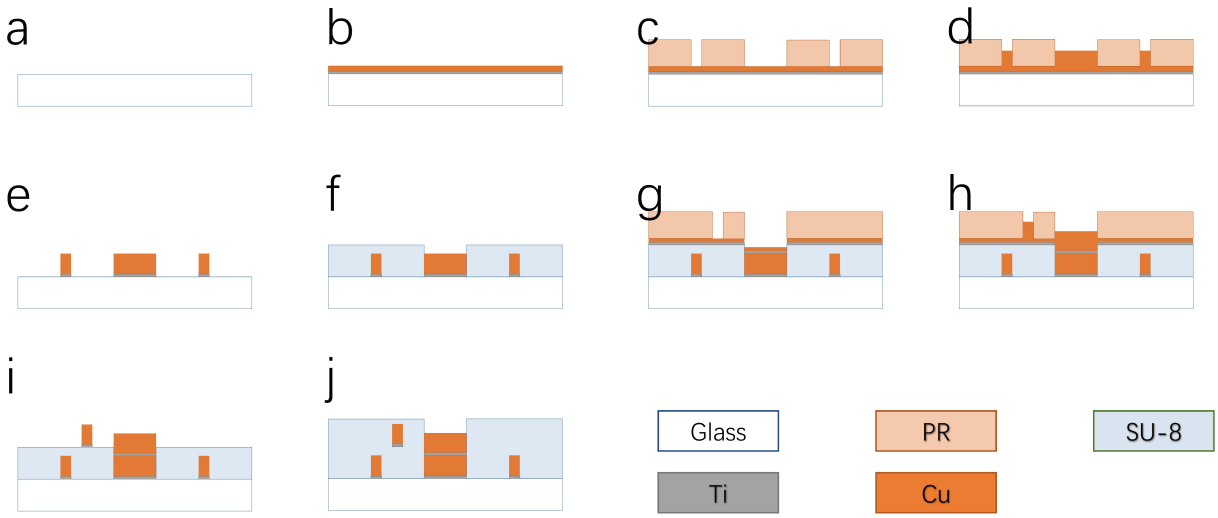

Figure 2. 2 Microfabrication process for the planar spiral detection coil.

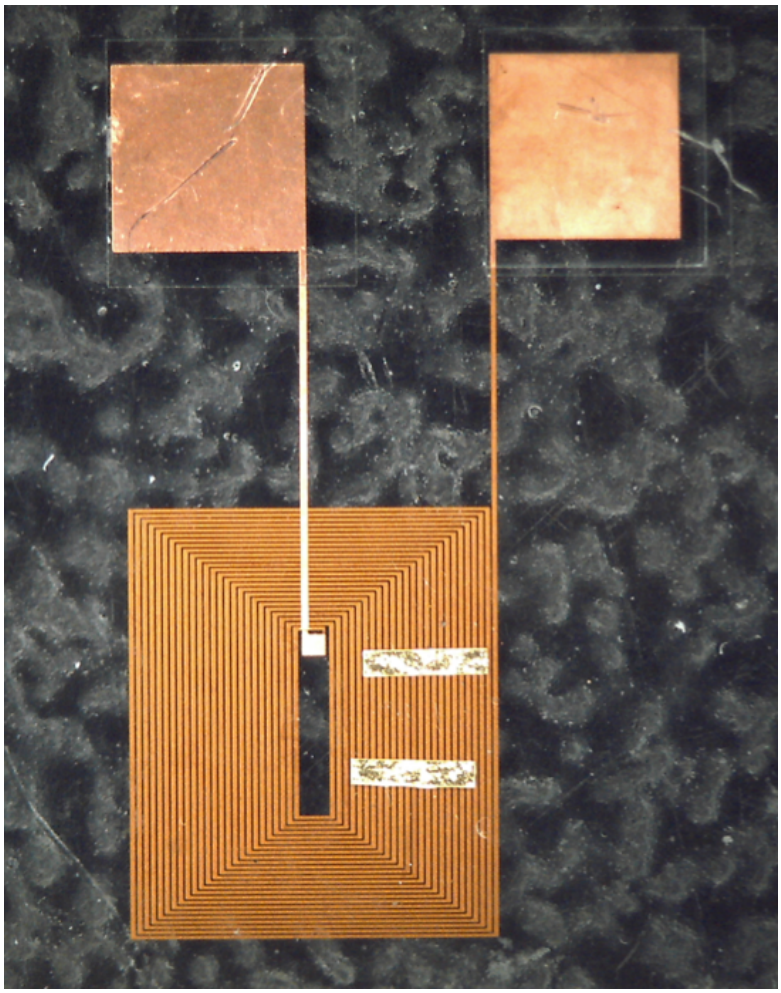

Figure 2. 3 An as-fabricated planar spiral coil with 1 mm ME platforms.

2.2.2 Fabrication of ME platforms

ME platforms were fabricated from METGLAS 2826MB alloy (Honeywell International Inc.). An automatic dicing saw (DAD 3220, Disco Corp, Tokyo, Japan) was employed to dice the metallic glass ribbon into 1×0.2×0.028 mm^3 platforms. The platforms were cleaned with methanol and acetone, and then annealed at 220℃ in a vacuum (10^3 Torr) for 2 h to remove residual stress generated by the dicing process. Cr and Au were deposited onto the platform surfaces using sputtering so that the Au layer could provide corrosion resistance and a surface ready for bio-probe immobilization.

2.2.3 E2 phage immobilization and surface blocking

Both E2 phage and *Salmonella* used in the research were provided by Dr. Tung-shi Huang's lab in the Poultry Science Department at Auburn University. The E2 phage, which is specific for *Salmonella* Typhimurium, was developed by Dr. Valery Petrenko at Auburn University [98]. The E2 phage suspension was diluted to 5×10^{11} vir/mL from 1×10^{12} vir/mL in Tris-buffered saline (TBS) solution. The ME platforms were immersed in the phage suspension for 1 h for physical loading. Then, the sensors were washed with deionized water twice to remove unbound phage and salt originating from the TBS solution. To avoid any nonspecific binding, the phage-loaded ME sensors were immersed into a blocking solution (SuperBlock™ (PBS) Blocking Buffer, Thermo Fisher Scientific Inc.) for 1 h, and then it was washed twice with deionized water. To compensate for environmental effects and non-specific binding, matched control biosensors without E2 phage were tested. Besides the control sensors which were on various populations of *Salmonella*, a series of 12 negative control measurements which use ME sensors loaded with phage to detect as-cleaned PE board surface without *Salmonella* was performed.

2.2.4 Bacterial contamination on plastic food preparing surfaces

An ultra-high-molecular-weight polyethylene (UHMW-PE) (food-grade) board was used to simulate the plastic food preparation plate in this work. The suspension of *Salmonella* Typhimurium with a population of 5×10^{8} CFU/ml was diluted into 5×10^{3} - 5×10^{7} CFU/ml using deionized water. The same volume (30 μL) of pathogen suspensions were pipetted and inoculated onto the UHMW-PE surface, forming a contamination area, circular in shape with a diameter of about 3 - 4 mm. Equation 3 was used to determine the corresponding surface *Salmonella typhimurium* populations.

$$\rho = \frac{\rho_0 V}{\pi R^2} \quad (7)$$

where ρ is the surface population of *Salmonella*, ρ_0 is the population of *Salmonella* in the suspension, V is the volume of the suspension which dropped onto the surface, and R is the radius of the drop on the surface. Using this equation, the surface population of *Salmonella* was calculated to be 1.5×10 CFU/mm^2 to 1.5×10^6 CFU/mm^2.

2.2.5 Real-time, *in-situ* surface detection process

After 1 h of drying in a fuming hood, two ME biosensors, in which one is a measurement sensor loaded with phage, and the other is a control sensor all blocked with SuperBlock, were placed on contaminated regions on the UHMW-PE board and the sample with biosensors was placed in a two planar coils measurement system, shown in Fig. 2.4. A network analyzer was used for signal generation and data collection. Each real-time detection was performed by placing both measurement and control sensors on contaminated areas and about 1mm under detector coils for 10 min detection. Humidity was provided by a humidifier as soon as the measurement started, to make sure the dried *Salmonella* on the board surface and phage on the sensor could be activated and start combination [70], [128]. A LabVIEW VI (by the author) allowed the recording to be as fast as 10 s per data point, which is much more efficient than manual input. The data plots and fitted curves were generated by DataGraph 4.5.1 (by David Adalsteinsson). The differences between measurement sensors and control sensors (without *Salmonella*) were compared by Student's independent t-test in GraphPad Prism7 (GraphPad Software, San Diego, CA, USA). Student's independent t-test (t-test), is a statistical test to determine if there is significant difference between two different treatments in two separate sets of data. In statistical tests, P-value indicates the probability that the sample observation or a more extreme result obtained when the null hypothesis is true. In this research, if the P-

value is smaller than 0.05, it means that there is a significant difference between measurement and control sensors. The smaller the value of P, the more significant the difference is.

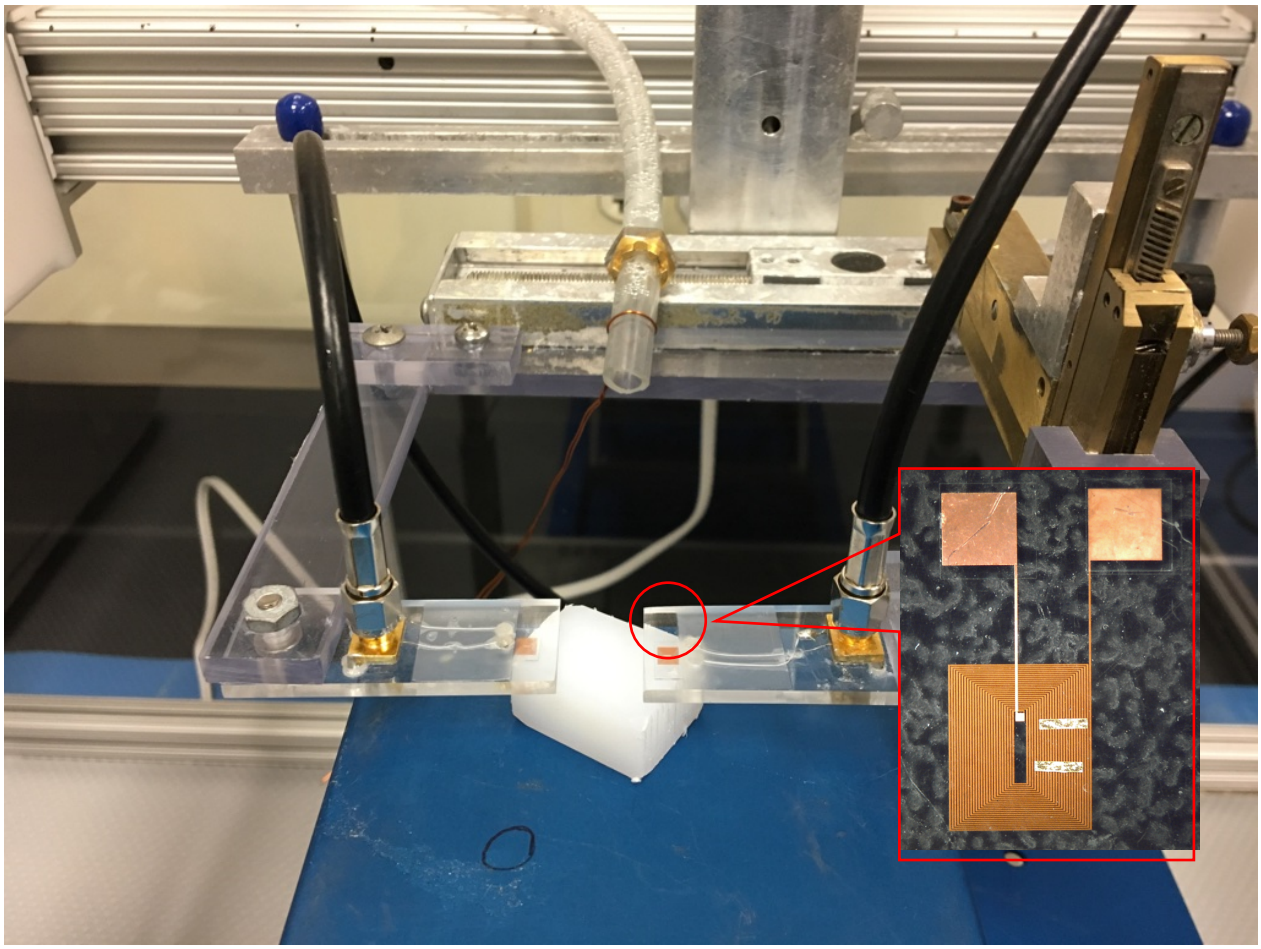

Figure 2. 4 The 2-coil ME measurement system

2.3 Results & discussion

The resonant frequency behaviors of sensors on the surface of the plastic board with different populations of *Salmonella* (1.5×10^{6}-1.5×10 CFU/mm^2) were recorded as a function of exposure time and shown in Fig. 2.5. From the plot, the ME measurement sensors exhibit larger changes in resonant frequencies with the increase of populations of *Salmonella*. Indicated by the equation 2, it means that more pathogens have been bonded to the ME sensor

at higher population. At the same time, the resonant frequency changes of control sensors were constantly low, where only minimal noise (less than 100 Hz) was found. This demonstrates that the phage on our ME sensors can bond with *Salmonella* specifically and has no interaction with other bacteria or materials [187].

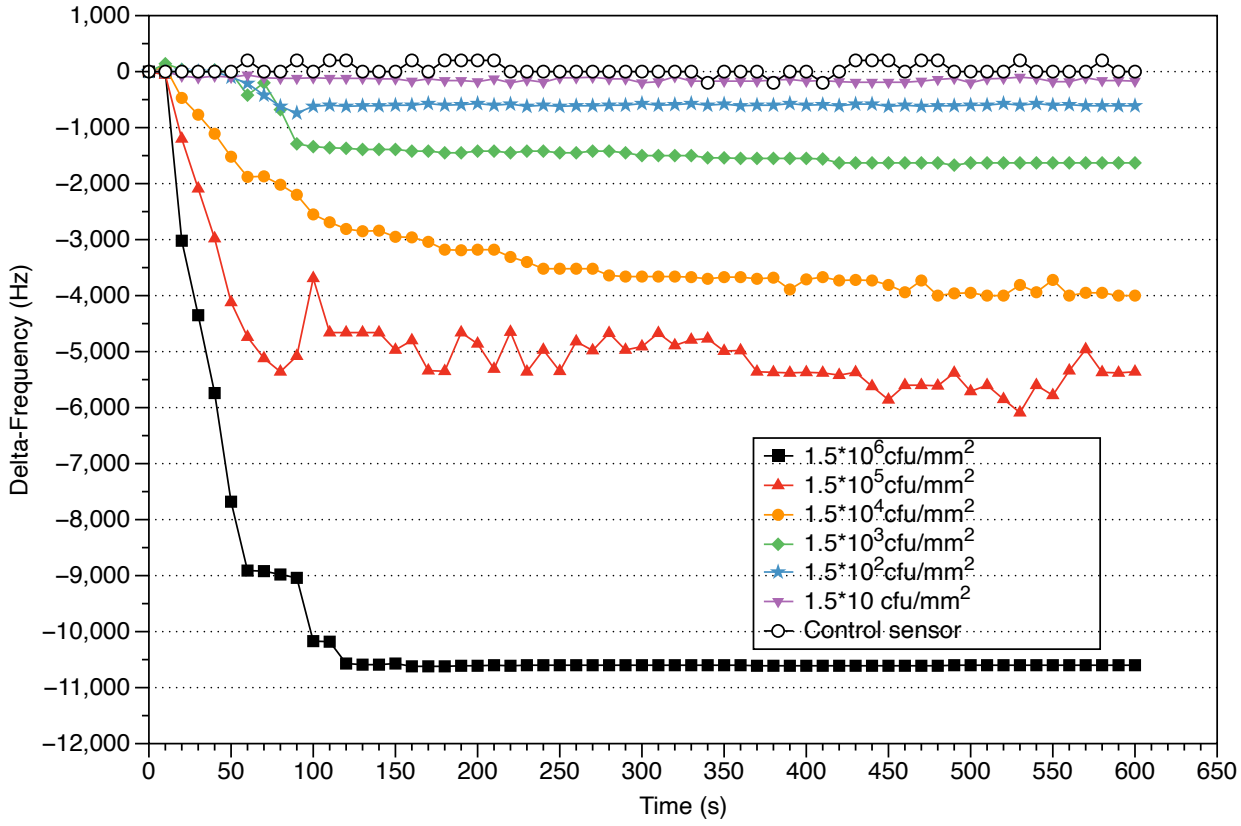

Figure 2. 5 Resonant frequency changes of measurement and control sensors as a function of time.

To further confirm the results, all the sensors were stained with dye and then observed under an optical microscope at the magnification of 50× (Fig. 2.6). The *Salmonella* Typhimurium has a cylindrical rod-like cell with the size at about 0.5 µm × 2 µm. They are shown as dark rods or dots in the figures. It is apparent that the populations of *Salmonella* on the sensors drop dramatically with the drop-in population of *Salmonella* on the sample

surfaces. No obvious *Salmonella* CFU was found on the measurement sensor from the lower populations (1.5×10^2 CFU/mm^2 and 1.5×10^1 CFU/mm^2).

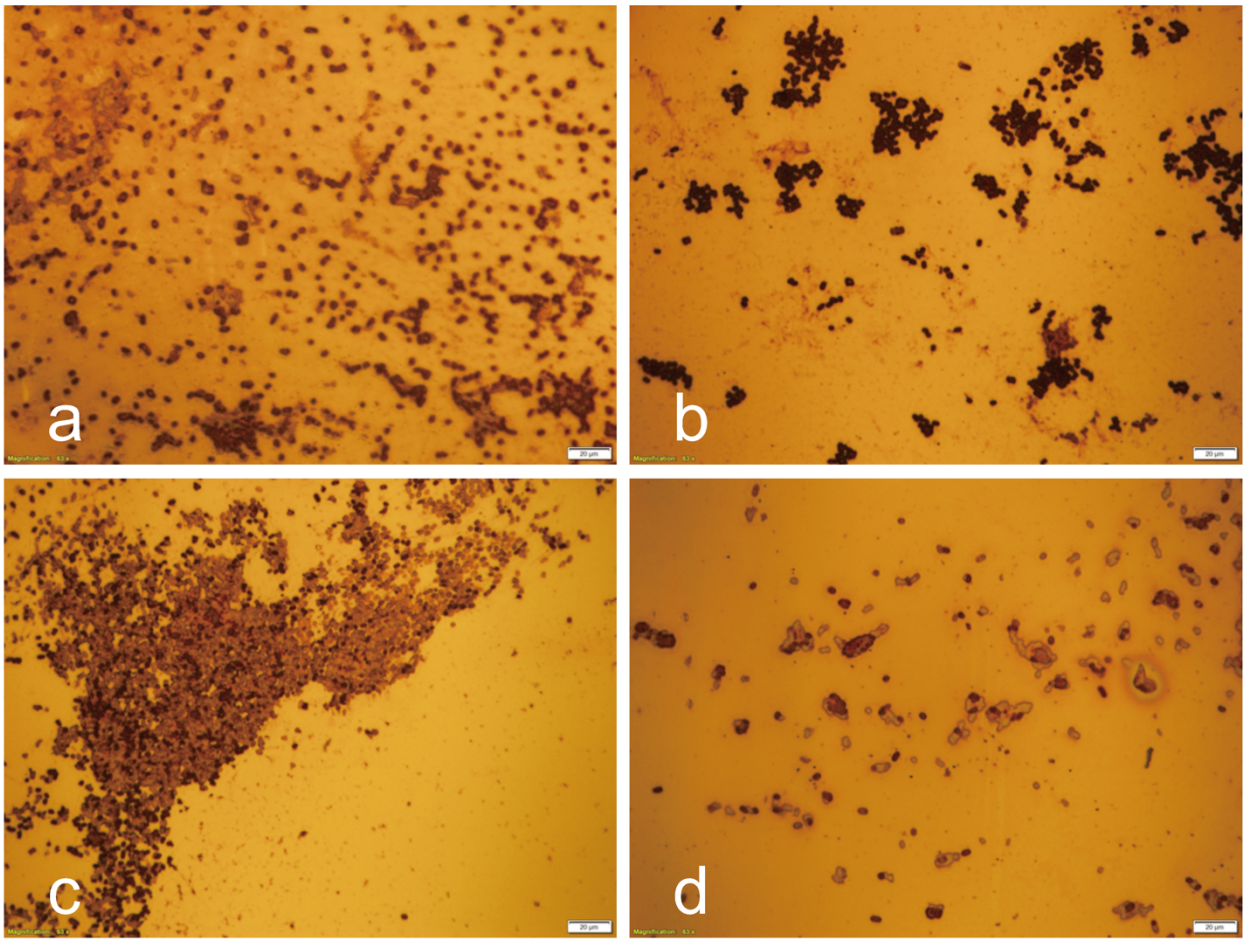

Figure 2. 6 Surfaces of sensors after measuring the population of *Salmonella* at: a. 1.5×10^6 CFU/mm^2; b. 1.5×10^5 CFU/mm^2; c. 1.5×10^4 CFU/mm^2; d. 1.5×10^3 CFU/mm^2.

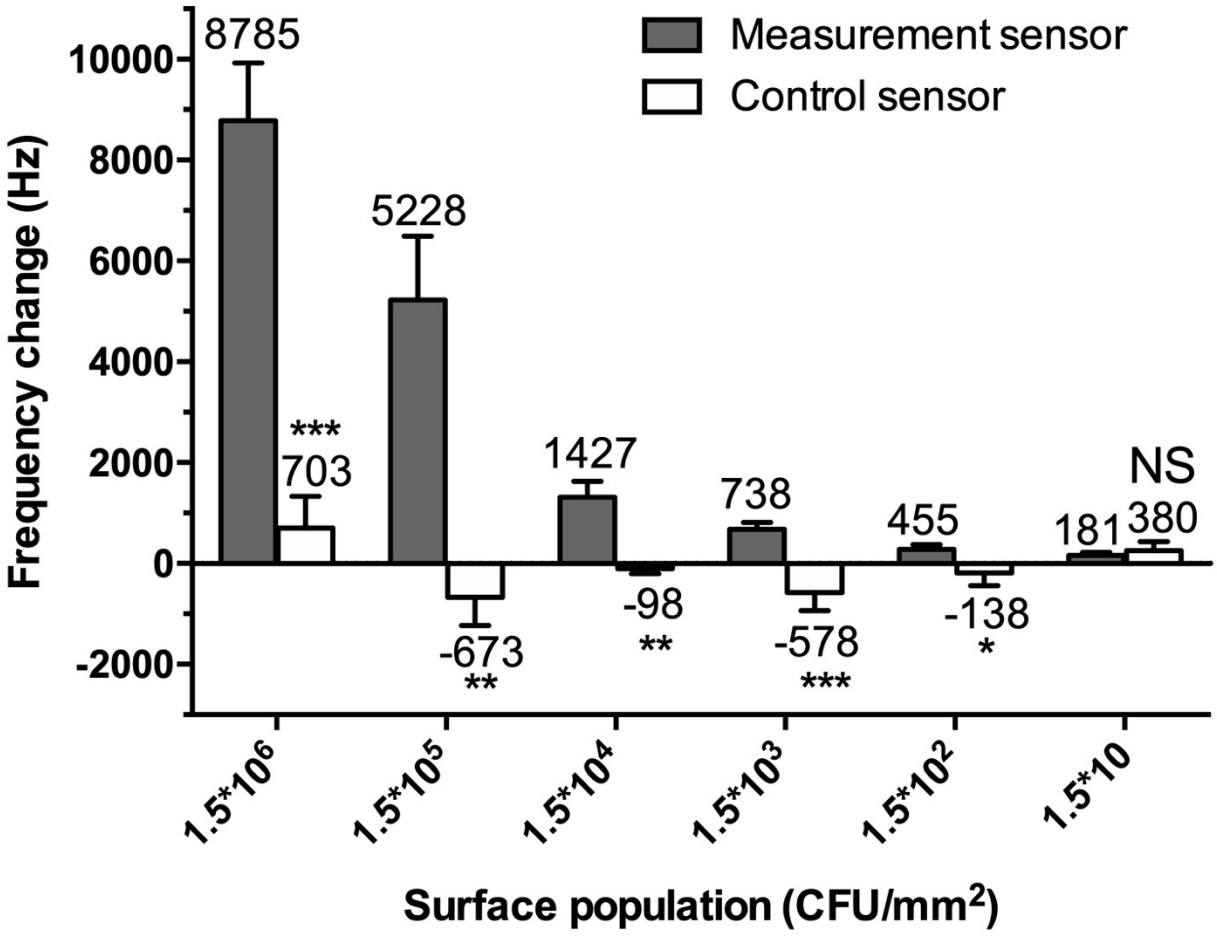

Figure 2. 7 Comparison between measurement and control sensors of different population of *Salmonella* on PE boards. Asterisks in the figures indicated significant differences between measurement and control at the level of "*", P<0.05; "**", P<0.01; and "***", P<0.001. "NS" means no significant difference.

The comparison between measurement sensors and control sensors was shown in Fig. 2.7. According Student's independent t-test, no significant difference was observed at the population at 15 CFU/mm^2 (P=0.5445, t=0.6184). For all *Salmonella* surface population higher than 15 CFU/mm^2, significant differences were found between measurement and control sensors (1.5×10^2 CFU/mm^2: P=0.0473, t=2.138; 1.5×10^3 CFU/mm^2: P=0.0007, t=4.123; 1.5×10^4 CFU/mm^2: P=0.008, t=2.997; 1.5×10^5 CFU/mm^2: P=0.007, t=3.066;

1.5×10^6 CFU/mm^2: P=0.0003, t=4.593). The observed significances confirmed that the change in resonant frequency is affected by the bonding of *Salmonella* to the sensor. Based on the statistical analysis, the LOD of this series of measurements was between 15 - 150 CFU/mm^2. For detection of *Salmonella* at this population, considering the sensor size was 1×0.2 mm^2, the average number of *Salmonella* cells it could bond with was only 30. Calculated by equation 2, the mass of 30 *Salmonella* cells was not supposed to cause a resonant frequency change as large as 100 Hz. According to Zhang's research [55], comparing with a uniform attached mass, a ununiform mass coating of the ME sensor would be able to cause a much larger resonant frequency.

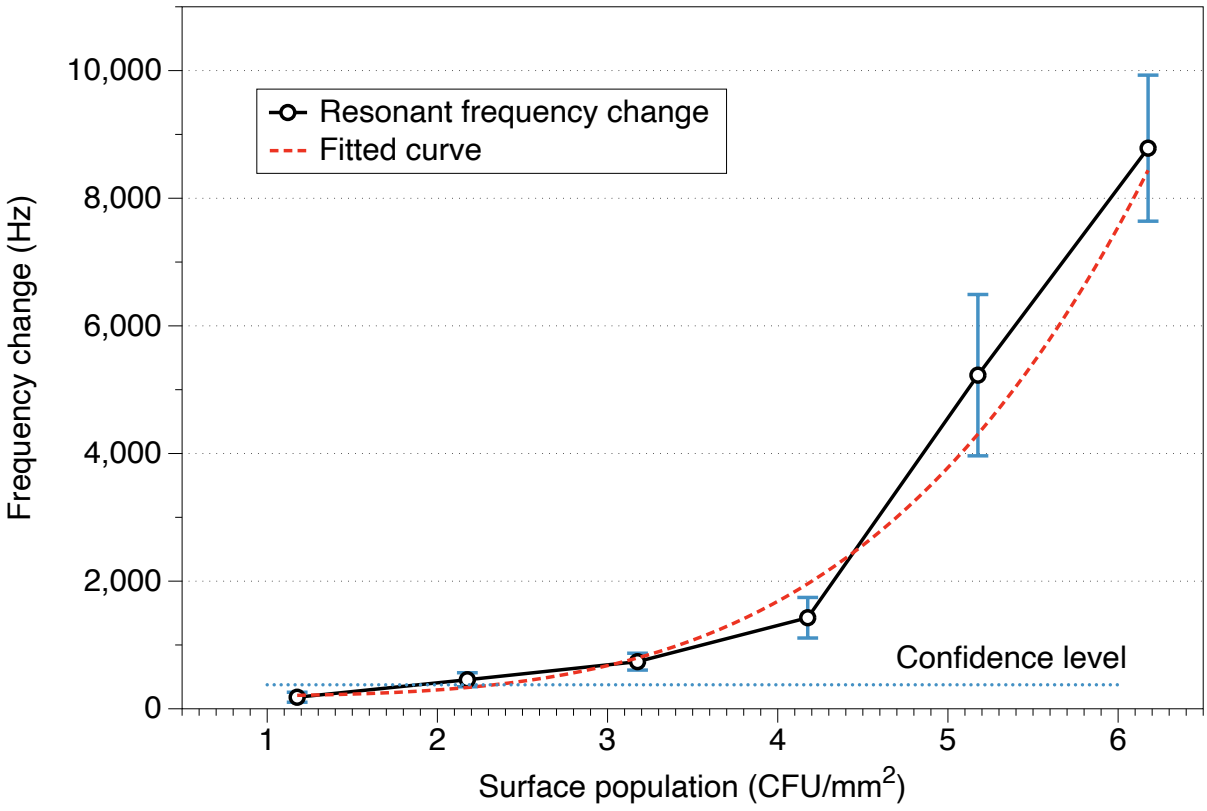

Figure 2. 8 Average resonant frequency changes and standard deviations of different population of *Salmonella* on PE boards.

In order to determine the LOD of ME biosensors on the PE board surface, Fig. 2.8 shows the frequency change plot of the measurement sensors. The mean value of each population was shown as data points with an error bar which represents the standard error. The trend of the resonant frequency change with different population of *Salmonella* on the samples is replicated well. The red dash plot in Fig. 2.8 is the fitting curve by Sigmoidal function [91],

$$y = A_1 + \frac{A_1 - A_2}{1 + (x/x_0)^p} \quad (8)$$

Where A_1, A_2, x_0, and p are fitting constants, x and y are the population of the culture and the resonant frequency changes, respectively. In this case, $A_1 = 198.9$, $A_2 = 1.84 \times 10^8$, $x_0 = 78.2$, $p = 3.95$, and R^2 of the fitting was 0.976. According to the 12 replicates of negative control measurements, the average standard deviation at 125.4 Hz was treated as the noise of the measurements. Substitute 3 times of this value as the confidence level of the series of measurements into the fitted equation, the LOD was calculated as 199 CFU/mm^2.

2.4 Summary

In this research, the direct ME sensor detection of *Salmonella* on sample surfaces using the planar spiral coil was demonstrated for the first time. A measurement system with which both measurement sensor (E2 phage treated) and control sensor (without E2 phage) could be tested simultaneously was built. A food-grade PE board was used to simulate the food preparation plate. A series of measurement with different populations (1.5×10^6 CFU/mm^2 to 1.5×10 CFU/mm^2) was performed, and the results were discussed. The resonant frequency of ME measurement sensors was found to change to a larger degree at higher populations of *Salmonella*. The limit of detection of this system was determined as 199 CFU/mm^2 by statistics method.

Chapter 3. Detection of pathogens in liquid using ME sensors combined with membrane

3.1 Introduction

Estimated by CDC, in the U.S., 1.2 million foodborne illnesses and 450 deaths are caused by Salmonellosis every year [2]. The outbreaks of *Salmonella* often link to food, such as pre-cut fruit, ground or cut meat products, and various kinds of salads [188]. To minimize the impact of *Salmonella*, the entire food chain, including not only the surfaces of fruits [70], [189] and food preparation boards [190], but also the tap water, wash water or other liquid [176], [177], needs to be monitored. Considering the time-consuming of our gold standard, the PCR [184], [185], ME sensing which can do cheaper, faster, and more efficient detection on-site was developed.

In previous research of ME sensors, the measurements required placing the sensor inside a solenoid detector to measure the initial value, and then process it before measuring the completed value [100],[91]. With the invention of the planar spiral coil, *in-situ* continuous measurement on sample surfaces was realized [128]. Based on the ability of direct sensing on surface, a hypothesis is proposed that the use of a membrane filter to transfer the target pathogens from liquid to membrane surface to achieve one of the biggest challenges of rapid detection of low concentration bacteria, pre-concentration. As a process which allows solvents and small molecules to pass and leave debris larger than the designed pore size,

membrane filtration can significantly increase the bacterial concentration. In this way, during the actual bacterial detection process, if the bacterial concentration required by the regulations is too low and the LOD of the biosensor is insufficient to meet the standard, this pre-concentration is necessary. Since the membrane filtration method can highly concentrate a small amount of target particles contained in large-capacity solutions to a point in a short time, the measurement time can also be greatly reduced, and the measurement accuracy can also be improved. Based on this, a laboratory membrane filtration system for cells often consists of a membrane filter with a pore size much smaller than the cell size, a suitable funnel, a flask, and a pump which was used to create vacuum or negative pressure (Fig. 3.1).

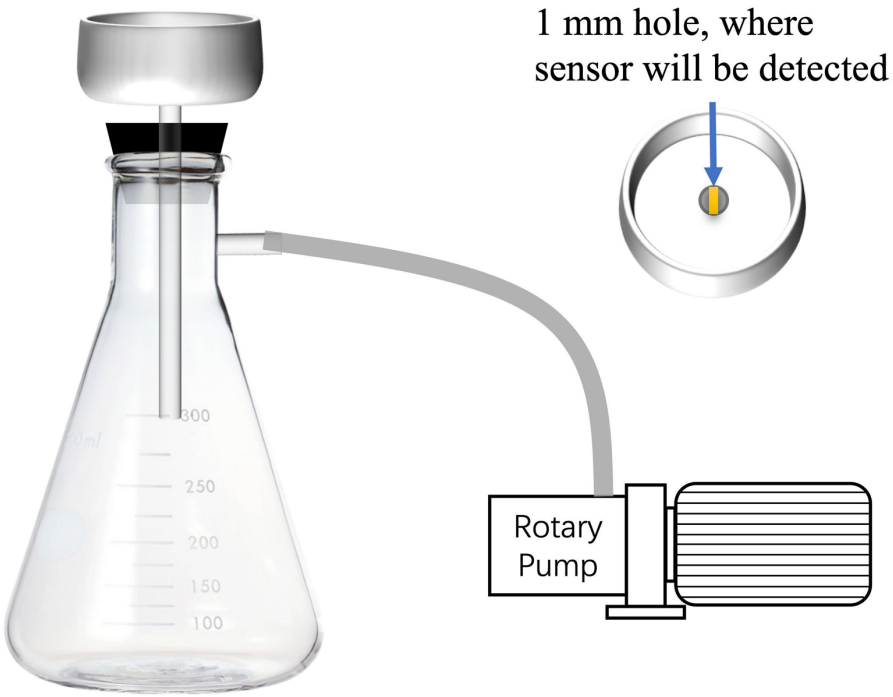

Figure 3. 1 Schematic illustration of the membrane filtration system. The top right corner shows a top view of the funnel with 1 mm diameter hole. ME sensors will be placed on the hole for further detection after filtration.

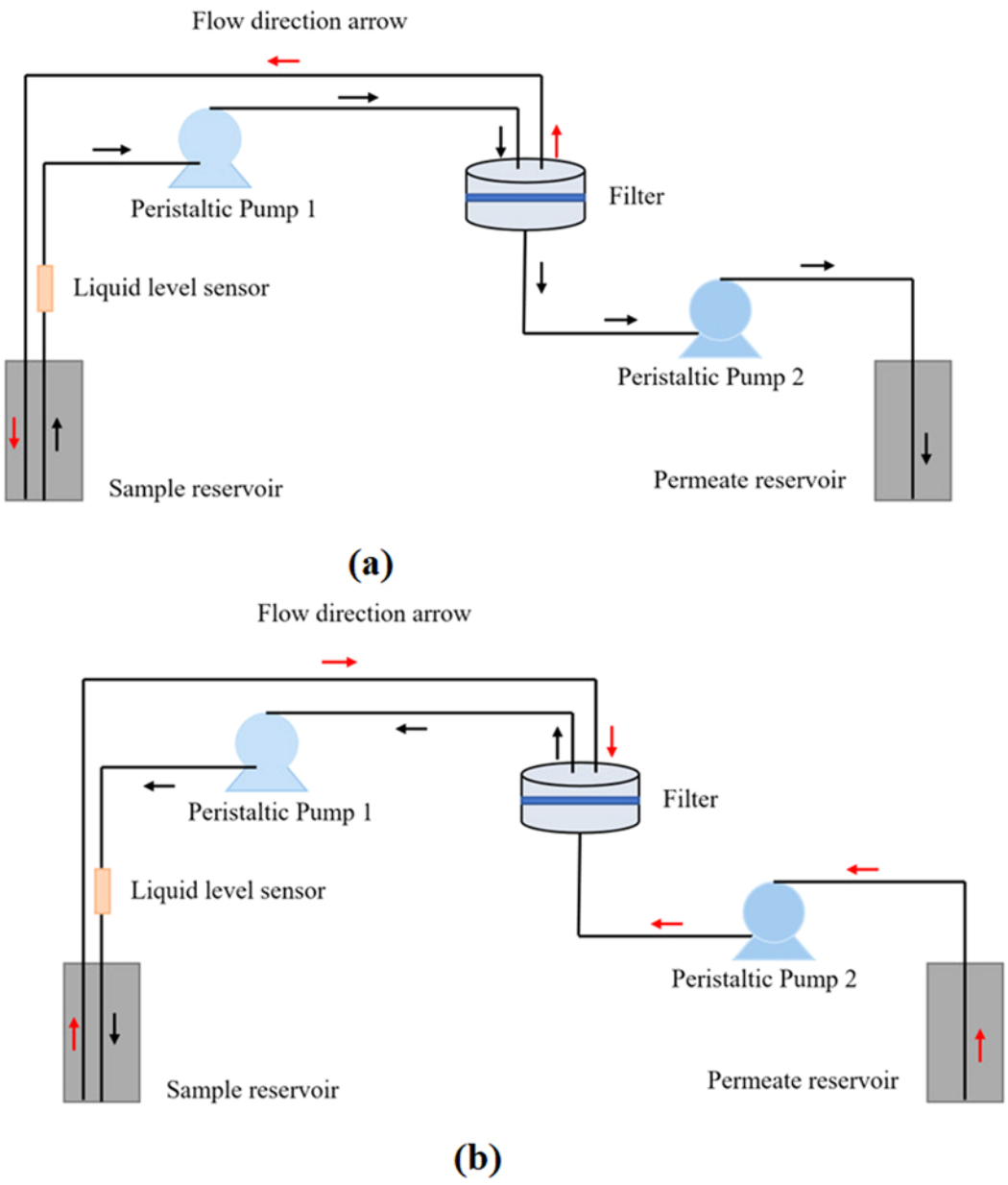

Figure 3. 2 Schematic illustration of an automated bacterial concentration and recovery system. [191]

Membranes are often used as components of biosensors, including mechanical support structures [192], transduction parts [193], pathogen filtration or concentration [191], etc. For pathogen concentration, polycarbonate membrane filters have unique advantages that they consist of arrays of series of cylindrical holes that penetrate the entire membrane [180]. In

this case, the uniformly distributed through-holes on the polycarbonate materials of the membrane filter present a very good filtration effect on relatively small and uniform bacteria cells. It can effectively keep bacteria on the surface of the membrane filter instead on being stuck in the complex network [180]. In the research of Zhang et al. [191], a ceramic membrane was used for the concentration and recovery of *E. coli*. By concentrating 500 mL *E. coli* suspension with total population around 20-80 CFU into 10 mL, 82% recovery rate was achieved. This way, an *E. coli* liquid sample with extremely low concentration became possible for detection. Considering the ME sensing technique equipped with a planar spiral coil can do detections on membrane surface directly, no back to water recovery process is needed, the detection limit of this system is more imaginative.

In this chapter, the membrane filtration and ME sensors are combined to transform the former detection in liquid to the *in-situ* detection on a membrane filter surface. By hypothesis, to combine the surface *in-situ* detection method with the membrane filter sampling, the LOD for *Salmonella* in liquid could be improved. The aim of this study is to: 1) use the polycarbonate membrane filter to concentrate *Salmonella* cells from the suspension before the measurement with the ME sensors that was coupled with the planar spiral coil; 2) use the fluorescence microscopy to examine the accumulation of *Salmonella* on the membrane surface after filtration and the bacterial grasping of ME sensors after detection.

3.2 Materials and methods

3.2.1 Construction of the filtering system

The filtering system consisted of a membrane filter, a funnel and a rotary pump (Fig. 3.1). Membrane filters (Millipore ISOPORE^{TM}) with an average pore size of 0.4 μm were employed to separate *Salmonella* cells from the liquid and expose them on the surface of

filters. It is a white glossy hydrophilic polycarbonate membrane filter fabricated by track etching on the surface of polycarbonate. This production process guarantees that the filter has a relatively uniform caliber (porosity 10-20%), which means it would have a good filtration performance on *Salmonella* cells whose normal size at 1-3 μm. A special plastic funnel with a 1 mm diameter hole was designed for this filtering experiment. During the filtering process, all the *Salmonella* suspensions passed through the single hole to make sure that all bacteria would be located within one spot for further measurement. Since the size of the funnel hole matched the size of 1 mm ME sensor, it maximized the possibility of sensors capturing bacteria. A rotary pump was used to create a vacuum environment so that the filtering process could be shortened to seconds.

3.2.2 Filtering processes

Both *Salmonella* Typhimurium and E2 phage suspension used in this research was provided by Dr. Tung-shi Huang's Lab in the Poultry Science Department at Auburn University. The *Salmonella* suspension was dyed by a *Bac*Light bacterial viability kit (Invitrogen™) diluted from its initial population (5×10^8 CFU/mL) into 5×10^1-5×10^6 CFU/mL with DI water. To mark the location of *Salmonella*, 1 μL of food dye was dropped on the filter so the position of the funnel hole was shown as blue. 100 μL of *Salmonella* suspension in each population was then dripped onto the marker when the pump was on. The surface population of *Salmonella* cells on filter was calculated by equation:

$$\rho = \frac{\rho_0 V}{\pi R^2} \tag{7}$$

where ρ is the surface population of *Salmonella* after filtration, ρ_0 is the original population of *Salmonella* in the suspension, V is the volume of the suspension which passed through the membrane filter, and R is the radius of the hole in the funnel. Take the highest

population of *Salmonella* suspension, ρ_0=5×10^6 CFU/mL used in this measurement as an example, the sample volume was 100 μL, the radius was 1/2 mm. By calculation, the surface population was 6.36×10^5 CFU/mm^2. So, the tested surface populations of *Salmonella* on membrane filters were from 6.36×10^0 CFU/mm^2 to 6.36×10^5 CFU/mm^2.

The whole volume of *Salmonella* suspension could be filtered in 10 - 30 s. The filter paper was then peeled off from the funnel and dried for 10 min before measurement. Fluorescence micrographs of *Salmonella* cells on membrane filter and ME sensors were captured with an Olympus BX51 microscope equipped with a Lumen 200 metal halide fluorescence light source and a fluorescein isothiocyanate (FITC) filter set (Olympus, Tokyo, Japan). The image processing, including time-lapse shooting and cell counting, was performed by the GNU Image Manipulation Program (GIMP).

3.2.3 ME sensing system

The planar spiral coil which was used as the wireless detector was prepared by micro-electronic fabrication methods, including photolithography, electroplating, and sputtering. The ME resonant elements were directly diced from METGLAS 2826MB alloy ribbon (Honeywell International Inc.) by an automatic dicing saw (DAD 3220, Disco Corp, Tokyo, Japan) into 1×0.2×0.028 mm^3. After cleansing and annealing, Cr and Au thin film layers were coated for corrosion resistance and biocompatible. This way the sensors were ready for phage immobilization. A network analyzer (ZNC, Rohde & Schwarz) was connected with the coil detector to provide and receive signals.

3.2.4 Measurement processes

The E2 phage as a bio-probe was diluted from 1×10^{12} vir/mL to 1×10^{11} by TBS solution. Gold coated ME sensors were rotated in the phage suspension for 1 h, to make sure that the

phage was immobilized on the gold surfaces to form measurement sensor. Both measurement and control sensors were immobilized with SuperBlock (SuperBlock^{TM} (PBS) Blocking Buffer, ThermoFisher Scientific Inc.) to prevent non-specific binding. Measurement and control sensors were tested on the marked spot under the planar spiral coil alternately. Data was collected by a LabVIEW VI every 10 s for as long as 10 min. Since food dye was used in this experiment as a marker, one more negative control with food dye and 0 CFU/mL *Salmonella* suspension (DI water) was performed to check the influence of the dye on the measurements. In order to demonstrate the detection, a series of experiments with 6 replicates were done and analyzed. The LOD was calculated and compared with the previous *in-situ* detection on plastic board.

3.3 Results & discussion

Due to the smooth surface of the polycarbonate material, fluorescently labeled *Salmonella* cells can be easily observed through a microscope as small green rods (Fig. 3.3) after the filtration process. And because the *Salmonella* separated by the filter from the suspension was collected on the smooth surface, it also facilitated the further detection by the ME sensors. The sensor sheet will have a greater chance of meeting *Salmonella* cells within the marked area. In addition, because of the smooth polycarbonate surface, the membrane filter is not easily contaminated, so unnecessary interference can be reduced during the experiment. The non-hygroscopic nature makes it easy to dry, which can also shorten the test time.

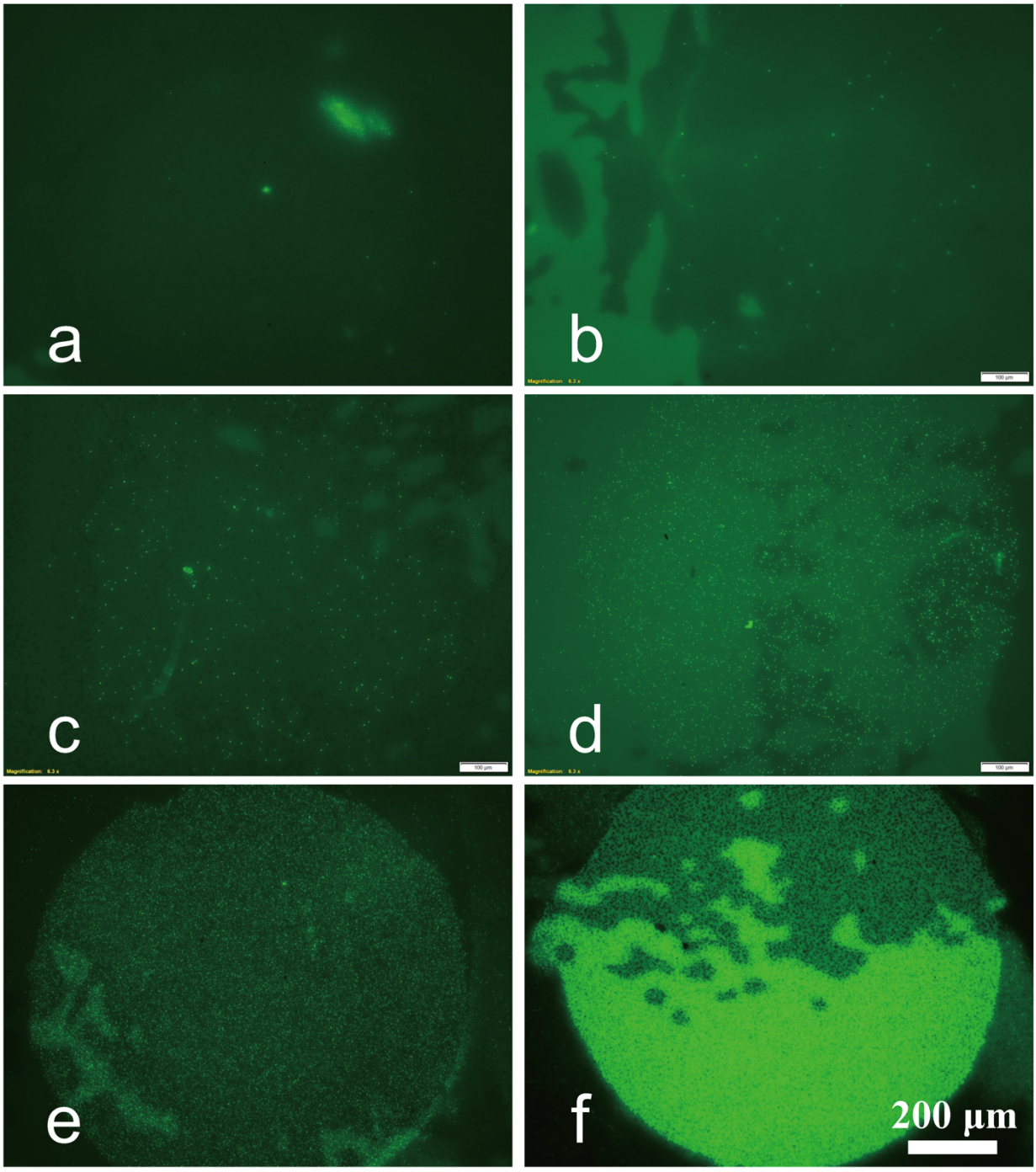

Figure 3. 3 The fluorescence images of *Salmonella* on filters with different populations: a, 6.36 CFU/mm^2, b, 6.36×10^1 CFU/mm^2, c, 6.36×10^2 CFU/mm^2, d, 6.36×10^3 CFU/mm^2, e, 6.36×10^4 CFU/mm^2, f, 6.36×10^5 CFU/mm^2.

Fig. 3.3 shows the fluorescence images of the *Salmonella* on filters with different populations. The population of the *Salmonella* suspension used in the experiment was diluted from the initial number, 5×10^8 CFU/mL, to a minimum of 5×10^1 CFU/mL. The lower six populations were used for the filtration, because the filtration of 100 µL of *Salmonella* suspension whose population higher than 5×10^6 CFU/mL would take a much longer time than 60 s which was not time efficient. Also, the *Salmonella* suspension with a population higher than 5×10^6 CFU/mL will show a clear sense of translucency and can be separated from the clean water by the naked eye without any food safety measurements. According to Fig. 3.3, as the *Salmonella* population increases, the number of bacteria on the filter increases exponentially. Fig 3.3 c-f show that *Salmonella* cells located on filters mostly clustered in circles. Fig. 3.3 a & b show 5 and 51 *Salmonella* cells respectively. Comparing with the nominated numbers of 5 and 50, almost 100% concentration rate was done by the membrane filter to the *Salmonella* cells. These results evidently indicate that most of the *Salmonella* cells from suspensions were concentrated on the experiment designed spot. Therefore, the nominated population of *Salmonella* on membrane filters (5×10^0-5×10^5 CFU) will be used in following figures and discussions.

Fig. 3.4 demonstrates the behavior of the resonant frequency over time for a set of sensors when measured at different *Salmonella* populations (5×10^0-5×10^5 CFU). In the negative control with no *Salmonella* (0 CFU/mL) (Fig. 3.4 white dots), the resonant frequency was stable, without a decreasing trend. Most of the measurements start their resonant frequency drop shortly after the measurement start and soon get stable after 3-5 min. The resonant frequency change increased according to the *Salmonella* population increase from 5×10^0 CFU to 5×10^4 CFU, while in the 5×10^5 CFU population measurement, the change in

resonant frequency didn't increase with the increase in the population. This phenomenon may be caused by several reasons: 1. Due to the excessive amount of *Salmonella* concentrated at the same point, the ME sensor floated above the bacteria during the testing process. The decrease in viscosity during floating and the loss of friction between the sensor and the membrane filter may bring new influencing factors to the measurement and prevent the resonant frequency from decreasing as expected. 2. The large number of *Salmonella* may also be attached to the ME sensor in layers, and the outer layers of *Salmonella* didn't contribute to the decrease of resonant frequency due to it was not attached to the ME sensor itself.

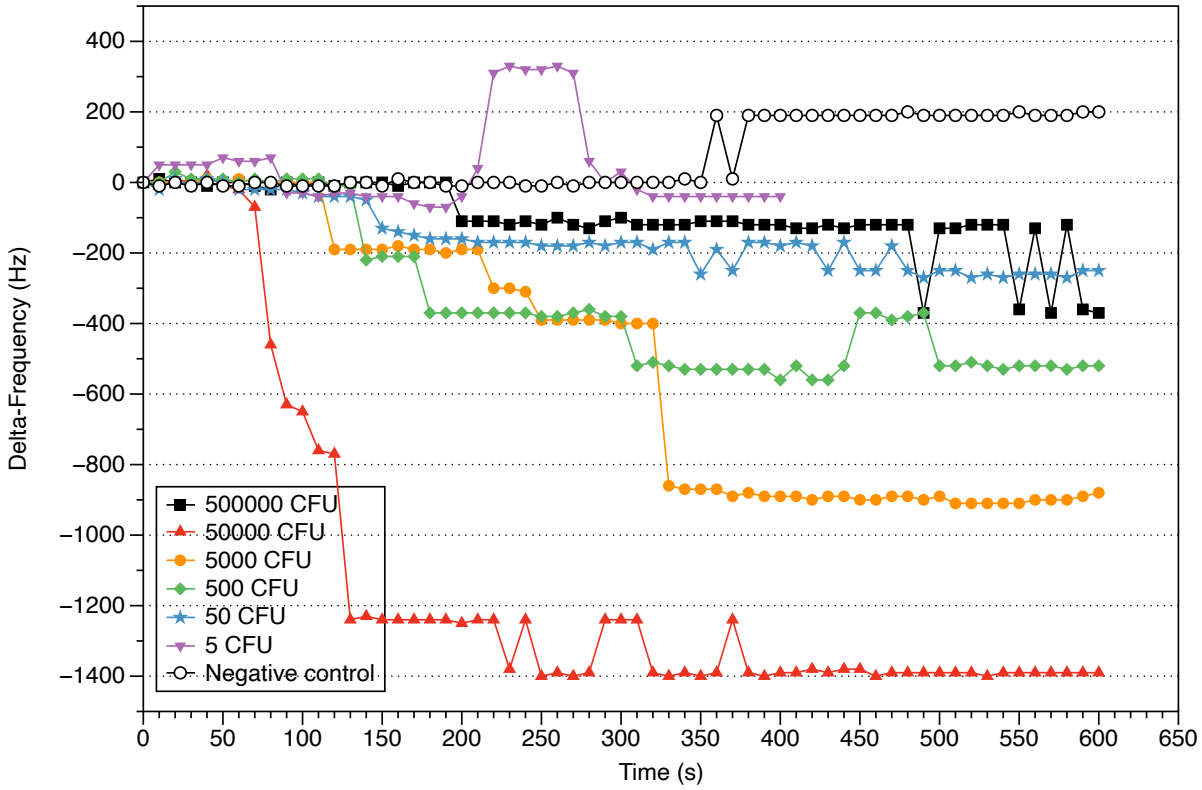

Figure 3. 4 resonant frequency changes of a group of measurements.

In order to check the bacterial adhesion effect of the measurement sensors after the test was completed, each sensor was observed under a fluorescence microscope and recorded as Fig. 3.5. As shown in Figure 3.5a, after ten minutes of reaction with the highest population

(5×10^5 CFU), the sensor surface showed large patches of green. The amount of *Salmonella* stuck on the sensor was large, and it was impossible to separate individual green rod-like *Salmonella* cells. This proves the possibility of the sensor floating above the *Salmonella* cells. In Fig. 3.5b, c, and d, measurement sensors which detected lower populations are attached with hundreds, dozens, and several bacteria, respectively. This decreasing trend is compounded by the expected decrease in the number of bacteria on the surface of the membrane filter. But comparing the bacteria captured by the sensor itself and the bacteria present on the surface of the filter, this number seems to be about 1-2%. On the sensor that responded to be the penultimately lowest population (Fig. 3.5e 5×10^1 CFU), only one *Salmonella* cell (shown as the green dot in the red circle) was found, and none at the lowest population (Fig. 3.5f 5×10^0 CFU).

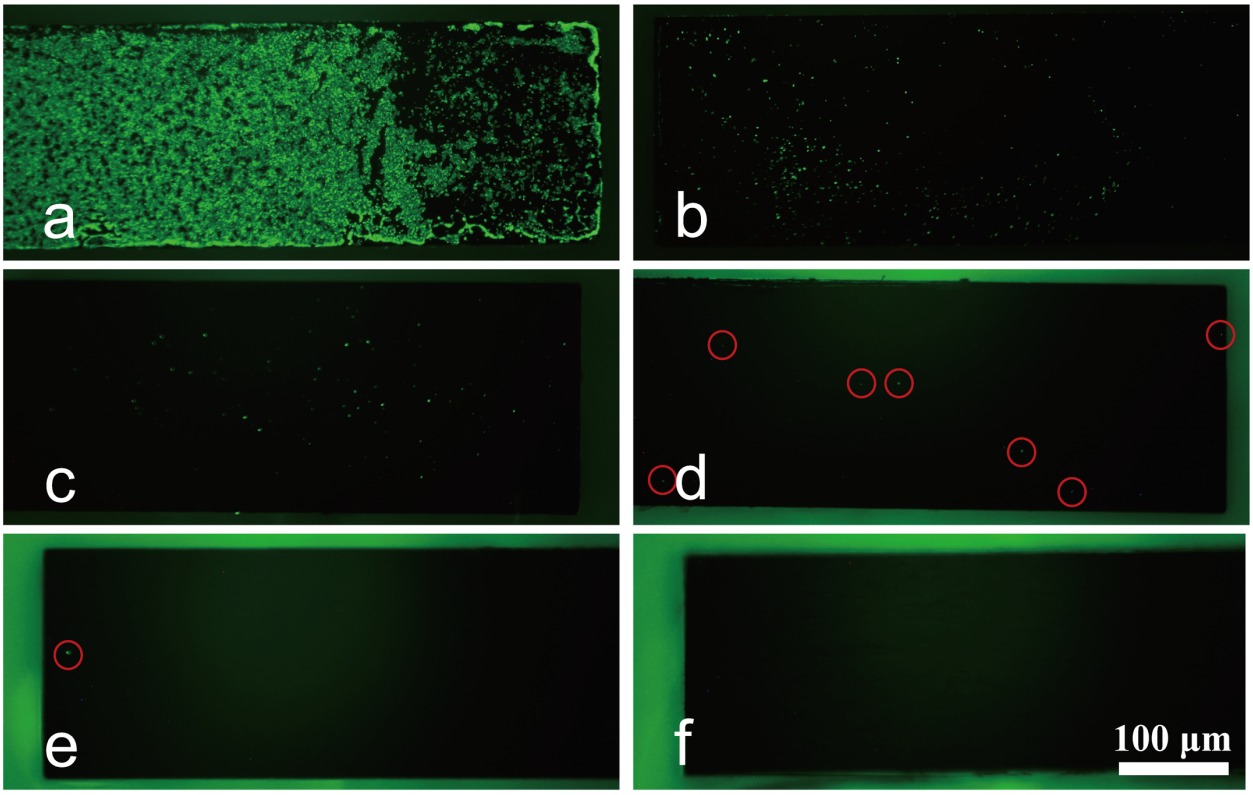

Figure 3. 5 The fluorescence images of *Salmonella* on sensors with different populations: a, 5×10^5 CFU, b, 5×10^4 CFU, c, 5×10^3 CFU, d, 5×10^2 CFU, e, 5×10^1 CFU, f, 5×10^0 CFU.

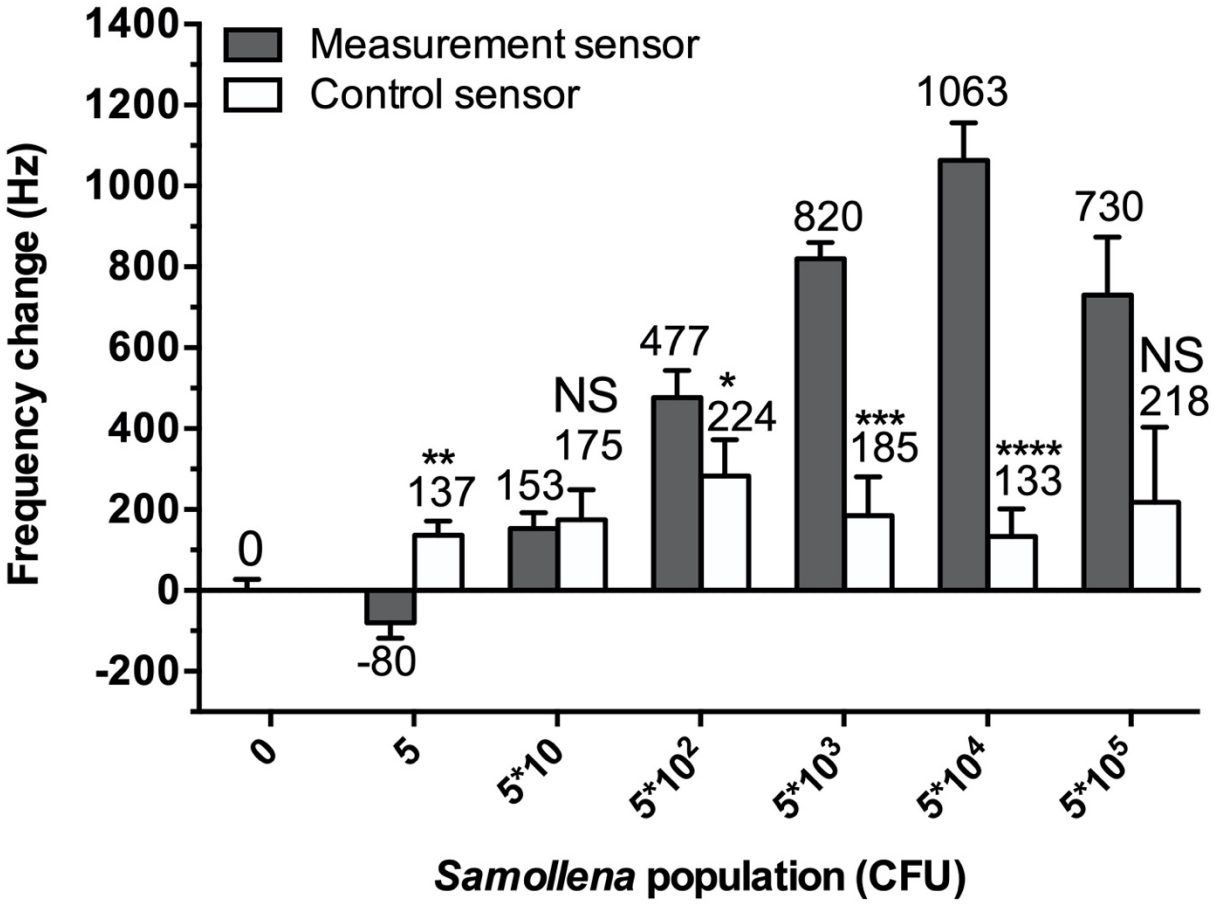

Figure 3. 6 Comparison between measurement and control sensors of different populations of *Salmonella* on membrane filters. Asterisks in the figures indicated significant differences between measurement and control at the level of "*", P<0.05; "**", P<0.01; "***", P<0.001; "****", P<0.0001. "NS" means no significant difference.

In order to study the performance of the membrane filter-assisted ME detection system for detecting *Salmonella* in suspensions of different populations, 6 groups of measurement biosensors and control biosensors were tested on the marked positions alternatively. As shown in Fig. 3.6, the lengths of bars are the mean value of resonant frequency changes; the error bars indicate standard deviations. According to a total 6 repeats of negative controls (Fig. 3.6 0 CFU), the average resonant frequency change (0 Hz) and the standard deviation

(66.3 Hz) indicate that the noise of this measurement system was limited to 199 Hz. In this case, the dye marker was safe to use for the detection. For the measurements from low to high populations (5×10^0-5×10^4 CFU), the frequency changes also vary from small to large, which accords with the tendency of the weight increase. According to Student's independent t-test, for the comparison between measurement and control sensors, the populations at 5×10^0 CFU (P=0.0018, t=4.203) showed significant difference and 5×10^1 CFU (P=0.8003, t=0.2598) didn't. However, the resonant frequency changes of 5×10^0 CFU were in noise level. For all *Salmonella* population on membrane filter higher than 5×10^1 CFU, significant differences were observed (5×10^2 CFU (P=0.396, t=2.405), 5×10^3 CFU (P=0.0001, t=6.109), 5×10^4 CFU (P<0.0001, t=8.098), 5×10^5 CFU (P=0.0544, t=2.179)). Therefore, the LOD of this measurement system is lower than 5×10^2 CFU or 6.36×10^2 CFU/mm^2.

The anomaly is still shown in Fig. 3.6 that the mean value of the frequency change at the highest population (5×10^5 CFU) is smaller than the lower populations. This has also been reflected in the discussion of Fig. 3.4 above. This may be due to the excessive influence of *Salmonella* on the real-time measurement process of the membrane filter surface. We proposed a solution to try to solve this problem: to record the resonant frequency of the clean sensor on a *Salmonella*-free spot of the membrane filter before test, and to record the resonant frequency of the contaminated sensor by flipping it around, so the side without *Salmonella* attached on to the *Salmonella*-free spot of membrane filter. This way, the variables can be controlled as small as possible and the mass of *Salmonella* should be the only factor which influenced the resonant frequency. According to Fig. 3.7, the resonant frequency changes of measurement sensors (1378±400 Hz) and control sensors (-78±310 Hz) are observed (P<0.0001, t=7.039). The results of measurement sensors in this test are used to replace the

test results of the same population in previous series direct measurements to obtain the resonant frequency trend chart in Fig. 3.8. In Fig. 3.8, the surface population x-axis was log transformed and presented as $log_{10}x$. It was found that this curve is a compound linear regression and could be fitted by linear function ($y = -312 + 296.1 * x$). Considering the noise level of this measurement system was 199 Hz, substitute it into the fitted equation, the LOD of the membrane filter-assisted ME sensing system was determined as 54 CFU (6.9×10^1 CFU/mm^2 on membrane surface or 5.4×10^2 CFU/mL in original suspension).

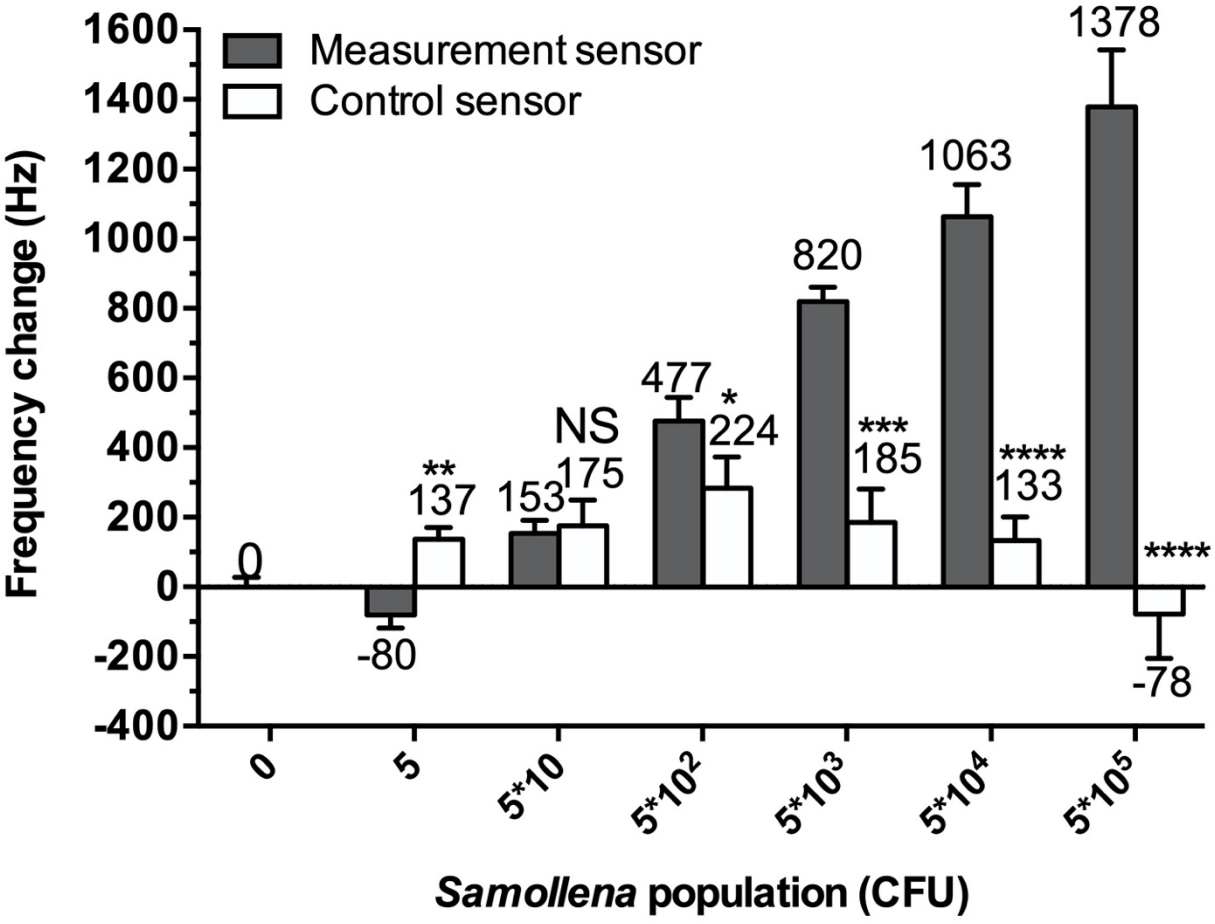

Figure 3. 7 Corrected comparison between measurement and control sensors of different populations of *Salmonella* on membrane filters. Asterisks in the figures indicated significant

differences between measurement and control at the level of "*", P<0.05; "**", P<0.01; "***", P<0.001; "****", P<0.0001. "NS" means no significant difference.

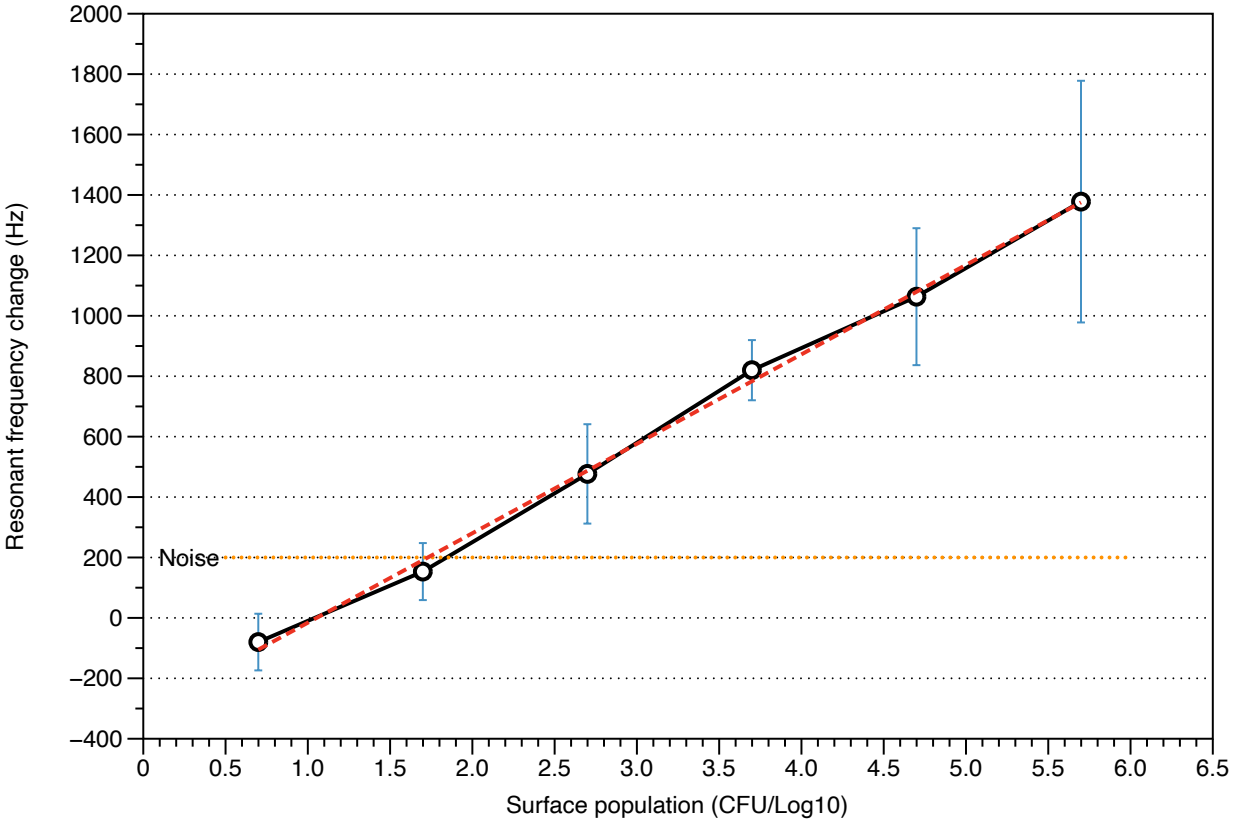

Figure 3. 8 The resonant frequency changes according to a different population of *Salmonella* on membrane filters.

Limited by lab experiments, 100 µL was chosen as the sampling size in this research. For real detections of water quality in real daily life, the bacterial concentration will be extremely low, and the sample volume and the filtration time can be very sufficient. Referring to Zhang's research [191], an E. coli suspension with an initial bacterial concentration as low as 0.1 CFU/mL could be recovered at around 80%. For the membrane filter assisted ME sensing, as long as the water sample amount can be larger than 540 mL, the detection is possible.

3.4 Summary

In this research, the membrane filter was applied to the ME sensing system for the first time, and it helped to transfer the former detection of *Salmonella* from liquid to membrane filter surface. The surface *in-situ* detection method of ME sensing system with planar spiral coil built-in can offer its fast and accurate characteristics for the detections of *Salmonella* in liquid. Based on the design of the funnel, most of the *Salmonella* in the suspension can be concentrated into a small circle to fit the size of the sensor, so the possibility of the sensor to get contaminated with the target pathogen was maximized. According the results and analysis, the detection limit of this system can reach 54 CFU (6.9×10^1 CFU/mm^2 on membrane surface or 5.4×10^2 CFU/mL in original suspension). Comparing the traditional ME sensor detection in solenoid coil, this system can make the detection of *Salmonella* in liquid faster (10 min vs 1 h), and more accurate (5.4×10^2 CFU/mL vs 5×10^3 CFU/mL) [194]. Since the filtration capability of membrane filters does not necessarily limit to 100 μL as tested in this research, as long as enough volume of tested liquid passed through the membrane filter, the LOD of *Salmonella* population in the liquid can be even lower.

Chapter 4. Swabs and peelable gel as large-scale sampling methods of *Salmonella* Typhimurium

4.1 Introduction

People suffer from foodborne diseases caused by microorganisms because food can be contaminated at any stage of the food supply chain. *Salmonella*, which we target in this research, is one of the main pathogens that causes food poisoning, fever and even hundreds of deaths every year [5], [6]. To prevent the *Salmonella* outbreaks, an ME biosensing system which consists of a wireless acoustic wave sensor platform [195] and a coil detector [70], [186] was employed for real-time, low-cost, and portable *Salmonella* detection on site [196]. Due to the basic theory of the acoustic wave sensor platform, a higher sensitivity could be offered by a smaller sensor [33]. Here comes the dilemma that if the sensor size is too small, the detection area it could touch would also be small. Even though the multiple sensors fast measurement can provide very good information of the existence of targeted pathogens by statistics [197], a sampling method which can cover the whole desired area may serve as an simpler alternative.

After its invention around a century ago [157], the swab soon became one of the most useful surface sampling techniques. Due to the characteristics such as low cost, easy-to-use, and highly efficient, the swab has been widely used in hospitals, labs [146], and homes for the pathogen collection. With the development in the past decades, Q-tips with cotton fibers

wrapped around the head of wooden rods are no longer the only architecture of swabs. Different synthetic fibers, such as rayon [148], foam [151], polyester [152], and nylon [153] have been synthesized and used for the applicators of swabs. These applicators usually have excellent water absorbability which helps them by collecting the particles from sample surfaces. Besides the application of new materials, the construction of the applicators also experienced a revolution from the wrapped structure to a flocked one [153], in which a large number of short nylon fibers stand perpendicular to the handler tip and form a head. This fabrication method provides a more ordered structure of the applicators. Tightly aligned fibers can act as brushes on the sample surfaces and then hold liquid samples by its strong capillary effect. This flocked structure was claimed to have better ability to collect cells from surfaces and have a faster elution rate back into liquid [153].

Swabs wetted by DI water can pick up and recover more pathogens than using swabs only [148]. To enhance the *Salmonella* recovery rates from dry surfaces, we need a better wetting agent than DI water which can help us pick up more pathogens. So, this wetting agent should have the following abilities: 1. It should be able to lower the surface tension between the pathogen and sample surface; 2. It should be able to offer stable oil-in-water emulsion; 3. It should be widely accepted for the usage in the biology lab; 4. It should be safe for food applications. Comparing with DI water, Tween 20, which is a nonionic detergent widely used in biochemical applications, fits these requirements. In Buttner et al.'s research [175], a 0.05% Tween 20 solution was used to suspend B. *atrophaeus* before swab tests. The high recovery rate was hypothesized to be influenced by the low coherence between spores and the sample surface. By comparing 11 different solutions in a series of experiments to identify the best for swab wetting, Moore and Griffith showed that the high recovery rate of pathogens in the

diluent was mainly influenced by the pick-up and release rates [169]. Although their performance varied, all the surfactants significantly improved the two processes, it mitigated the damage to bacterial cells during dry swabbing, and maximized elution.

Instead of collecting particles in a mechanical way, a method of applying a peelable gel to sample surfaces to remove *Salmonella* was proposed. By hypothesis, we should be able to find a gel that can be spread evenly over a large surface area. The gel should be able to form a thin film and pick up bacteria from sample surfaces. The gel film should be able to keep bacteria alive and then easily peel off from the surface. It also should be able to dissolve into water in a short time, so that the pathogen collected by the gel can be recovered quickly.

Regarding the choice of peelable gel, the first consideration is the safety to bacteria and operators. Commonly used edible gels are generally natural products and considered as safe. Among them, agar and carrageenan are seaweed extracts with high gelling and melting points (85 °C), so they cannot be spread on the sample surface at room temperature. Also, because their water-soluble temperature is too high, *Salmonella* would be killed at a temperature higher than 71 °C. Even if in some way the bacteria were picked up by these gels, it cannot be restored to water. Gum arabic (acacia gum) is an exudate obtained from the bark of African legumes. Because of its suitable viscosity, it is often used to make fudge. In the preliminary tests, we found that gum arabic can dissolve well in water at room temperature and form a viscous and odorless gel. However, the dried gum arabic film is very fragile and easy to break and cannot be peeled off from the sample surfaces.

Gelatin, derived from various animal by-products, is a commonly used translucent, colorless, flavorless food additive. At around 30 °C, it transforms between a semi-solid phase and a liquid-like one. This melting point of gelatin is a little lower than the incubation

temperature (37 °C) and much lower than the killing temperature of *Salmonella* (71 °C), so the melting process of the gelatin won't hurt the pathogen. According to an FDA study [198], *Salmonella* can survive in gelatin gel and recover by a certain incubation process. Not only can gelatin keep *Salmonella* alive in it [199], it also allows the micro-organisms to break it down into smaller molecules [200]. Based on Brocklehurst's research [201], the *Salmonella* Typhimurium can even grow in gelatin gel under a suitable environment. In this case, gelatin is chosen for the peelable gel test.

The goal of this study is to find the most suitable large-scale sampling method of environmental surfaces. To simulate a real food processing environment, three normal food processing plate materials were selected: a food grade PE board (with different roughness), a stainless steel sheet, and glass slides. Five commercially available swabs (Fig. 4.1 a. Rayon; b. Cotton; c. Purflock; d. Hydraflock; e. ESwab) were compared by their structures, water capacities, and *Salmonella* Typhimurium recovery rates from both wet and dry surfaces. The effect of a wetting agent for swabs, Tween 20, was tested for improving the *Salmonella* sampling efficiency from dry surfaces. Finally, gelatin was compared with swabbing for *Salmonella* recovery in different roughness of PE boards and from various kinds of sample surfaces.

4.2 Materials and methods

4.2.1 The selection and treatment of swabs and gelatin

The five typical swabs, which represent different applicator fibers and structures, are traditional rayon swabs (Fig. 4.1a) and cotton swabs (Fig. 4.1b), the Purflock (Fig. 4.1c) swabs and Hydraflock swabs (Fig. 4.1d) (Puritan Medical Products, Lenexa, KS), and the eSwab (Fig. 4.1e) (Copan Diagnostics, Murrieta, CA). All the swabs used in this work were

sterile and single packaged. Photos and SEM images were taken to demonstrate the fibers, structures, and characteristics of the different applicators. Tween 20 was provided by Dr. Tung-shi Huang's lab with a concentration of 0.1% and diluted into a lower concentration of 0.05% for the comparison.

Figure 4. 1 Swabs used in this research. a. Rayon; b. Cotton; c. Purflock; d. Hydraflock; e. eSwab.

Gelatin (Knox, Englewood Cliffs, NJ, Fig. 4.2a) with different concentrations (0.025 g/mL, 0.05 g/mL, 0.075 g/mL, and 0.1 g/mL) were prepared for optimization. All the gelatin solution was prepared and kept at the *Salmonella* incubation temperature (37 °C). A water bath (Thermo NESLAB RTE 7, Newington, NH, Fig. 4.2b) was used to heat the mixture and maintain a precise temperature.

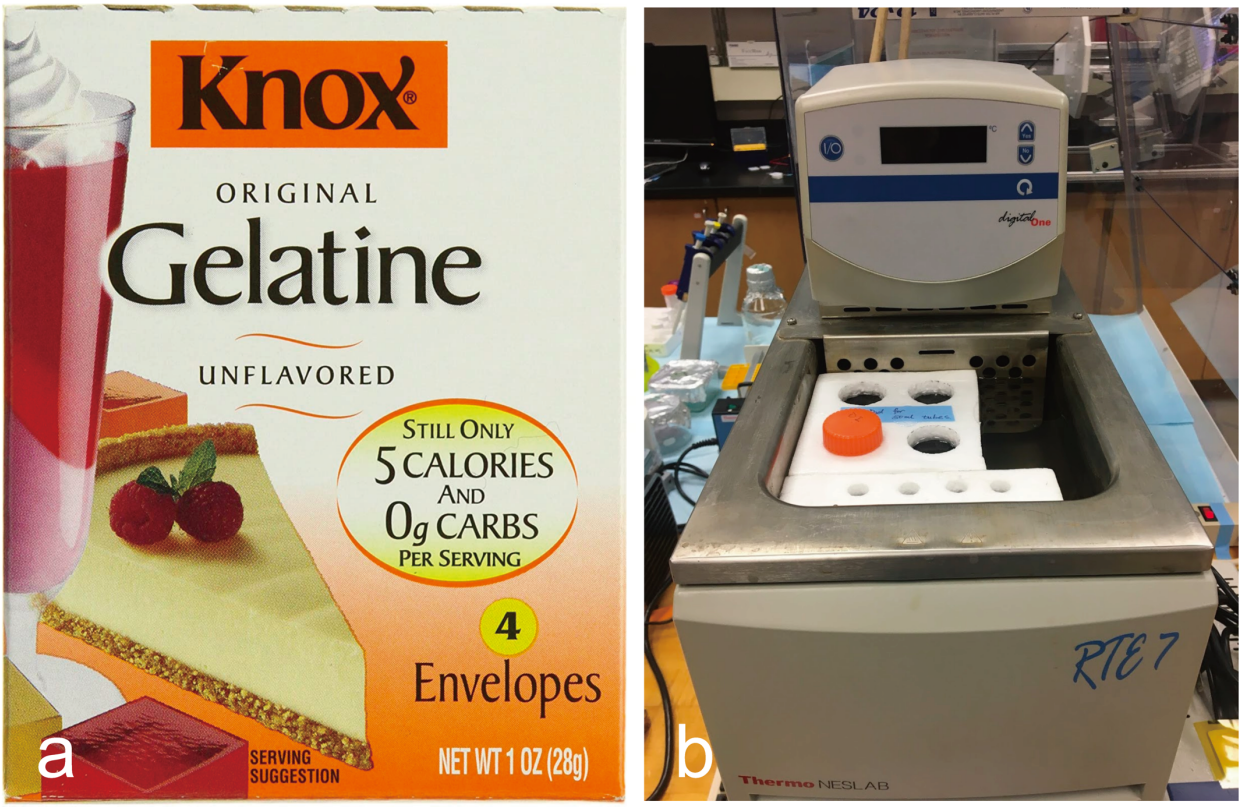

Figure 4. 2 a. box of unflavored gelatin, b. water bath heater.

4.2.2 *Salmonella* sample preparation

A food grade PE board, a 304 stainless steel sheet, and glass slides were used to simulate the environment of food preparation surfaces. The PE board was diced into 3×3 cm^2 squares by a band saw; and the stainless steel sheet and glass slides were cut into the same size by wire cutting and diamond blade, respectively. Three surface roughness of PE plates were prepared using sandpapers with grits at 120 (120PE), 320 (320PE), 600 (600PE) to

correspond to the long-term used, mild used, and brand-new plastic food cutting board. The corresponding roughness of each PE plate was expressed as 115 μm, 36 μm, 16 μm, respectively. The suspension of *Salmonella* Typhimurium with a population of 5×10^8 CFU/ml was diluted into 5×10^4 - 5×10^7 CFU/ml using deionized water. Five drops of a *Salmonella* suspension, 20 μL per drop, were loaded onto each PE square. Calculated by equation 7, the surface population of *Salmonella* in this research range from 5 CFU/mm^2 to 55000 CFU/mm^2. For wet surface tests, swabbing was carried out on the samples immediately, while for the dry surface tests, all the samples were located in the hood for a drying time of about 2 h.

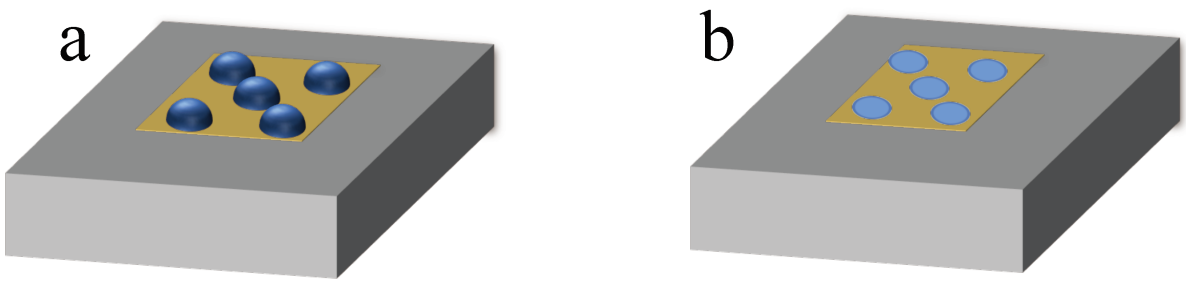

Figure 4. 3 The sample preparation process: a. 5 droplets on sample surface; b. *Salmonella* suspensions dried in the hood.

4.2.3 Sampling and recovering process

Swabbing:

First, a preliminary test to measure the water absorption capacity of different kinds of swabs was conducted (Fig. 4.4) to determine the volume of water should be used in the following tests. Three replicates were done by dipping each fresh swab into water and measure the weight loss of the water tank. It was found that the rayon and cotton tipped traditional swabs can absorb more water than the flocked ones. All the five kinds of swabs could take more than 100 μL DI water.

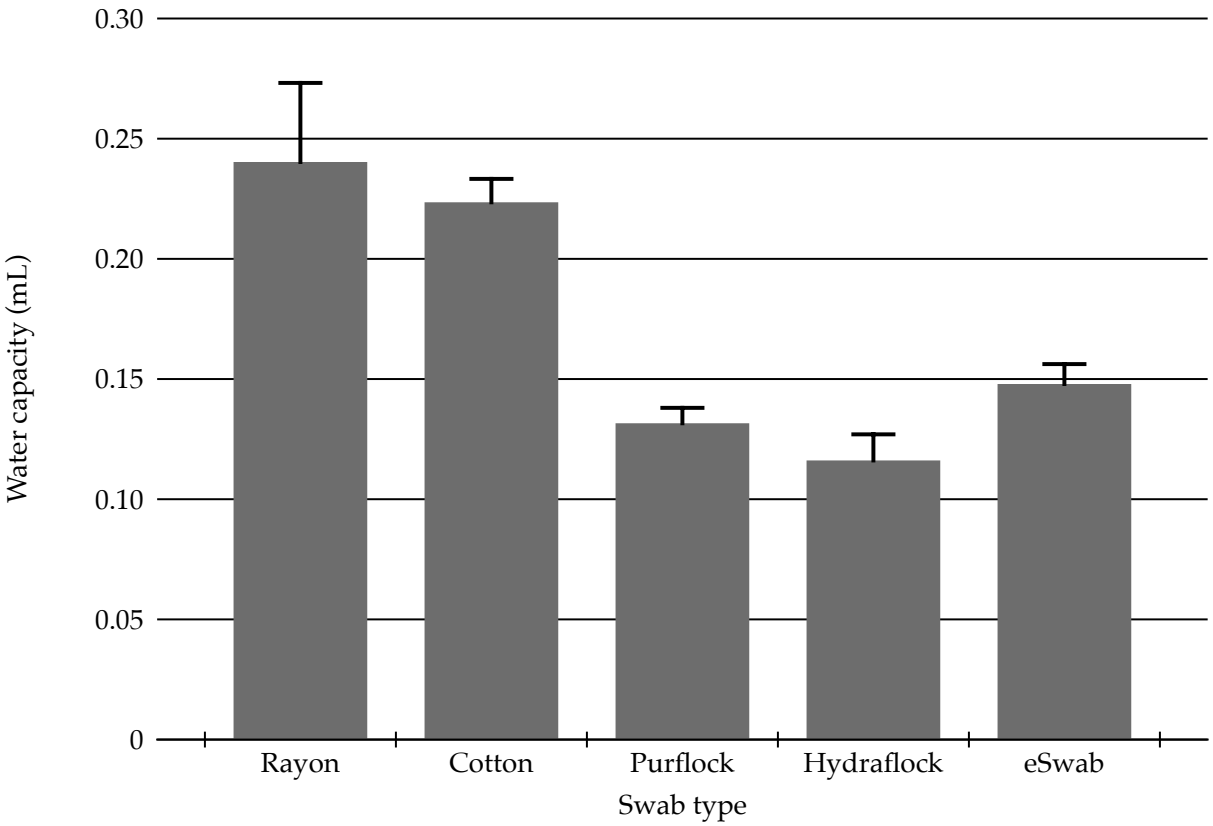

Figure 4. 4 Water capacity (mL) of the different swabs.

100 μL DI water was loaded onto the PE squares. Immediately afterward, a swab was applied to absorb the moisture so dried *Salmonella* is picked up by the humidified swab as much as possible. The swab was then pressed down so its tip could fully contact the board surface and move in the three directions illustrated in Fig. 4.5, 30 times per direction. Each movement was as uniform as possible to make sure that the swab covered the sample surface evenly. The swab was rotated about its axis by 90 degrees after swabbing on each direction, so that the pathogen capture rate can be maximized. The swab tip was then submerged in 900 μL DI water in a plastic tube, followed by 15 s vortexing. After that, the suspension was diluted by factors of 10^1,10^2 and 10^3, and each population was marked on petri dishes as -1/-2/-3. For each population 2 drops of 10 μL were placed on to the petri dish and formed a line

by slipping down. After 16 h of incubation at 37 °C, bacteria colonies grew and were suitable for plate counting.

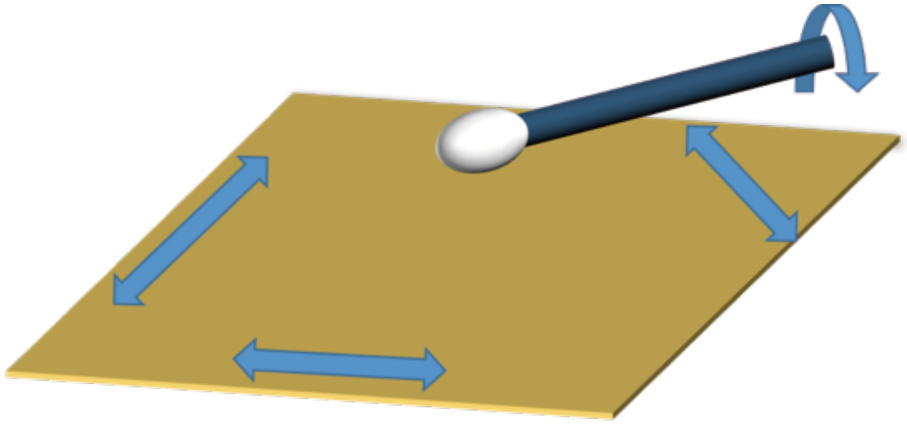

Figure 4. 5 The sampling processes: swabbing and rotation.

Peelable gel:

The same boards which were used in swab tests were also used as sample surface in the gelatin test. The cleaning, *Salmonella* dropping, and drying procedures were also following the procedures used in the swab tests. 100 µL of fully dissolved gelatin solution was then pipetted onto sample plates and dried for 2 h. The thickness of each gelatin film which formed from different concentrations was measured by a height meter. 0.05 g/mL was the concentration which could form the thinnest film with a complete and uniform structure. After the gelatin dried on the *Salmonella* contaminated surface, it could easily be peeled off by tweezers.

The peeled off gelatin film was dissolved in 1 mL of DI water, heated by the external water bath controlled at 37 °C. This temperature was used to decrease the time to dissolve the gelatin without killing the bacteria. The plate count procedure also follows the swab testing.

4.3 Results & discussion

4.3.1 Photo and SEM observation of swabs and structure analysis

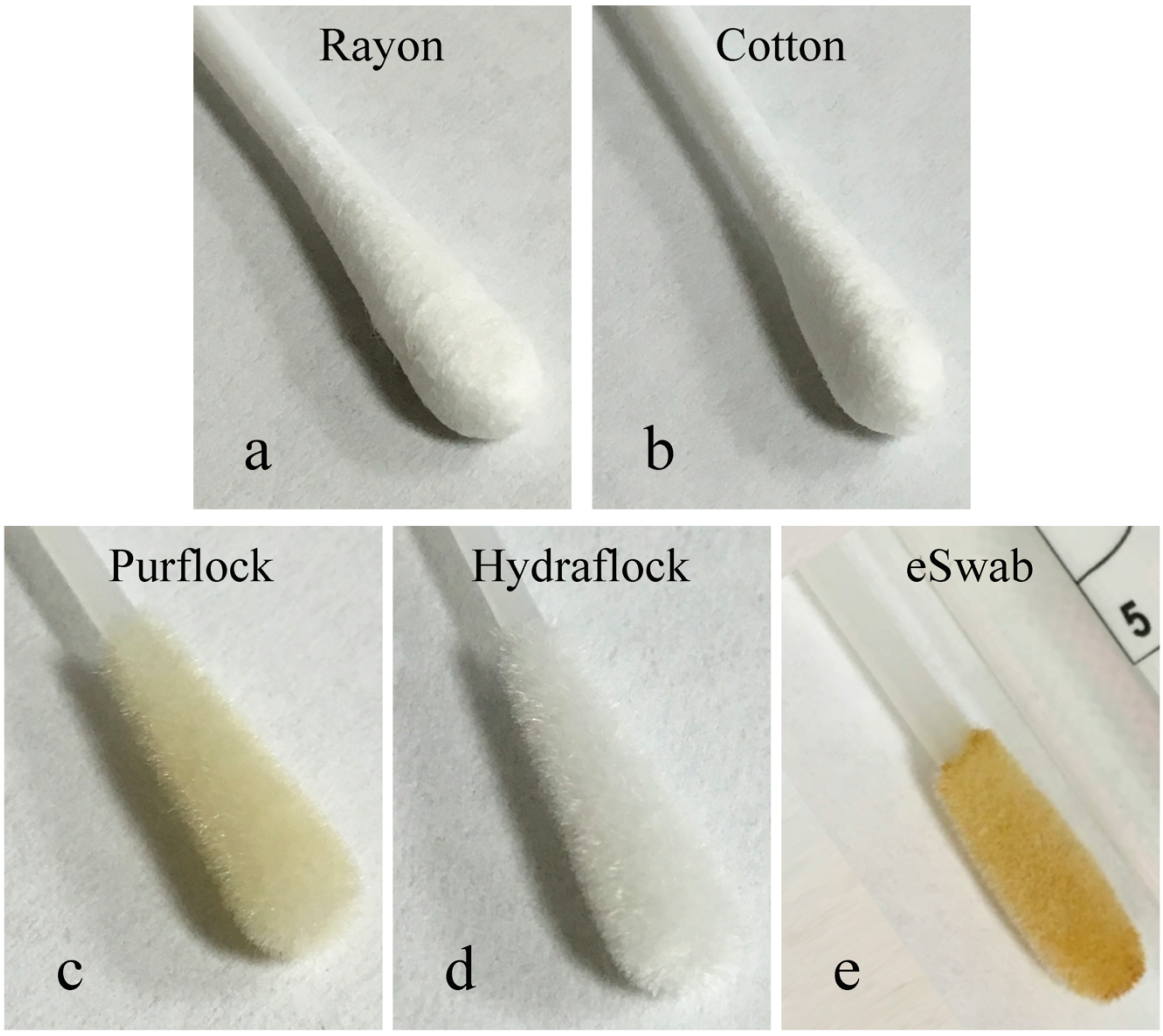

Figure 4. 6 Swabs used in this research. a. Rayon; b. Cotton; c. Purflock; d. Hydraflock; e. eSwab.

Photos of all the five swabs with different tip materials and their isolated sterile packages are shown in Fig. 4.6. The variations of swab sizes are controlled in a small range ($5 \pm 0.2\ mm$ in diameter / $16.5 \pm 1\ mm$ in length) to keep the capture ability and recovery rate

only depend on the architecture of applicators. Observed by the naked eyes, rayon & cotton swabs are traditional ones whose fiber was twined around one head of the plastic handles to make the tips, while the other three are flocked designs, where all the fibers stand as arrays on the heads to make tips.

To further determine the microstructures of these swabs, the SEM images (Fig. 4.7) were taken. The SEM magnification of rayon and cotton swabs (Fig. 4.7a and 4.7b) reveals that the fibers tangle together since they are wrapped around the head of the handle. The rayon fiber seemed very smooth and uniform, with an average diameter at 13.28 μm. Quite different from the rayon one, the cotton fibers were rough, flat, and always twisted. The width of cotton fibers varied a lot, ranging from 5-13 μm. As is called, the Purflock swab had very clean, smooth, and uniform fibers, whose average diameter was 18.29 μm, flocked around the head. The microstructure of the Hydraflock swab was quite unique. Its special 3D design not only makes the fibers flocked around the head of handle, but also keeps branching very uniform on top of each fiber. The average diameter of the Hydraflock swab fibers was 17.2 μm, while the diameter of each branch was around 2.52 μm. The structure of eSwab is very similar with the Purflock's, but the surface of the fibers seems to be very unsmooth. It might be caused by the protein added by Copan on this swab.

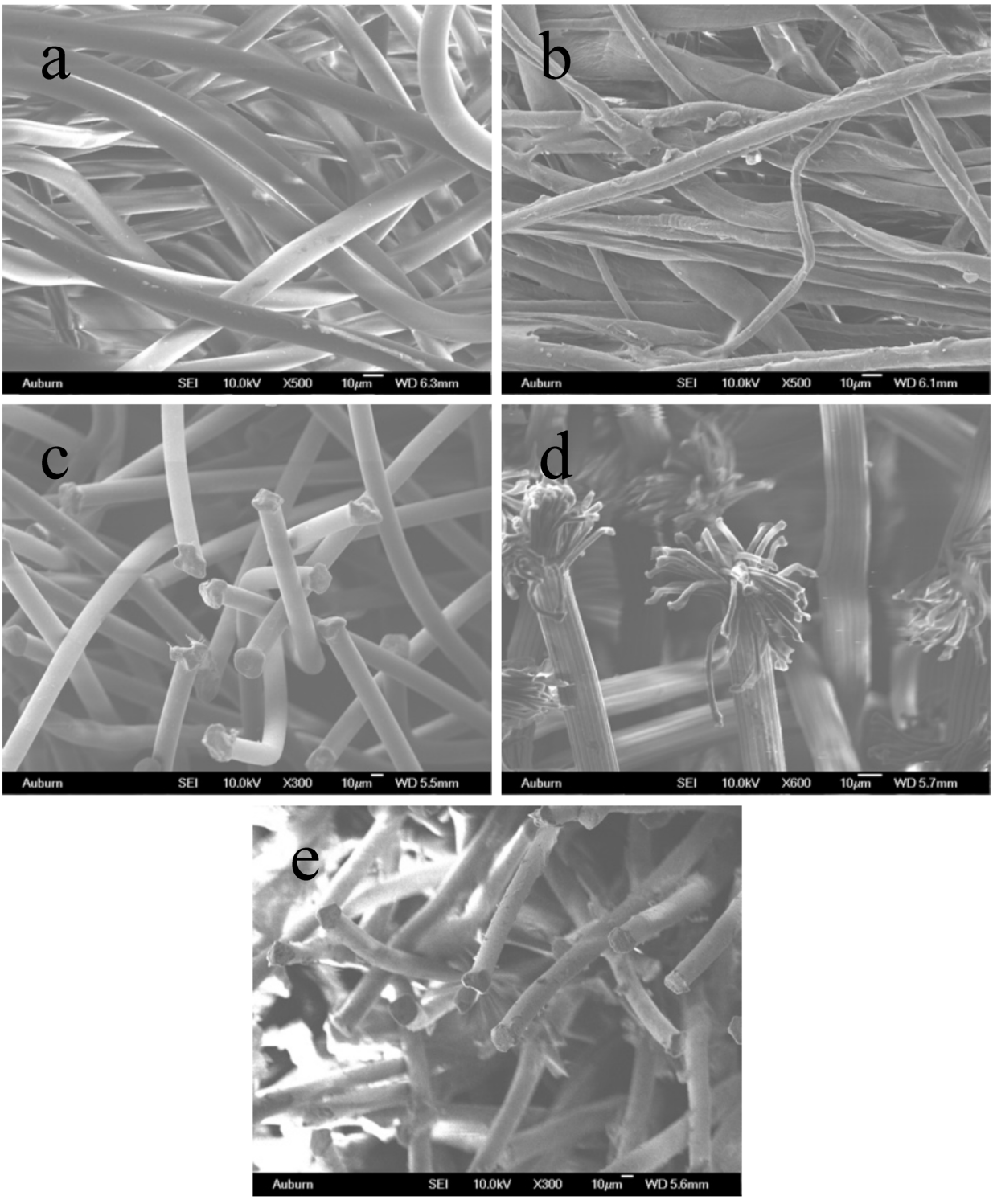

Figure 4. 7 SEM images of swabs. a. Rayon; b. Cotton; c. Purflock; d. Hydraflock; e. eSwab.

4.3.2 Comparison of swabs on the *Salmonella* recovery from wet surfaces

The recovery results on wet plastic surfaces quantified by plate counting are shown in Fig. 4.8. The recovery rates of the three flocked swabs were higher than the two traditional ones. Compared them in pairs by t-test, significant differences were found between Purflock swabs and traditional ones (Rayon: P=0.0357; Cotton: P=0.044). Significant differences also showed between Hydraflock swabs and traditional ones (Rayon: P=0.0184; Cotton: P=0.021). However, the comparison between eSwab and Rayon/Cotton didn't show any significant difference (Rayon: P=0.0596; Cotton: P=0.0596). The differences in *Salmonella* recovery rate seem to be caused by the differences of tip microstructures. The wrapped fibers of traditional swabs may trap the bacteria, while the flocked structure would not have an apparent block for the pathogens. The branching tips of Hydraflock fibers was able to sweep more detailed than other flocked swabs, so it gets the highest *Salmonella* recovery rate on wet surface detection.

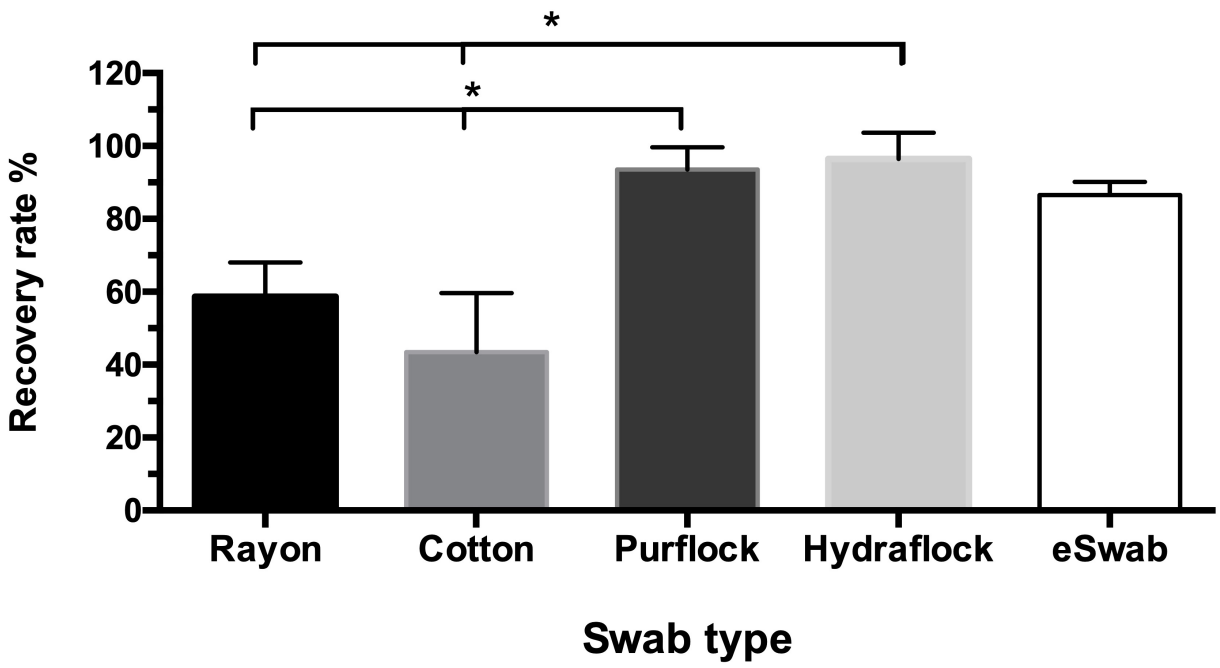

Figure 4. 8 *Salmonella* recovery rate of different swabs on wet surfaces. (Asterisks in the figures indicated significant differences among glass, steel, and plastic boards at the level of "*", $P<0.05$.)

4.3.3 Comparison of swabs on the *Salmonella* recovery from dry surfaces

The *Salmonella* recovery rate of different swabs on dried 600PE board surfaces was shown in Fig. 4.9. To find out a swab that can be used for various surfaces universally, experiments were conducted on three different surfaces – steel, glass and PE board. Across all swabbing methods, eSwab has the highest recovery rate on plastic surfaces but the lowest on the glass ones ($P=0.01$). The Hydraflock swab showed similar levels of recovery rates ($P=0.32$) for all the three surfaces. When compared with other swabbing methods, it presented similar or relatively higher recovery rates. Similar with eSwab, Purflock swab also showed a significant difference ($P=0.04$) in recovery rates among three surfaces with the plastic board

the highest. The two traditional swabs, rayon and cotton, showed relatively lower recovery rates than other methods, and no significant differences (Rayon: P=0.24; Cotton: P=0.45) were observed among the three surfaces. Purflock and eSwab behave very similarly on surfaces of different materials, which may be related to their similar microstructure (Fig. 4.7c&e).

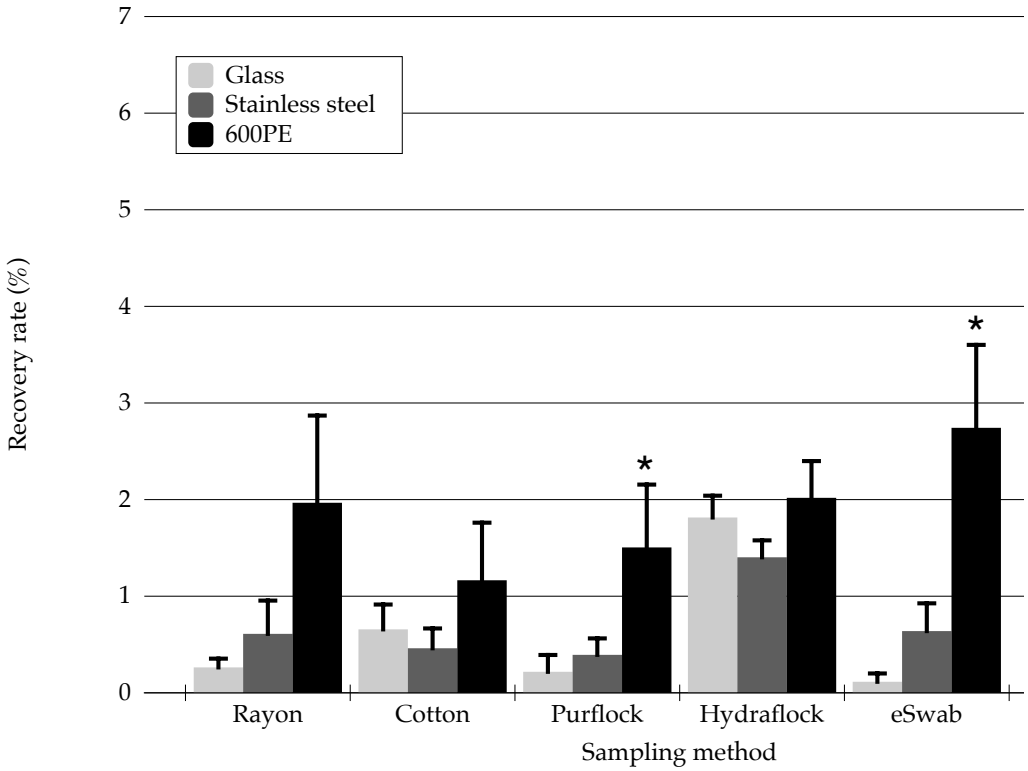

Figure 4. 9 Comparison of *Salmonella* recovery rates of different swabs on 600PE boards; Stainless steel sheets, and glass slides. (Asterisks in the figures indicated significant differences among glass, steel, and plastic boards at the level of "*", P<0.05.)

4.3.4 Wetting agent assisted swabbing from dry surfaces

A preliminary screening to compare the recovery rates by using the wetting agent, Tween 20, with different concentration (0.1% & 0.05%). When the Tween 20 modified swabs

were applied on the dry surface, the recovery rates of both concentrations (0.1% & 0.05%) were consistently higher with 0.05% on all swab methods. Further tests on both 600PE board and stainless steel sheet showed about 10-fold increases after adding the surfactant. Significant differences between with/without 0.05% Tween20 were detected (600PE: $P<0.01$; Stainless steel: $P<0.01$). In Moore and Griffith's discussion about in-house swabbing standards [169], the addition of surfactants to wetting solutions significantly increased the number of recovered E. coli colonies from dry surfaces compared to solutions lacking surfactant. This is because the sublethal damage to the cell membrane in a dry environment makes the bacteria very sensitive to excessive agitation and strong shear forces [202]. The wetting solution containing surfactants will reduce the surface tension of the liquid on sample surfaces, thereby reducing the mechanical energy generated by the wiping action and minimizes the damage of bacteria [169].

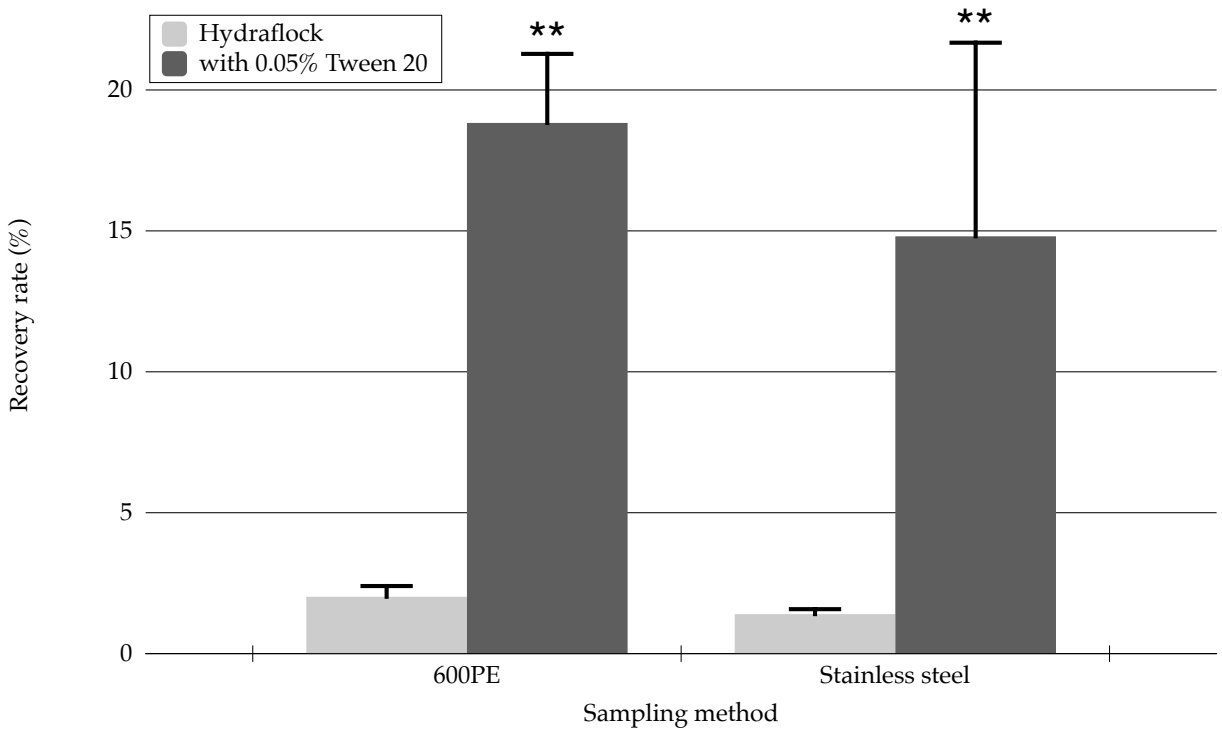

Figure 4. 10 Comparison of *Salmonella* recovery rates on Hydraflock swab with/without 0.05% Tween 20. (Asterisks in the figures indicated significant differences between with/without 0.05% Tween 20 at the level of "**", P<0.01).

4.3.5 Screening data for peelable gel sampling

The ability of gelatin to remove and recover *Salmonella* cells was then examined by fluorescence optical microscope. Fig. 4.11 shows a series of fluorescence microscopy images of *Salmonella* at 5×10^6 CFU/mL: a) *Salmonella* cells after drying on PE board; b) PE board surface after gelatin was peeled off. In the 0.038 mm×2 mm image-taking area, there were a total of 777 live *Salmonella* colonies counted in Fig. 4.11a and very few live *Salmonella* colonies counted in Fig. 4.11c. Obviously, gelatin does have the ability to remove almost all the *Salmonella* cells from PE board surface. It may solve the difficulty of detection on rough surfaces.

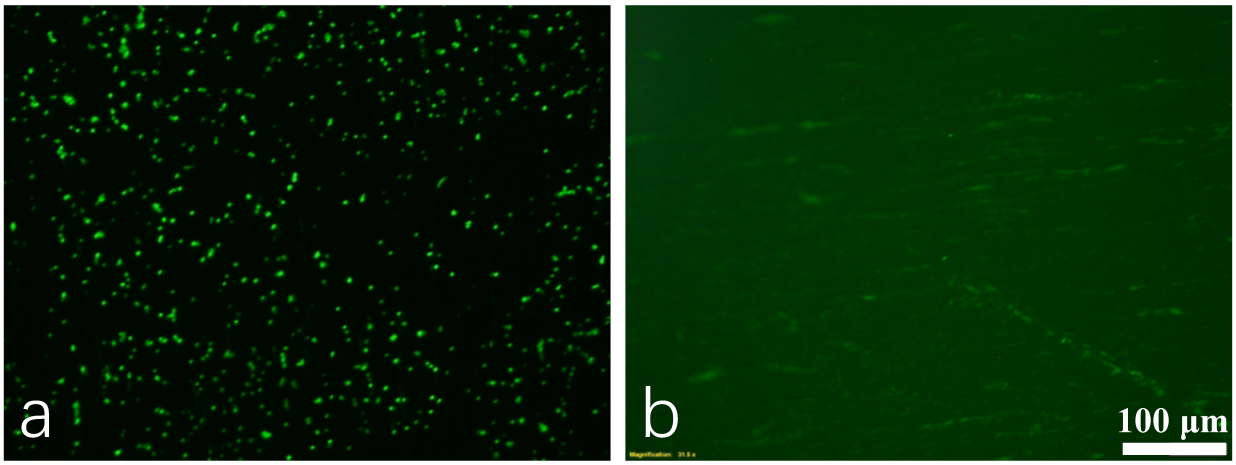

Figure 4. 11 a. *Salmonella* on PE board; b. PE board after gelatin treatment.

To minimize the influence caused by gelatin on bacteria and maximize the recovery rate of *Salmonella*, using a less amount of gelatin to pick up as much as *Salmonella* is needed. At the same time, a too thin layer of gelatin won't be smoothly peeled off completely. Various concentrations (0.025 g/mL, 0.05 g/mL, 0.075 g/mL, and 0.1 g/mL) of gelatin solution was prepared and measured after drying. 0.05 g/mL was the one which would form a thin film with a thickness at only 0.02 mm.

No data was recorded for the test of gelatin on glass (Fig. 4.12) because gelatin films are not able to be removed from the glass surfaces. When compared between the plastic boards and stainless steel sheets, significant higher recovery rates ($P=0.03$) were observed on plastic boards. On the stainless steel sheets, the recovery rates by gelatin was similar with all the swabs ($P>0.05$). However, on a plastic board, gelatin had achieved relatively higher recovery rates than the swab sampling methods, while the differences were not statistically different ($P>0.05$). Overall, gelatin showed a good recovery rate when used as a sampling method for *Salmonella* on surface. Comparing with swab sampling, the peelable gel sampling method represented by gelatin has three major advantages: 1, large scale. Gelatin solution can be applied on any area of surfaces as the experiment designed, while the swabbing can only

cover a relatively small range. 2, repeatability. The bacterial recovery results of swab sampling are highly dependent on the operation of the experimenter, because the force applied on sample surfaces can be different. For the peelable gel sampling method, the application of gel can be much more repeatable. 3, no trained personal required. Gelatin is a commonly used food additive in households, its usage in bacterial surface sampling is just a repurposing utilization.

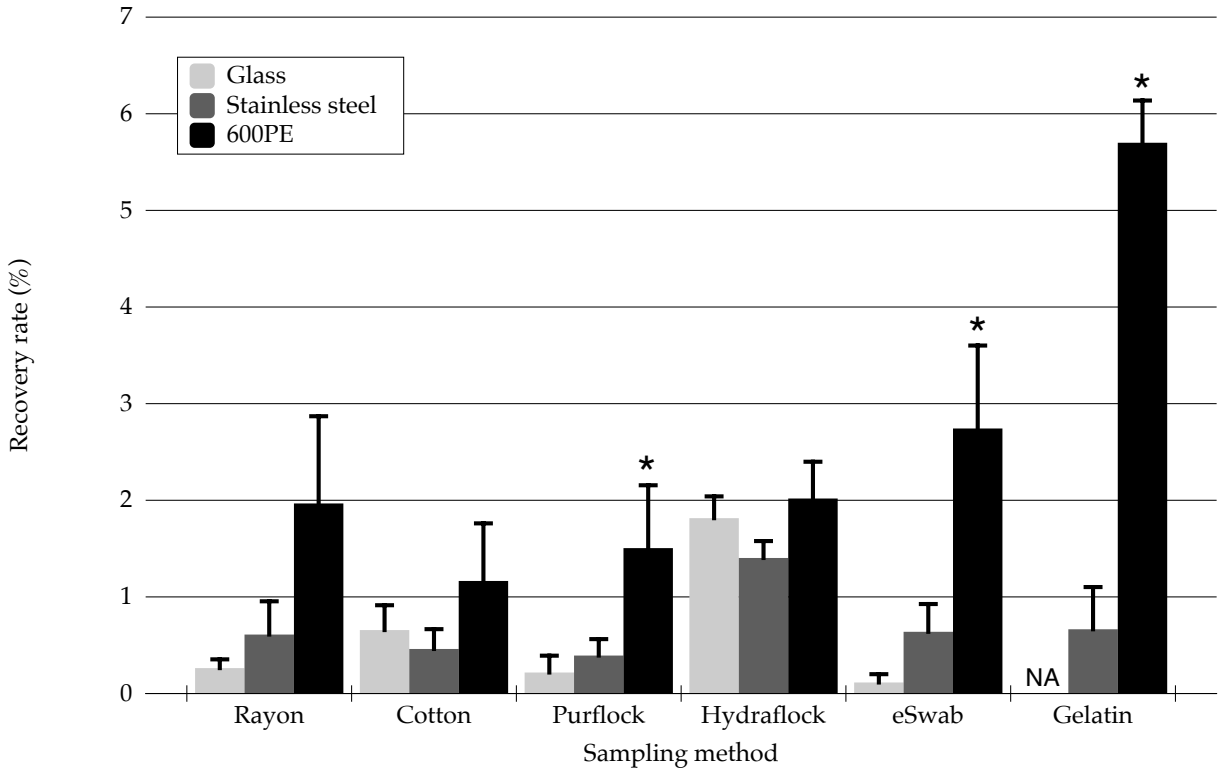

Figure 4. 12 Comparison of *Salmonella* recovery rates of gelatin and swabs on 600PE boards; Stainless steel sheets, and glass slides. (Asterisks in the figures indicated significant differences among glass, steel, and plastic boards at the level of "*", $P<0.05$. "NA" means no available for tests.)

4.3.6 Comparison the effect of different roughness on recovery rates of *Salmonella* by gelatin and Hydraflock swab.

Salmonella with surface density range from 5 CFU/mm^2 to 55000 CFU/mm^2 was tested for the recovery rates from PE board with different roughness (120PE, 320PE, and 600PE) by gelatin and Hydraflock swab (with 0.05% Tween 20) (Fig. 4.13). At 5 CFU/mm^2 and 55 CFU/mm^2, low recovery rates were found. By gelatin sampling method (Fig. 4.13a), the recovery rates on 600PE were significantly higher than 320PE ($P<0.01$) and 120PE ($P=0.0104$); no significant difference was found between 120PE and 320PE ($P=0.13$) at 550 CFU/mm^2. For 5500 CFU/mm^2, a similar pattern was observed with 550 CFU/mm^2 (600PE vs 320PE: $P<0.01$; 600PE vs 120PE: $P<0.01$; 320PE vs 120PE: $P=0.74$). However, for the highest surface population 55000 CFU/mm^2, no significant difference was found among three surfaces ($P>0.05$). This finding indicates that the efficiency of *Salmonella* captured by gelatin was affected by surface roughness. Especially at low population, the capture efficiency on smoother plastic surfaces was better.

By Hydraflock swab (with 0.05% Tween 20) sampling method (Fig. 4.13b), no significant difference was found on all surfaces with different roughness at any tested *Salmonella* population. This result is consistent with our previous finding that the sampling efficiency of Hydraflock swab was not affected by the surface materials. The perpendicular nylon fibers of the flocked swab served as a soft brush, which contributed to their suitability for the pathogen capture on flat surfaces as well as rough environmental surfaces. The well-designed compact perpendicular fibers caused a strong capillary action and a robust hydraulic uptake of liquid samples, which allowed for better collection of cells or other microorganisms from environmental surfaces and faster elution into liquid after capture [153].

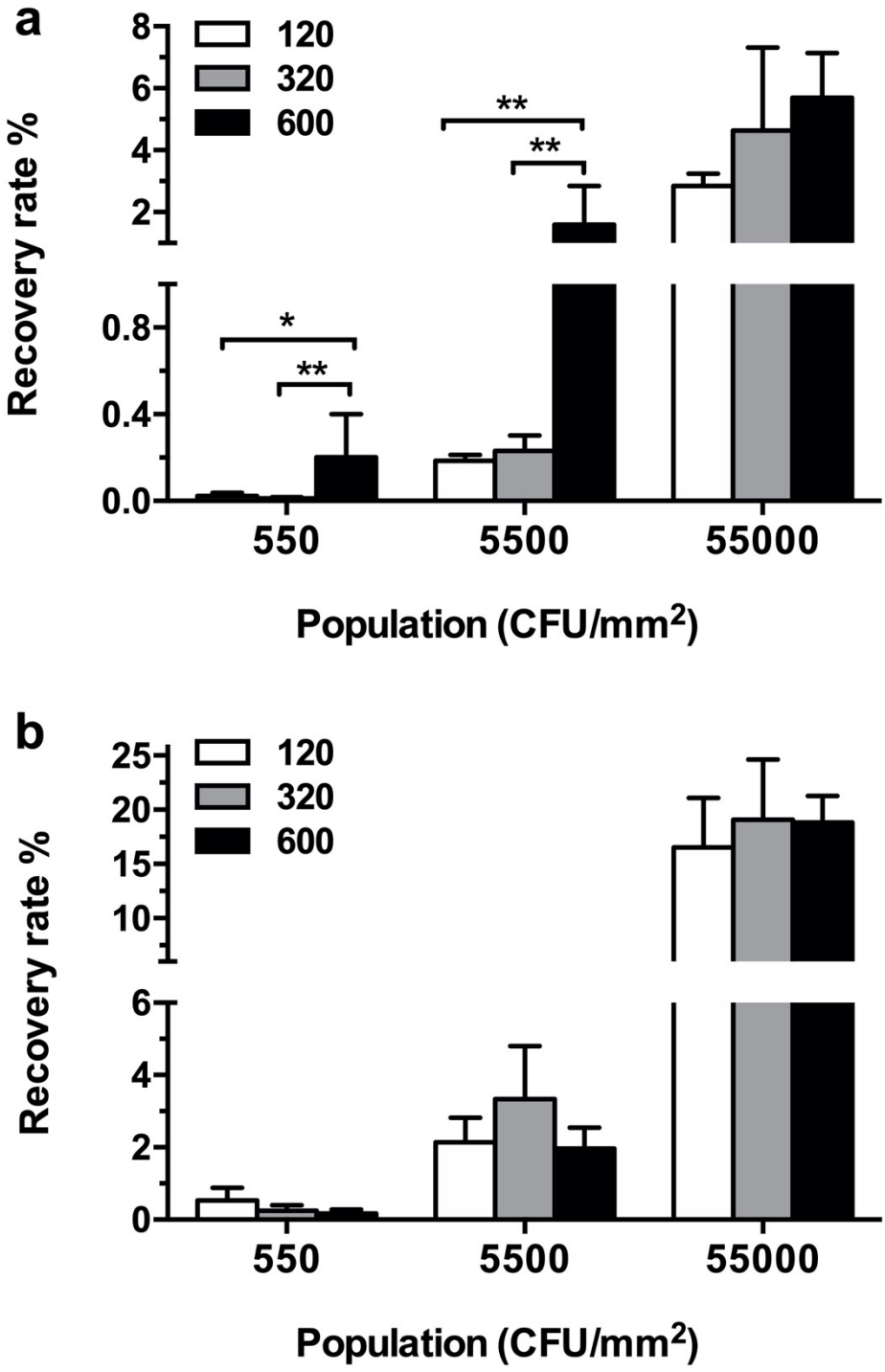

Figure 4. 13 Comparison on the recovery rates of *Salmonella* from various populations among different roughness (120PE, 320PE, 600PE) by a. Gelatin; b. Hydraflock swab (with

0.05% Tween 20). (Asterisks in the figures indicated significant differences among different roughness PE boards at the level of "*", $P<0.05$; "**", $P<0.01$.)

4.3.7 Comparison the effect of different materials on recovery rates of *Salmonella* by gelatin and Hydraflock swab.

When tested on 600PE, the only significant difference was observed between gelatin and Hydraflock swabs (with 0.05% Tween 20) at the highest population (55000 CFU/mm^2) ($P<0.01$). However, on the stainless steel, significant differences were observed between gelatin and Hydraflock swabs at all tested population ($P<0.01$). This finding indicates that the efficiency of *Salmonella* capture by Hydraflock swab assisted by surfactant was better than gelatin, especially when tested with a larger population of *Salmonella*. The difference these two methods was also affected by materials.

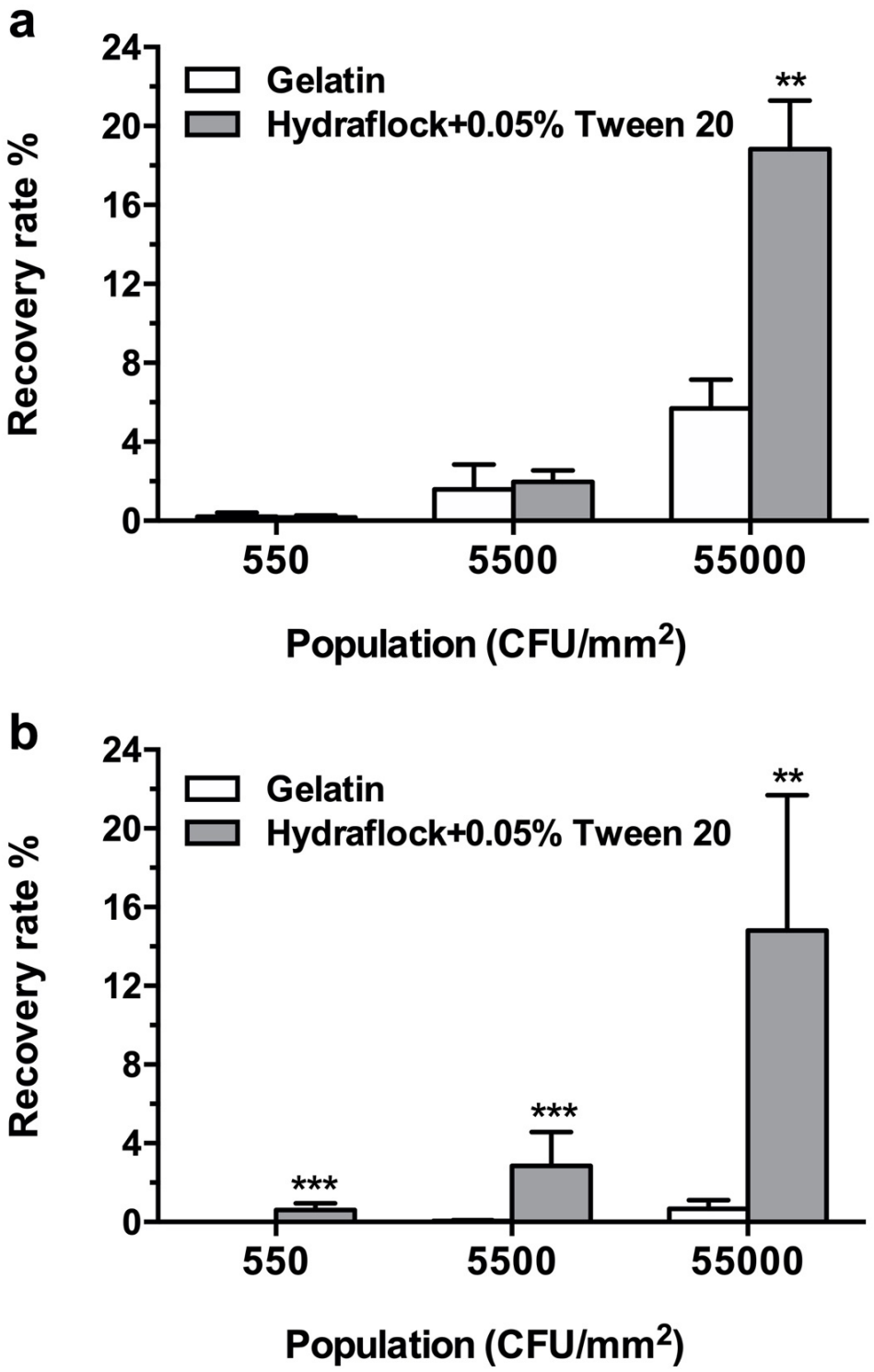

Figure 4. 14 Comparison on the recovery rates of *Salmonella* from various populations between Gelatin and HydraFlock swab (with 0.05% Tween 20) on a. 600PE; b. Stainless

steel. (Asterisks in the figures indicated significant differences between gelatin and HydraFlock swab at the level of "**", $P<0.01$; "***", $P<0.001$.)

4.4 Summary

In previous research, the surface direct detection using ME sensors met a dilemma that smaller sensor may provide higher sensitivity but also result in a smaller detection area. In this chapter, five commercially available swabs and gelatin were compared and analyzed for their large-scale sampling ability of *Salmonella* from normal food processing plates: plastic, stainless steel, and glass. First, the microstructures of different swabs were compared by SEM. Considering the recovery rates of *Salmonella* from wet and dry surfaces, the flocked structure swabs, especially the Hydraflock ones, have higher performance than the traditional ones, because of their brush-like construction, capillary effect, and faster elution. Hydraflock swabs showed constantly good performance on different materials and different surface roughness. Gelatin was found to have a similar or better recovery ability against *Salmonella* on the 600PE board than tested swabs, while it was not compatible with a glass surface detection due to tight bonding. The wetting agent Tween 20 was used to assist the experiment of swabs and found a significant improvement in the bacterial recovery. The recovery rates of Hydraflock swabs assisted by Tween 20 were better than gelatin on different surfaces. Therefore, the Hydraflock swab with the wetting agent is the most suitable sampling method to restore large scale *Salmonella* for further ME testing.

Our finding provides the possibility of using gelatin as an alternative sampling method other than the swab. Comparing with swabbing, gelatin showed three advantages: large-scale, repeatability, and no trained personnel requirement. With further modifications of physical and chemical properties, such as changing the size of its particle, increasing its viscosity, or

mixing it with additives (i.e. nutrition, surfactant, etc.), its efficiency of bacterial recovery could be improved.

Chapter 5 Conclusion

For more realistic on-site detection of *Salmonella* to protect our food safety, we need more efficient surface detection methods and the detection capability of a few colonies in high-throughput liquids. With the application of the planar spiral detection coil which offers higher magnetic flux change, a measurement system with which both a measurement sensor (E2 phage treated) and a control sensor (without E2 phage) could be directly tested on sample surfaces simultaneously was built. In order to simulate the real food processing environment, a food grade PE board was used as a cutting board for *Salmonella* surface detection. By series measurements, it was found that the resonant frequencies of ME measurement sensors change to a larger degree at higher populations of *Salmonella*.

Based on the good performance of the planar spiral coil on surface direct detection, the method by using a membrane filter to transfer *Salmonella* cells from in-liquid to membrane surface was introduced. The result confirmed that most of the *Salmonella* colonies could be concentrated to fit the ME sensor size for detection. This process maximized the possibility of the ME sensor for the detection *Salmonella* in liquid. The LOD of 54 CFU (69 CFU/mm^2) was achieved in this measurement. Because the detection limit at this circumstance is only related to the *Salmonella* population on the membrane surface, low concentration of *Salmonella* samples could be measured when given at a larger volume.

To solve the limit of small surface coverage of the ME sensor size, a large-scale sampling method is needed without changing the size of the ME sensor in the aim of preserving its sensitivity. Five kinds of swabs and gelatin sampling methods were compared on sample surfaces with different roughness and materials. Without adding wetting agents to swabs, gelatin performed similar or better efficiency than the swabs. Among all sampling methods, the efficiencies of bacterial recovery rates of Purflock, eSwab and gelatin were affected by the surface materials; constant higher efficiency was observed on PE boards than other materials. When tested with different roughness of PE boards, the gelatin performed better on smoother surfaces, while Hydraflock swabs showed no difference. After adding Tween 20 as the wetting agent, the efficiency of Hydraflock swabs was increased and showed even higher efficiency than gelatin.

The result indicates that Hydraflock swabs with a suitable wetting agent is good for general surface sampling, and the gelatin also showed its potential as an alternative sampling method. With further modifications of physical and chemical properties of gelatin, such as changing the size of its particle, increasing its viscosity, or mixing it with additives (i.e. nutrition, surfactant, etc.), its efficiency of bacterial recovery could be improved. Further study of the application of swabbing or gelatin onto food surfaces is required. The large-scale sampling methods may be a possible path to solve the detection problem caused by the curvature of foods.

Chapter 6 Future work

In chapter 2, a planar spiral coil was microfabricated and utilized for the detection of Salmonella on plastic board surface directly. There are still some issues worth optimizing. Although the planar spiral coil has improvements comparing with the cuboid coil on the signal, the distance between the sensor and the coil was still limited to about 1 mm. This poses difficulties for wireless detection on site. Future researchers may design new detection coils or test methods to increase the detection distance.

In chapter 4, a new pathogen sampling method by using peelable gel was introduced. Gelatin was selected as the representative of edible gels from agar, carrageenan, and gum arabic. According to M. Glicksman [203], edible gel can be divided into six categories with more than 60 kinds. In addition to what was mentioned above, the most commonly used gels are xanthan gum, guar gum, sodium alginate, locust bean gum and konjac gum, etc. Further research is possible on two directions: 1. To find another kind of gel which also fit the requirements of peelable gel to replace gelatin and achieve a higher recovery rate. 2. Referring to the practice of mixing additives in the food industry, future researchers may add other gels into gelatin to make it adapt better to more surfaces.

References

[1] "Food Safety Home Page | CDC," *cdc.gov*. [Online]. Available: https://www.cdc.gov/foodsafety/index.html. [Accessed: 01-Mar-2020].

[2] E. Scallan, R. M. Hoekstra, F. J. Angulo, R. V. Tauxe, M.-A. Widdowson, S. L. Roy, J. L. Jones, and P. M. Griffin, "Foodborne Illness Acquired in the United States—Major Pathogens," *Emerging Infect. Dis.*, vol. 17, no. 1, pp. 7–15, Jan. 2011.

[3] CDC, "CDC - Estimates of Foodborne Illness in the United States," *cdc.gov*, 2012. [Online]. Available: http://www.cdc.gov/foodborneburden/. [Accessed: 22-Oct-2015].

[4] S. E. Majowicz, J. Musto, E. Scallan, F. J. Angulo, M. Kirk, S. J. O'Brien, T. F. Jones, A. Fazil, R. M. Hoekstra, International Collaboration on Enteric Disease 'Burden of Illness' Studies, "The global burden of nontyphoidal Salmonella gastroenteritis.," *Clin Infect Dis.*, vol. 50, no. 6, pp. 882–889, Mar. 2010.

[5] C. Bell and A. Kyriakides, *Salmonella*. Oxford, UK: John Wiley & Sons, 2008.

[6] J. A. Crump and J. Wain, *Salmonella*, Second Edition. 2017, pp. 425–433.

[7] FDA, "Guidance for Industry: Testing for *Salmonella* Species in Human Foods and Direct-Human-Contact Animal Foods," *fda.gov*, Mar-2012. [Online]. Available:

http://www.fda.gov/regulatory-information/search-fda-guidance-documents/guidance-industry-testing-salmonella-species-human-foods-and-direct-human-contact-animal-foods. [Accessed: 01-Mar-2020].

[8] "Multistate Outbreak of Salmonella Infections Linked to Coconut Tree Brand Frozen Shredded Coconut | January 2018 | Salmonella | CDC," *cdc.gov*. [Online]. Available: https://www.cdc.gov/salmonella/coconut-01-18/index.html. [Accessed: 06-Apr-2020].

[9] "Multistate Outbreak of Salmonella Montevideo Infections Linked to Raw Sprouts | January 2018 | Salmonella | CDC," *cdc.gov*. [Online]. Available: https://www.cdc.gov/salmonella/montevideo-01-18/index.html. [Accessed: 06-Apr-2020].

[10] "Multistate Outbreak of Salmonella I 4,[5],12:b:- Infections Linked to Kratom Products | February 2018 | Salmonella | CDC," *cdc.gov*. [Online]. Available: https://www.cdc.gov/salmonella/kratom-02-18/index.html. [Accessed: 06-Apr-2020].

[11] "Multistate Outbreak of Salmonella Typhimurium Linked to Chicken Salad | February 2018 | Salmonella | CDC," *cdc.gov*. [Online]. Available: https://www.cdc.gov/salmonella/typhimurium-02-18/index.html. [Accessed: 06-Apr-2020].

[12] "Multistate Outbreak of Salmonella Typhimurium Infections Linked to Dried Coconut | March 2018 | Salmonella | CDC," *cdc.gov*. [Online]. Available: https://www.cdc.gov/salmonella/typhimurium-03-18/index.html. [Accessed: 06-Apr-2020].

[13] "Outbreak of Salmonella Infections Linked to Gravel Ridge Farms Shell Eggs - Final Update | Outbreak of Salmonella Infections Linked to Gravel Ridge Farms Shell Eggs | September 2018 | Salmonella | CDC," *cdc.gov*. [Online]. Available: https://www.cdc.gov/salmonella/enteritidis-09-18/index.html. [Accessed: 06-Apr-2020].

[14] "Multistate Outbreak of Salmonella Adelaide Infections Linked to Pre-Cut Melon (Final Update) | Multistate Outbreak of Salmonella Adelaide Infections Linked to Pre-Cut Melon | June 2018 | Salmonella | CDC," *cdc.gov*. [Online]. Available: https://www.cdc.gov/salmonella/adelaide-06-18/index.html. [Accessed: 06-Apr-2020].

[15] "Multistate Outbreak of Salmonella Mbandaka Infections Linked to Kellogg's Honey Smacks Cereal (Final Update) | Multistate Outbreak of Salmonella Mbandaka Infections Linked to Honey Smacks Cereal | June 2018 | Salmonella | CDC," *cdc.gov*. [Online]. Available: https://www.cdc.gov/salmonella/mbandaka-06-18/index.html. [Accessed: 06-Apr-2020].

[16] "Outbreak of Salmonella Infections Linked to Hy-Vee Spring Pasta Salad - Final Update | Outbreak of Salmonella Infections Linked to Hy-Vee Spring Pasta Salad | July 2018 | Salmonella | CDC," *cdc.gov*. [Online]. Available: https://www.cdc.gov/salmonella/sandiego-07-18/index.html. [Accessed: 06-Apr-2020].

[17] "Outbreak of Multidrug-Resistant Salmonella Infections Linked to Raw Turkey Products | Multidrug-Resistant Salmonella Infections Linked to Raw Turkey Products | July 2018 | Salmonella | CDC," *cdc.gov*. [Online]. Available:

https://www.cdc.gov/salmonella/reading-07-18/index.html. [Accessed: 06-Apr-2020].

[18] "Outbreak of Salmonella Infections Linked to Chicken (Final Update) | Outbreak of Salmonella Infections Linked to Chicken | August 2018 | Salmonella | CDC," *cdc.gov*. [Online]. Available: https://www.cdc.gov/salmonella/chicken-08-18/index.html. [Accessed: 06-Apr-2020].

[19] "Outbreak of Salmonella Infections Linked to Ground Beef | Outbreak of Salmonella Infections Linked to Ground Beef | October 2018 | Salmonella | CDC," *cdc.gov*. [Online]. Available: https://www.cdc.gov/salmonella/newport-10-18/index.html. [Accessed: 06-Apr-2020].

[20] "Outbreak of Multidrug-Resistant Salmonella Infections Linked to Raw Chicken Products | Multistate Outbreak of Salmonella Infections Linked to Raw Chicken Products | October 2018 | Salmonella | CDC," *cdc.gov*. [Online]. Available: https://www.cdc.gov/salmonella/infantis-10-18/index.html. [Accessed: 06-Apr-2020].

[21] "Outbreak of Salmonella Infections | Multistate Outbreak of Salmonella Agbeni Infections | November 2018 | Salmonella | CDC," *cdc.gov*. [Online]. Available: https://www.cdc.gov/salmonella/agbeni-11-18/index.html. [Accessed: 06-Apr-2020].

[22] "Outbreak of Salmonella Infections Linked to Tahini from Achdut Ltd. | Outbreak of Salmonella Infections Linked to Tahini from Achdut Ltd. | November 2018 | Salmonella | CDC," *cdc.gov*. [Online]. Available: https://www.cdc.gov/salmonella/concord-11-18/index.html. [Accessed: 06-Apr-

2020].

[23] "Outbreak of Salmonella Infections Linked to Butterball Brand Ground Turkey | Outbreak of Salmonella Infections Linked to Butterball Ground Turkey | March 2019 | Salmonella | CDC," *cdc.gov*. [Online]. Available: https://www.cdc.gov/salmonella/schwarzengrund-03-19/index.html. [Accessed: 06-Apr-2020].

[24] "Outbreak of Salmonella Infections Linked to Pre-Cut Melons | Outbreak of Salmonella Infections Linked to Pre-Cut Melon | April 2019 | Salmonella | CDC," *cdc.gov*. [Online]. Available: https://www.cdc.gov/salmonella/carrau-04-19/index.html. [Accessed: 06-Apr-2020].

[25] "Outbreak of Salmonella Infections Linked to Frozen Raw Tuna | Outbreak of Salmonella Infections Linked to Frozen Raw Tuna| April 2019 | Salmonella | CDC," *cdc.gov*. [Online]. Available: https://www.cdc.gov/salmonella/newport-04-19/index.html. [Accessed: 06-Apr-2020].

[26] "Outbreak of Salmonella Infections Linked to Cavi Brand Whole, Fresh Papayas | Outbreak of Salmonella Infections Linked to Whole, Fresh Papayas Imported from Mexico | June 2019 | Salmonella | CDC," *cdc.gov*. [Online]. Available: https://www.cdc.gov/salmonella/uganda-06-19/index.html. [Accessed: 06-Apr-2020].

[27] "Outbreak of Salmonella Infections Linked to Ground Beef | Outbreak of Salmonella Infections Linked to Ground Beef | November 2019 | Salmonella | CDC," *cdc.gov*. [Online]. Available: https://www.cdc.gov/salmonella/dublin-11-19/index.html. [Accessed: 06-Apr-2020].

[28] "Outbreak of Salmonella Infections Linked to Cut Fruit | Outbreak of Salmonella Infections Linked to Cut Fruit | December 2019 | Salmonella | CDC," *cdc.gov*. [Online]. Available: https://www.cdc.gov/salmonella/javiana-12-19/index.html. [Accessed: 06-Apr-2020].

[29] C. Fançony, Y. V. Sebastião, J. E. Pires, D. Gamboa, and S. V. Nery, "Performance of microscopy and RDTs in the context of a malaria prevalence survey in Angola: a comparison using PCR as the gold standard," *Malaria Journal 2013 12:1*, vol. 12, no. 1, p. 284, Aug. 2013.

[30] T. W. Alexander, T. Reuter, E. Okine, R. Sharma, and T. A. McAllister, "Conventional and real-time polymerase chain reaction assessment of the fate of transgenic DNA in sheep fed Roundup Ready rapeseed meal," *British Journal of Nutrition*, vol. 96, no. 6, pp. 997–1005, Dec. 2006.

[31] T. B. White, A. M. McCoy, V. A. Streva, J. Fenrich, and P. L. Deininger, "A droplet digital PCR detection method for rare L1 insertions in tumors," *Mobile DNA 2014 5:1*, vol. 5, no. 1, p. 30, Dec. 2014.

[32] D. Dean, R. S. Turingan, H.-U. Thomann, A. Zolotova, J. Rothschild, S. J. Joseph, T. D. Read, E. Tan, and R. F. Selden, "A Multiplexed Microfluidic PCR Assay for Sensitive and Specific Point-of-Care Detection of Chlamydia trachomatis," *PLOS ONE*, vol. 7, no. 12, p. e51685, Dec. 2012.

[33] S. Horikawa, "Low-Cost, Rapid, Sensitive Detection of Pathogenic Bacteria Using Phage-Based Magnetoelastic Biosensors," pp. 1–166, Apr. 2013.

[34] J. M. Eijkelkamp, H. J. M. Aarts, and H. J. van der Fels-Klerx, "Suitability of Rapid Detection Methods for Salmonella in Poultry Slaughterhouses," *Food Anal.*

Methods, vol. 2, no. 1, pp. 1–13, Jul. 2008.

[35] R. M. Lequin, *Enzyme immunoassay (EIA)/enzyme-linked immunosorbent assay (ELISA)*. Clinical chemistry, 2005.

[36] R. Kumar, P. K. Surendran, and N. Thampuran, "Evaluation of culture, ELISA and PCR assays for the detection of *Salmonella* in seafood," *Letters in Applied Microbiology*, vol. 46, no. 2, pp. 221–226, Jan. 2008.

[37] S. Perelle, F. Dilasser, B. Malorny, J. Grout, J. Hoorfar, and P. Fach, "Comparison of PCR-ELISA and LightCycler real-time PCR assays for detecting *Salmonella* spp. in milk and meat samples," *Molecular and Cellular Probes*, vol. 18, no. 6, pp. 409–420, Dec. 2004.

[38] P. Damborský, J. Švitel, and J. Katrlík, "Optical biosensors," *Essays in Biochemistry*, vol. 60, no. 1, pp. 91–100, Jun. 2016.

[39] X. Liu, Y. Hu, S. Zheng, Y. Liu, Z. He, and F. Luo, "Surface plasmon resonance immunosensor for fast, highly sensitive, and in situ detection of the magnetic nanoparticles-enriched Salmonella enteritidis," *Sensors and Actuators B: Chemical*, vol. 230, pp. 191–198, Jul. 2016.

[40] M. Janczuk, J. Niedziolka-Joensson, and K. Szot-Karpinska, "Bacteriophages in electrochemistry: A review," *J. Electroanal. Chem.*, vol. 779, pp. 207–219, Oct. 2016.

[41] G. Zhang, "Foodborne Pathogenic Bacteria Detection: An Evaluation of Current and Developing Methods," *The Meducator*, vol. 1, no. 24, Dec. 2013.

[42] J. Pollet, F. Delport, K. P. F. Janssen, K. Jans, G. Maes, H. Pfeiffer, M. Wevers, and J. Lammertyn, "Fiber optic SPR biosensing of DNA hybridization and DNA–protein

interactions," *Biosensors and Bioelectronic*, vol. 25, no. 4, pp. 864–869, Dec. 2009.

[43] T. T. Goodrich, H. J. Lee, and R. M. Corn, "Direct Detection of Genomic DNA by Enzymatically Amplified SPR Imaging Measurements of RNA Microarrays," *J. Am. Chem. Soc.*, vol. 126, no. 13, pp. 4086–4087, Apr. 2004.

[44] S. D. Mazumdar, M. Hartmann, P. Kämpfer, and M. Keusgen, "Rapid method for detection of Salmonella in milk by surface plasmon resonance (SPR)," *Biosensors and Bioelectronic*, vol. 22, no. 9, pp. 2040–2046, Apr. 2007.

[45] E. Helmerhorst, D. J. Chandler, M. Nussio, and C. D. Mamotte, "Real-time and Label-free Bio-sensing of Molecular Interactions by Surface Plasmon Resonance: A Laboratory Medicine Perspective," *The Clinical Biochemist Reviews*, vol. 33, no. 4, p. 161, Nov. 2012.

[46] C. Song, S. Zhang, and H. Huang, "Choosing a suitable method for the identification of replication origins in microbial genomes," *Front. Microbiol.*, vol. 6, no. 5279, p. 17816, 2015.

[47] N. Wang, Y. Liu, Y. Fu, and F. Yan, "AC Measurements Using Organic Electrochemical Transistors for Accurate Sensing.," *ACS Appl. Mater. Interfaces*, p. acsami.7b07668, Aug. 2017.

[48] L. Zhou, M. A. Arugula, B. A. Chin, and A. L. Simonian, "Simultaneous Surface Plasmon Resonance/Fluorescence Spectroelectrochemical in Situ Monitoring of Dynamic Changes on Functional Interfaces: A Study of the Electrochemical Proximity Assay Model System," *ACS Appl. Mater. Interfaces*, vol. 10, no. 48, pp. 41763–41772, Oct. 2018.

[49] N. F. D. Silva, J. M. C. S. Magalhães, C. Freire, and C. Delerue-Matos,

"Electrochemical biosensors for Salmonella: State of the art and challenges in food safety assessment," *Biosensors and Bioelectronic*, vol. 99, pp. 667–682, Jan. 2018.

[50] B. Ilic, H. G. Craighead, S. Krylov, W. Senaratne, C. Ober, and P. Neuzil, "Attogram detection using nanoelectromechanical oscillators," *J. Appl. Phys.*, vol. 95, no. 7, pp. 3694–3703, Mar. 2004.

[51] J. W. Yi, W. Y. Shih, and W.-H. Shih, "Effect of length, width, and mode on the mass detection sensitivity of piezoelectric unimorph cantilevers," *J. Appl. Phys.*, vol. 91, no. 3, pp. 1680–1686, Jan. 2002.

[52] C. A. Grimes, P. G. Stoyanov, D. Kouzoudis, and K. G. Ong, "Remote query pressure measurement using magnetoelastic sensors," *Rev. Sci. Instrum.*, vol. 70, no. 12, p. 4711, 1999.

[53] K. Zhang, L. Zhang, L. Fu, S. Li, H. Chen, and Z. Y. Cheng, "Magnetostrictive resonators as sensors and actuators," *Sensors and Actuators A: Physical*, vol. 200, pp. 2–10, Oct. 2013.

[54] K. Zhang, L. Zhang, and Y. Chai, "Mass Load Distribution Dependence of Mass Sensitivity of Magnetoelastic Sensors under Different Resonance Modes," *Sensors*, vol. 15, no. 8, pp. 20267–20278, Aug. 2015.

[55] K. Zhang and Y. Chai, "Numerical Study on Mass Sensitivity of Magnetoelastic Biosensors with Concentrated Mass Load under Different Resonance Modes," *Journal of Sensors*, vol. 2016, pp. 1–5, 2016.

[56] P. Cheng, S. Gao, W. Zhang, T. Wang, A. Jian, and S. Sang, "Resonance modes of freestanding magnetoelastic resonator and the application in viscosity measurement," *Smart Mater. Struct.*, vol. 24, no. 4, p. 045029, Apr. 2015.

[57] S. Horikawa, D. Bedi, S. Li, W. Shen, S. Huang, I.-H. Chen, Y. Chai, M. L. Auad, M. J. Bozack, J. M. Barbaree, V. A. Petrenko, and B. A. Chin, "Effects of surface functionalization on the surface phage coverage and the subsequent performance of phage-immobilized magnetoelastic biosensors," *Biosensors and Bioelectronics*, vol. 26, no. 5, pp. 2361–2367, Jan. 2011.

[58] S. R. Green, R. S. Kwon, G. H. Elta, and Y. B. Gianchandani, "In vivo and in situ evaluation of a wireless magnetoelastic sensor array for plastic biliary stent monitoring," *Biomedical Microdevices*, vol. 15, no. 3, pp. 509–517, Jun. 2013.

[59] J. Tang, S. R. Green, and Y. B. Gianchandani, "Scalable, high-performance magnetoelastic tags using frame-suspended hexagonal resonators," *JOURNAL OF MICROMECHANICS AND MICROENGINEERING*, vol. 24, no. 6, p. 065006, Jun. 2014.

[60] N. Pacella, A. DeRouin, B. Pereles, and K. G. Ong, "Geometrical modification of magnetoelastic sensors to enhance sensitivity," *Smart Mater. Struct.*, vol. 24, no. 2, p. 025018, Feb. 2015.

[61] P. G Saiz, D. Gandia, A. Lasheras, A. Sagasti, I. Quintana, M. L. Fdez-Gubieda, J. Gutierrez, M. I. Arriortua, and A. C. Lopes, "Enhanced mass sensitivity in novel magnetoelastic resonators geometries for advanced detection systems," *Sensors and Actuators B: Chemical*, vol. 296, p. 126612, Oct. 2019.

[62] A. Kittmann, P. Durdaut, S. Zabel, J. Reermann, J. Schmalz, B. Spetzler, D. Meyners, N. X. Sun, J. McCord, M. Gerken, G. Schmidt, M. Hoeft, R. Knoechel, F. Faupel, and E. Quandt, "Wide Band Low Noise Love Wave Magnetic Field Sensor System," *SCIENTIFIC REPORTS*, vol. 8, no. 1, p. 278, Jan. 2018.

[63] K. Krueger, K. Seemann, H. Leiste, M. Stueber, and S. Ulrich, “High-frequency magnetoelastic measurements on Fe-Co-Hf-N/Ti-N multilayer coatings,” *JOURNAL OF MAGNETISM AND MAGNETIC MATERIALS*, vol. 343, pp. 42–48, Oct. 2013.

[64] S. Atalay, V. S. Kolat, N. Bayri, and T. Izgi, “Magnetoelastic Sensor Studies on Amorphous Magnetic FeSiB Wire and the Application in Viscosity Measurement,” *JOURNAL OF SUPERCONDUCTIVITY AND NOVEL MAGNETISM*, vol. 29, no. 6, pp. 1551–1556, Jun. 2016.

[65] A. M. Aragon, M. Hernando Rydings, A. Hernando, and P. Marin, “Liquid pressure wireless sensor based on magnetostrictive microwires for applications in cardiovascular localized diagnostic,” *AIP ADVANCES*, vol. 5, no. 8, p. 087132, Aug. 2015.

[66] C. Herrero-Gomez, P. Marin, and A. Hernando, “Bias free magnetomechanical coupling on magnetic microwires for sensing applications,” *Appl. Phys. Lett.*, vol. 103, no. 14, p. 142414, Sep. 2013.

[67] C. Hlenschi, S. Corodeanu, and H. Chiriac, “Magnetoelastic Sensors for the Detections of Pulse Waves,” *Magnetics, IEEE Transactions on*, vol. 49, no. 1, pp. 117–119, Jan. 2013.

[68] H. Chiriac, C. Hlenschi, S. Corodeanu, M. Grecu, T.-A. Ovari, and N. Lupu, “Pulse Wave Detection Magnetoelastic Sensing Device Based on Nanocrystalline Microwires for the Indirect Diagnosis of Paroxysmal Rhythm Disorders,” *Magnetics, IEEE Transactions on*, vol. 52, no. 7, Jul. 2016.

[69] W. Shen, S. Li, M.-K. Park, Z. Zhang, Z. Cheng, V. A. Petrenko, and B. A. Chin, “Blocking Agent Optimization for Nonspecific Binding on Phage Based

Magnetoelastic Biosensors," *J. Electrochem. Soc.*, vol. 159, no. 10, pp. B818–B823, Jan. 2012.

[70] Y. Chai, S. Horikawa, S. Li, H. C. Wikle, and B. A. Chin, "A surface-scanning coil detector for real-time, in-situ detection of bacteria on fresh food surfaces," *Biosensors and Bioelectronic*, vol. 50, no. C, pp. 311–317, Dec. 2013.

[71] N. Du, L. Liao, Y. Xiao, X. Xiao, Z. Zhao, and Y. Lin, "Determination of radon using solid state nuclear tracks wireless sensing method," *ANALYTICA CHIMICA ACTA*, vol. 686, no. 1, pp. 121–125, Feb. 2011.

[72] T. Baimpos, V. Nikolakis, and D. Kouzoudis, "A new method for measuring the adsorption induced stresses of zeolite films using magnetoelastic sensors," *JOURNAL OF MEMBRANE SCIENCE*, vol. 390, pp. 130–140, Feb. 2012.

[73] J. Kiser, R. Lacomb, K. Bussmann, C. J. Hawley, J. E. Spanier, X. Zhuang, C. Dolabdjian, S. Lofland, and P. Finkel, "Magnetostrictive stress reconfigurable thin film resonators for near direct current magnetoelectric sensors," *Appl. Phys. Lett.*, vol. 104, no. 7, p. 072408, Feb. 2014.

[74] C. Liang, C. Gooneratne, D. Cha, L. Chen, Y. Gianchandani, and J. Kosel, "Development of FeNiMoB thin film materials for microfabricated magnetoelastic sensors," *J. Appl. Phys.*, vol. 112, no. 11, p. 113912, Dec. 2012.

[75] M. Staruch, C. Kassner, S. Fackler, I. Takeuchi, K. Bussmann, S. E. Lofland Jr, C. Dolabdjian, R. Lacomb, and P. Finkel, "Effects of magnetic field and pressure in magnetoelastic stress reconfigurable thin film resonators," *Appl. Phys. Lett.*, vol. 107, no. 3, p. 032909, Jul. 2015.

[76] J. Kiser, P. Finkel, J. Gao, C. Dolabdjian, J. Li, and D. Viehland, "Stress

reconfigurable tunable magnetoelectric resonators as magnetic sensors," *Appl. Phys. Lett.*, vol. 102, no. 4, p. 042909, Jan. 2013.

[77] A. Lasheras, J. Gutierrez, A. Balza, J. M. Barandiaran, and A. Rodriguez Pierna, "Radiofrequency magnetoelastic resonators for magnetoelectric applications," *J. Phys. D: Appl. Phys.*, vol. 47, no. 31, Aug. 2014.

[78] J. Gutierrez, A. Lasheras, P. Martins, N. Pereira, J. M. Barandiaran, and S. Lanceros-Mendez, "Metallic Glass/PVDF Magnetoelectric Laminates for Resonant Sensors and Actuators: A Review," *Sensors*, vol. 17, no. 6, p. 1251, Jun. 2017.

[79] S. Sang, P. Cheng, W. Zhang, P. Li, J. Hu, G. Li, and A. Jian, "Investigation on a new Fe83Ga17 wire-based magnetoelastic resonance biosensor," *J INTEL MAT SYST STR*, vol. 26, no. 8, pp. 980–987, May 2015.

[80] B. Adolphi, J. McCord, M. Bertram, C.-G. Oertel, U. Merkel, U. Marschner, R. Schaefer, C. Wenzel, and W.-J. Fischer, "Improvement of sputtered Galfenol thin films for sensor applications," *Smart Mater. Struct.*, vol. 19, no. 5, p. 055013, May 2010.

[81] S.-M. Na, M. Rice, G. Raghunath, V. Klimchenko, and A. B. Flatau, "Magnetostrictive Alfenol Whisker Sensor Performance and Sensitivity to Whisker Thickness," *Magnetics, IEEE Transactions on*, vol. 50, no. 11, Nov. 2014.

[82] V. L. Othero de Brito, S. A. Cunha, L. V. Lemos, and C. B. Nunes, "Magnetic Properties of Liquid-Phase Sintered CoFe2O4 for Application in Magnetoelastic and Magnetoelectric Transducers," *Sensors*, vol. 12, no. 8, pp. 10086–10096, Aug. 2012.

[83] P. N. Anantharamaiah and P. A. Joy, "Enhancing the strain sensitivity of CoFe2O4 at low magnetic fields without affecting the magnetostriction coefficient by

substitution of small amounts of Mg for Fe," *Phys. Chem. Chem. Phys.*, vol. 18, no. 15, pp. 10516–10527, Apr. 2016.

[84] K. Khaja Mohaideen and P. A. Joy, "High magnetostriction parameters for low-temperature sintered cobalt ferrite obtained by two-stage sintering," *JOURNAL OF MAGNETISM AND MAGNETIC MATERIALS*, vol. 371, pp. 121–129, Dec. 2014.

[85] V. R. Monaji and D. Das, "Influence of Zr doping on the structural, magnetic and magnetoelastic properties of cobalt-ferrites," *Journal of Alloys and Compounds*, vol. 634, pp. 99–103, Jun. 2015.

[86] P. Klein, K. Richter, R. Varga, and M. Vazquez, "Frequency and temperature dependencies of the switching field in glass-coated FeSiBCr microwire," *Journal of Alloys and Compounds*, vol. 569, pp. 9–12, Aug. 2013.

[87] R. Sabol, R. Varga, J. Hudak, J. Blazek, D. Praslicka, P. Vojtanik, G. Badini, and M. Vazquez, "Stress dependence of the switching field in glass-coated microwires with positive magnetostriction," *JOURNAL OF MAGNETISM AND MAGNETIC MATERIALS*, vol. 325, pp. 141–143, Jan. 2013.

[88] T. Baimpos, L. Gora, V. Nikolakis, and D. Kouzoudis, "Selective detection of hazardous VOCs using zeolite/Metglas composite sensors," *Sensors and Actuators A: Physical*, vol. 186, no. SI, pp. 21–31, Oct. 2012.

[89] V. Tsukala and D. Kouzoudis, "Zeolite micromembrane fabrication on magnetoelastic material using electron beam lithography," *MICROPOROUS AND MESOPOROUS MATERIALS*, vol. 197, pp. 213–220, Oct. 2014.

[90] C. D. Tormes, M. Beltrami, R. C. D. Cruz, and F. P. Missell, "Characterization of drying behavior of granular materials using magnetoelastic sensors," *NDT&E*

INTERNATIONAL, vol. 66, pp. 67–71, Sep. 2014.

[91] K. Zhang, L. Fu, L. Zhang, Z. Y. Cheng, and T.-S. Huang, "Magnetostrictive particle based biosensors for in situ and real-time detection of pathogens in water," *Biotechnology and Bioengineering*, vol. 111, no. 11, pp. 2229–2238, Nov. 2014.

[92] X. Guo, S. Gao, S. Sang, A. Jian, Q. Duan, J. Ji, and W. Zhang, "Detection system based on magnetoelastic sensor for classical swine fever virus," *Biosensors and Bioelectronic*, vol. 82, pp. 127–131, Aug. 2016.

[93] X. Guo, S. Sang, J. Guo, A. Jian, Q. Duan, J. Ji, Q. Zhang, and W. Zhang, "A magnetoelastic biosensor based on E2 glycoprotein for wireless detection of classical swine fever virus E2 antibody," *SCIENTIFIC REPORTS*, vol. 7, no. 1, p. 15626, Nov. 2017.

[94] C. Menti, M. Beltrami, M. D. Pozza, S. T. Martins, J. A. P. Henriques, A. D. Santos, F. P. Missell, and M. Roesch-Ely, "Influence of antibody immobilization strategies on the analytical performance of a magneto-elastic immunosensor for Staphylococcus aureus detection," *MATERIALS SCIENCE and ENGINEERING C-MATERIALS FOR BIOLOGICAL APPLICATIONS*, vol. 76, pp. 1232–1239, Jun. 2017.

[95] M. R. T. Rahman, Z. Lou, H. Wang, and L. Ai, "Aptamer Immobilized Magnetoelastic Sensor for the Determination of *Staphylococcus Aureus*," *ANALYTICAL LETTERS*, vol. 48, no. 15, pp. 2414–2422, Oct. 2015.

[96] L. V. R. Beltrami, M. Beltrami, M. Roesch-Ely, S. R. Kunst, F. P. Missell, E. J. Birriel, and C. de F. Malfatti, "Magnetoelastic sensors with hybrid films for bacteria detection in milk," *J. Food Eng.*, vol. 212, pp. 18–28, Nov. 2017.

[97] V. A. Petrenko and V. J. Vodyanoy, “Phage display for detection of biological threat agents,” *Journal of Microbiological Methods*, vol. 53, no. 2, pp. 253–262, May 2003.

[98] I. B. Sorokulova, E. V. Olsen, I.-H. Chen, B. Fiebor, J. M. Barbaree, V. J. Vodyanoy, B. A. Chin, and V. A. Petrenko, “Landscape phage probes for *Salmonella* typhimurium,” *Journal of Microbiological Methods*, vol. 63, no. 1, pp. 55–72, Oct. 2005.

[99] I.-H. Chen, S. Horikawa, S. Du, Y. Liu, H. C. Wikle, J. M. Barbaree, and B. A. Chin, “Thermal Stability of Phage Peptide Probes Vs. Aptamer for Salmonella Detection on Magnetoelastic Biosensors Platform,” *ECS Trans.*, vol. 75, no. 16, pp. 165–173, Aug. 2016.

[100] Y. Chai, S. Li, S. Horikawa, M.-K. Park, V. Vodyanoy, and B. A. Chin, “Rapid and Sensitive Detection of Salmonella Typhimurium on Eggshells by Using Wireless Biosensors,” *j food prot*, vol. 75, no. 4, pp. 631–636, Apr. 2012.

[101] F. Wang, S. Horikawa, J. Hu, H. C. Wikle, I.-H. Chen, S. Du, Y. Liu, and B. A. Chin, “Detection of *Salmonella* Typhimurium on Spinach Using Phage-Based Magnetoelastic Biosensors.,” *Sensors*, vol. 17, no. 2, p. 386, Feb. 2017.

[102] I.-H. Chen, S. Horikawa, K. Bryant, R. Riggs, B. A. Chin, and J. M. Barbaree, “Bacterial assessment of phage magnetoelastic sensors for *Salmonella* enterica Typhimurium detection in chicken meat,” *Food Control*, vol. 71, pp. 273–278, Jan. 2017.

[103] V. A. Petrenko, “Landscape phage as a molecular recognition interface for detection devices,” *Microelectronics Journal*, vol. 39, no. 2, pp. 202–207, Feb. 2008.

[104] H. Chiriac, E. Hristoforou, M. Neagu, and F. Borza, “Force measurements using Fe-rich amorphous wire as magnetostrictive delay line,” *Sensors and Actuators A: Physical*, vol. 91, no. 1, pp. 223–225, Jun. 2001.

[105] C. Gomez-Polo, K. R. Pirota, and M. Knobel, “Stress dependence of second harmonic amplitude of giant magnetoimpedance in CoFeSiB amorphous samples,” *JOURNAL OF MAGNETISM AND MAGNETIC MATERIALS*, vol. 242, no. 1, pp. 294–296, Apr. 2002.

[106] E. S. Bastos, A. Dalponte, F. P. Missell, G. O. Fulop, M. B. de Souza Dias, and C. Bormio-Nunes, “Linear Wireless Strain Sensor Using FeAlB and Amorphous Alloys,” *Magnetics, IEEE Transactions on*, vol. 53, no. 11, pp. 1–4, 2017.

[107] B. D. Pereles, A. J. DeRouin, T. A. Dienhart, E. L. Tan, and K. G. Ong, “A Wireless, Magnetoelastic-Based Sensor Array for Force Monitoring on a Hard Surface,” *SENSOR LETTERS*, vol. 10, no. 3, pp. 806–813, Apr. 2012.

[108] J. Ferenc, M. Kowalczyk, G. Cieslak, and T. Kulik, “Magnetostrictive Iron-Based Bulk Metallic Glasses for Force Sensors,” *Magnetics, IEEE Transactions on*, vol. 50, no. 4, Apr. 2014.

[109] D. M. Stefanescu and M. A. Anghel, “Electrical methods for force measurement - A brief survey,” *MEASUREMENT*, vol. 46, no. 2, pp. 949–959, Feb. 2013.

[110] A. DeRouin, N. Pacella, C. Zhao, K.-N. An, and K. G. Ong, “A Wireless Sensor for Real-Time Monitoring of Tensile Force on Sutured Wound Sites,” *IEEE TRANSACTIONS ON BIOMEDICAL ENGINEERING*, vol. 63, no. 8, pp. 1665–1671, Aug. 2016.

[111] B. D. Pereles, A. J. DeRouin, and K. G. Ong, “A Wireless, Passive Magnetoelastic

Force-Mapping System for Biomedical Applications," *JOURNAL OF BIOMECHANICAL ENGINEERING-TRANSACTIONS OF THE ASME*, vol. 136, no. 1, p. 011010, Jan. 2014.

[112] T. Huber, B. Bergmair, C. Vogler, F. Bruckner, G. Hrkac, and D. Suess, "Magnetoelastic resonance sensor for remote strain measurements," *Appl. Phys. Lett.*, vol. 101, no. 4, p. 042402, Jul. 2012.

[113] Y. Tan, J. Hu, L. Ren, J. Zhu, J. Yang, and D. Liu, "A Passive and Wireless Sensor for Bone Plate Strain Monitoring," *Sensors*, vol. 17, no. 11, p. 2635, Nov. 2017.

[114] D. Jackiewicz, R. Szewczyk, and A. Bienkowski, "UTILIZING MAGNETOELASTIC EFFECT TO MONITOR THE STRESS IN THE STEEL TRUSS STRUCTURES," *Journal of Electrical Engineering-Elektrotechnicky Casopis*, vol. 66, no. 7, pp. 178–181, Dec. 2015.

[115] Y.-Q. Huang, J.-C. Yin, Y.-S. Wang, X.-L. Xiao, B. Zhou, J.-H. Xue, X. Tang, X.-F. Wang, Y.-F. Zhu, and S.-H. Chen, "Streptavidin and gold nanoparticles-based dual signal amplification for sensitive magnetoelastic sensing of mercury using a specific aptamer probe," *Sensors and Actuators B: Chemical*, vol. 235, pp. 507–514, Nov. 2016.

[116] J.-C. Yin, Y.-S. Wang, B. Zhou, X.-L. Xiao, J.-H. Xue, J.-C. Wang, Y.-S. Wang, and Q.-M. Qian, "A wireless magnetoelastic sensor for uranyl using DNAzyme-graphene oxide and gold nanoparticles-based amplification," *Sensors and Actuators B: Chemical*, vol. 188, pp. 147–155, Nov. 2013.

[117] L. Chen, J. Li, T. Tran ThanhThuy, L. Zhou, C. Huang, L. Yuan, and Q. Cai, "A wireless and sensitive detection of octachlorostyrene using modified AuNPs as

signal-amplifying tags," *Biosensors and Bioelectronic*, vol. 52, pp. 427–432, Feb. 2014.

[118] "A bovine serum albumin-coated magnetoelastic biosensor for the wireless detection of heavy metal ions," *Sensors and Actuators B: Chemical*, Oct. 2017.

[119] S. Sang, S. Gao, X. Guo, P. Cheng, and W. Zhang, "The detection of Pb2+ in solution using bare magnetoelastic resonator," *Appl. Phys. Lett.*, vol. 108, no. 5, p. 054102, Feb. 2016.

[120] R. Guntupalli, R. S. Lakshmanan, M. L. Johnson, J. Hu, T.-S. Huang, J. M. Barbaree, V. J. Vodyanoy, and B. A. Chin, "Magnetoelastic biosensor for the detection of Salmonella typhimurium in food products," *Sens. & Instrumen. Food Qual.*, vol. 1, no. 1, pp. 3–10, Feb. 2007.

[121] S. Butterworth and F. D. Smith, "The equivalent circuit of the magnetostriction oscillator," *Proc. Phys. Soc.*, vol. 43, no. 2, pp. 166–185, Mar. 1931.

[122] H. Xie, Y. Chai, S. Horikawa, S. Li, B. A. Chin, and H. C. Wikle III, "A pulsed wave excitation system to characterize micron-scale magnetoelastic biosensors," *Sensors and Actuators A: Physical*, vol. 205, pp. 143–149, Jan. 2014.

[123] N. V. Lavrik, M. J. Sepaniak, and P. G. Datskos, "Cantilever transducers as a platform for chemical and biological sensors," *Rev. Sci. Instrum.*, vol. 75, no. 7, pp. 2229–2253, Jun. 2004.

[124] C. Ziegler, "Cantilever-based biosensors," *Anal Bioanal Chem*, vol. 379, no. 7, pp. 946–959, Aug. 2004.

[125] P. Chen, Q. Jiang, S. Horikawa, and S. Li, "Magnetoelastic-Sensor Integrated Microfluidic Chip for the Measurement of Blood Plasma Viscosity," *J. Electrochem.*

Soc., vol. 164, no. 6, pp. B247–B252, 2017.

[126] B. Bergmair, T. Huber, F. Bruckner, C. Vogler, and D. Suess, "Removal of earth's magnetic field effect on magnetoelastic resonance sensors by an antisymmetric bias field," *Sensors and Actuators A: Physical*, vol. 183, pp. 11–15, Aug. 2012.

[127] W. Shen, L. C. Mathison, V. A. Petrenko, and B. A. Chin, "Design and characterization of a magnetoelastic sensor for the detection of biological agents," *J. Phys. D: Appl. Phys.*, vol. 43, no. 1, p. 015004, Jan. 2010.

[128] Y. Chai, S. Horikawa, H. C. Wikle, Z. Wang, and B. A. Chin, "Surface-scanning coil detectors for magnetoelastic biosensors: A comparison of planar-spiral and solenoid coils," *Appl. Phys. Lett.*, vol. 103, no. 17, p. 173510, Oct. 2013.

[129] S. Horikawa, S. Du, Y. Liu, X. Lu, I.-H. Chen, H. C. Wikle, P. Chen, M. Beidaghi, S.-J. Suh, Y. Feng, Z. Cheng, and B. A. Chin, "Effects of Surface-Scanning Detector Position on the Response of a Wireless Magnetoelastic Biosensor," *ECS Trans.*, vol. 80, no. 10, pp. 1579–1583, Oct. 2017.

[130] "World bioproducts." [Online]. Available: https://www.worldbioproducts.com/. [Accessed: 25-Mar-2020].

[131] "BIO-TAPE SLIDES, 50/BX." [Online]. Available: https://www.zefon.com/bio-tape-slides-50bx. [Accessed: 25-Mar-2020].

[132] "Storage, Use and Shipping of Surface Contact (RODAC) Testing Plates | TechTip | STERIS AST." [Online]. Available: https://www.steris-ast.com/techtip/storage-use-and-shipping-of-surface-contact-rodac-testing-plates/. [Accessed: 25-Mar-2020].

[133] R. Ismaïl, F. Aviat, V. Michel, I. Le Bayon, P. Gay-Perret, M. Kutnik, and M. Fédérighi, "Methods for Recovering Microorganisms from Solid Surfaces Used in

the Food Industry: A Review of the Literature," *International Journal of Environmental Research and Public Health 2014, Vol. 11, Pages 804-814*, vol. 10, no. 11, pp. 6169–6183, Nov. 2013.

[134] S. K. Tamminga and E. H. Kampelmacher, "Comparison of agar sausage, alginate swab and adhesive tape methods for sampling flat surfaces contaminated with bacteria," *Zentralbl Bakteriol Orig B*, Jan. 1978.

[135] A. NISKANEN and M. S. POHJA, "Comparative Studies on the Sampling and Investigation of Microbial Contamination of Surfaces by the Contact Plate and Swab Methods," *Journal of Applied Microbiology*, vol. 42, no. 1, pp. 53–63, Feb. 1977.

[136] R. E. A. WILLIAMS, A. G. GIBSON, T. C. AITCHISON, R. LEVER, and R. M. MACKIE, "Assessment of a contact-plate sampling technique and subsequent quantitative bacterial studies in atopic dermatitis," *British Journal of Dermatology*, vol. 123, no. 4, pp. 493–501, Oct. 1990.

[137] M. RÖNNQVIST, M. RÄTTÖ, P. TUOMINEN, S. SALO, and L. MAUNULA, "Swabs as a Tool for Monitoring the Presence of Norovirus on Environmental Surfaces in the Food Industry," *Journal of Food Protection*, vol. 76, no. 8, pp. 1421–1428, Nov. 2016.

[138] ISO, "ISO 18593:2004 - Microbiology of food and animal feeding stuffs -- Horizontal methods for sampling techniques from surfaces using contact plates and swabs," 2004.

[139] M. Osterblad, H. Jarvinen, K. Lonnqvist, S. Huikko, P. Laippala, J. Viljanto, H. Arvilommi, and P. Huovinen, "Evaluation of a New Cellulose Sponge-Tipped Swab for Microbiological Sampling: a Laboratory and Clinical Investigation," *J. Clin.*

Microbiol., vol. 41, no. 5, pp. 1894–1900, May 2003.

[140] A. S. Downey, S. M. Da Silva, N. D. Olson, J. J. Filliben, and J. B. Morrow, "Impact of Processing Method on Recovery of Bacteria from Wipes Used in Biological Surface Sampling," *Appl. Environ. Microbiol.*, vol. 78, no. 16, pp. 5872–5881, Aug. 2012.

[141] M. S. Favero, J. J. McDade, J. A. Robertsen, R. K. Hoffman, and R. W. Edwards, "Microbiological Sampling of Surfaces," *Journal of Applied Microbiology*, vol. 31, no. 3, pp. 336–343, Sep. 1968.

[142] N. Yamaguchi, A. Ishidoshiro, Y. Yoshida, T. Saika, S. Senda, and M. Nasu, "Development of an adhesive sheet for direct counting of bacteria on solid surfaces," *Journal of Microbiological Methods*, vol. 53, no. 3, pp. 405–410, Jun. 2003.

[143] S. W. Lemmen, H. Häfner, D. Zolldann, G. Amedick, and R. Lutticken, "Comparison of two sampling methods for the detection of Gram-positive and Gram-negative bacteria in the environment: moistened swabs versus Rodac plates," *International Journal of Hygiene and Environmental Health*, vol. 203, no. 3, pp. 245–248, Jan. 2001.

[144] A. Compass, "Standard Practices for Bulk Sample Collection and Swab Sample Collection of Visible Powders Suspected of Being Biological Agents and Toxins from Nonporous Surfaces."

[145] CDC, "Norovirus | Specimen Collection | CDC," *cdc.gov*. [Online]. Available: https://www.cdc.gov/norovirus/lab-testing/collection.html. [Accessed: 22-Jan-2018].

[146] C. A. Davidson, C. J. Griffith, A. C. Peters, and L. M. Fielding, "Evaluation of two

methods for monitoring surface cleanliness—ATP bioluminescence and traditional hygiene swabbing," *Luminescence*, vol. 14, no. 1, pp. 33–38, Jan. 1999.

[147] S. J. Dancer, "How do we assess hospital cleaning? A proposal for microbiological standards for surface hygiene in hospitals," *J. Hosp. Infect.*, vol. 56, no. 1, pp. 10–15, Jan. 2004.

[148] G. S. Brown, R. G. Betty, J. E. Brockmann, D. A. Lucero, C. A. Souza, K. S. Walsh, R. M. Boucher, M. S. Tezak, M. C. Wilson, T. Rudolph, H. D. A. Lindquist, and K. F. Martinez, "Evaluation of rayon swab surface sample collection method for Bacillus spores from nonporous surfaces," *J APPL MICROBIOL*, vol. 103, pp. 1074–1080, 2007.

[149] M. T. La Duc, R. Kern, and K. Venkateswaran, "Microbial Monitoring of Spacecraft and Associated Environments," *Microb Ecol*, vol. 47, no. 2, pp. 150–158, Feb. 2004.

[150] A. Probst, R. Facius, R. Wirth, and C. Moissl-Eichinger, "Validation of a Nylon-Flocked-Swab Protocol for Efficient Recovery of Bacterial Spores from Smooth and Rough Surfaces," *Appl. Environ. Microbiol.*, vol. 76, no. 15, pp. 5148–5158, Jul. 2010.

[151] S. Keeratipibul, T. Laovittayanurak, O. Pornruangsarp, Y. Chaturongkasumrit, H. Takahashi, and P. Techaruvichit, "Effect of swabbing techniques on the efficiency of bacterial recovery from food contact surfaces," *Food Control*, vol. 77, pp. 139–144, Jul. 2017.

[152] T. F. Landers, A. Hoet, and T. E. Wittum, "Swab type, moistening, and preenrichment for Staphylococcus aureus on environmental surfaces.," *J. Clin. Microbiol.*, vol. 48, no. 6, pp. 2235–2236, Jun. 2010.

[153] S. Nys, S. Vijgen, K. Magerman, and R. Cartuyvels, “Comparison of Copan eSwab with the Copan Venturi Transystem for the quantitative survival of Escherichia coli, Streptococcus agalactiae and Candida albicans,” *Eur J Clin Microbiol Infect Dis*, vol. 29, no. 4, pp. 453–456, Mar. 2010.

[154] P. Daley, S. Castriciano, M. Chernesky, and M. Smieja, “Comparison of flocked and rayon swabs for collection of respiratory epithelial cells from uninfected volunteers and symptomatic patients.,” *J. Clin. Microbiol.*, vol. 44, no. 6, pp. 2265–2267, Jun. 2006.

[155] J. Y. D'AOUST, C. MAISHMENT, P. STOTLAND, and A. BOVILLE, “Surfactants for the Effective Recovery of Salmonella in Fatty Foods,” *j food prot*, vol. 45, no. 3, pp. 249–252, Feb. 1982.

[156] G. W. Park, D. Lee, A. Treffiletti, M. Hrsak, J. Shugart, and J. Vinje, “Evaluation of a New Environmental Sampling Protocol for Detection of Human Norovirus on Inanimate Surfaces,” *Appl. Environ. Microbiol.*, vol. 81, no. 17, pp. 5987–5992, Sep. 2015.

[157] L. Gerstenzang, “Process and apparatus for manufacturing medical swabs,” 7~23-1929.

[158] Z. Gong, H. Du, F. Cheng, C. Wang, C. Wang, and M. Fan, “Fabrication of SERS Swab for Direct Detection of Trace Explosives in Fingerprints,” *ACS Appl. Mater. Interfaces*, vol. 6, no. 24, pp. 21931–21937, Dec. 2014.

[159] K. Scherer, D. Mäde, L. Ellerbroek, J. Schulenburg, R. Johne, and G. Klein, “Application of a Swab Sampling Method for the Detection of Norovirus and Rotavirus on Artificially Contaminated Food and Environmental Surfaces,” *Food*

Environ Virol, vol. 1, no. 1, pp. 42–49, Jan. 2009.

[160] S. J. Kadolph and S. B. Marcketti, ***Textiles (12th Edition)***. Pearson, 2016.

[161] M. Mokomane, I. Kasvosve, S. Gaseitsiwe, A. P. Steenhoff, J. M. Pernica, K. Lechiile, K. Luinstra, M. Smieja, and D. M. Goldfarb, "A comparison of flocked swabs and traditional swabs, using multiplex real-time PCR for detection of common gastroenteritis pathogens in Botswana," *Diagnostic Microbiology and Infectious Disease*, vol. 86, no. 2, pp. 141–143, Oct. 2016.

[162] A. Dolan, M. Bartlett, B. McEntee, E. Creamer, and H. Humphreys, "Evaluation of different methods to recover meticillin-resistant Staphylococcus aureus from hospital environmental surfaces," *J. Hosp. Infect.*, vol. 79, no. 3, pp. 227–230, Nov. 2011.

[163] E. Crawford and B. Musselman, "Evaluating a direct swabbing method for screening pesticides on fruit and vegetable surfaces using direct analysis in real time (DART) coupled to an Exactive benchtop orbitrap mass spectrometer," *Anal Bioanal Chem*, vol. 403, no. 10, pp. 2807–2812, Feb. 2012.

[164] L. Rose, B. Jensen, A. Peterson, S. N. Banerjee, and M. J. Arduino, "Swab Materials and *Bacillus anthracis* Spore Recovery from Nonporous Surfaces," *Emerging Infect. Dis.*, vol. 10, no. 6, pp. 1023–1029, Jun. 2004.

[165] L. R. Hodges, L. J. Rose, A. Peterson, J. Noble-Wang, and M. J. Arduino, "Evaluation of a macrofoam swab protocol for the recovery of Bacillus anthracis spores from a steel surface.," *Appl. Environ. Microbiol.*, vol. 72, no. 6, pp. 4429–4430, Jun. 2006.

[166] L. R. Hodges, L. J. Rose, H. O'Connell, and M. J. Arduino, "National validation

study of a swab protocol for the recovery of Bacillus anthracis spores from surfaces," *Journal of Microbiological Methods*, vol. 81, no. 2, pp. 141–146, May 2010.

[167] J. R. Hutchison, G. F. Piepel, B. G. Amidan, B. M. Hess, M. A. Sydor, and B. L. D. Kaiser, "Comparison of false-negative rates and limits of detection following macrofoam-swab sampling of Bacillus anthracis surrogates via Rapid Viability PCR and plate culture," *Journal of Applied Microbiology*, vol. 124, no. 5, pp. 1092–1106, May 2018.

[168] G. W. Park, D. Lee, A. Treffiletti, M. Hrsak, J. Shugart, and J. Vinje, "Evaluation of a New Environmental Sampling Protocol for Detection of Human Norovirus on Inanimate Surfaces," *Appl. Environ. Microbiol.*, vol. 81, no. 17, pp. 5987–5992, Sep. 2015.

[169] G. Moore and C. Griffith, "Problems associated with traditional hygiene swabbing: the need for in-house standardization," *Journal of Applied Microbiology*, vol. 103, no. 4, pp. 1090–1103, Oct. 2007.

[170] G. Dalmaso, M. Bini, R. Paroni, and M. Ferrari, "Qualification of high-recovery, flocked swabs as compared to traditional rayon swabs for microbiological environmental monitoring of surfaces.," *PDA J Pharm Sci Technol*, vol. 62, no. 3, pp. 191–199, May 2008.

[171] D. Triva, "Method of using flocked swab for collecting biological specimens," US 8,317,728B2, 11~27-2012.

[172] P. Verhoeven, F. Grattard, A. Carricajo, B. Pozzetto, and P. Berthelot, "Better Detection of Staphylococcus aureus Nasal Carriage by Use of Nylon Flocked

Swabs," *J. Clin. Microbiol.*, vol. 48, no. 11, pp. 4242–4244, Nov. 2010.

[173] G. Finazzi, M. N. Losio, and G. Varisco, "FLOQSwabTM: optimisation of procedures for the recovery of microbiological samples from surfaces," *Ital J Food Safety*, vol. 5, no. 3, Jun. 2016.

[174] K. H. Harry, J. C. Turner, and K. T. Madhusudhan, "Comparison of physical characteristics and collection and elution performance of clinical swabs," *AJMR*, vol. 7, no. 31, pp. 4039–4048, Aug. 2013.

[175] M. P. Buttner, P. Cruz-Perez, and L. D. Stetzenbach, "Enhanced detection of surface-associated bacteria in indoor environments by quantitative PCR.," *Appl. Environ. Microbiol.*, vol. 67, no. 6, pp. 2564–2570, Jun. 2001.

[176] A. M. Abdelzaher, H. M. Solo-Gabriele, M. E. Wright, and C. J. Palmer, "Sequential Concentration of Bacteria and Viruses from Marine Waters using a Dual Membrane System," *Journal of Environmental Quality*, vol. 37, no. 4, pp. 1648–1655, Jul. 2008.

[177] S. M. Lemma, A. Esposito, M. Mason, L. Brusetti, S. Cesco, and M. Scampicchio, "Removal of bacteria and yeast in water and beer by nylon nanofibrous membranes," *J. Food Eng.*, vol. 157, pp. 1–6, Jul. 2015.

[178] L. A. Goetz, B. Jalvo, R. Rosal, and A. P. Mathew, "Superhydrophilic anti-fouling electrospun cellulose acetate membranes coated with chitin nanocrystals for water filtration," *JOURNAL OF MEMBRANE SCIENCE*, vol. 510, pp. 238–248, Jul. 2016.

[179] L. Mocé-Llivina, J. Jofre, X. Méndez, D. Akkelidou, F. Lucena, and G. T. Papageorgiou, "Counting cytopathogenic virus adsorbed to cellulose nitrate membrane filters as a simple method for counting viruses in raw sewage and sewage

effluents," *J. Virol. Methods*, vol. 102, no. 1, pp. 83–92, Apr. 2002.

[180] S. Jain, S. Chattopadhyay, R. Jackeray, C. K. V. Z. Abid, G. S. Kohli, and H. Singh, "Highly sensitive detection of *Salmonella* typhi using surface aminated polycarbonate membrane enhanced-ELISA," *Biosensors and Bioelectronic*, vol. 31, no. 1, pp. 37–43, Jan. 2012.

[181] A. Cavallini, M. Notarnicola, P. Berloco, A. Lippolis, and A. Di Leo, "Use of macroporous polypropylene filter to allow identification of bacteria by PCR in human fecal samples," *Journal of Microbiological Methods*, vol. 39, no. 3, pp. 265–270, Feb. 2000.

[182] P. Feng, S. D. Weagant, M. A. Grant, W. B. Bacteriological, 2002, "BAM: Enumeration of Escherichia coli and the Coliform Bacteria," *innocua.net*

.

[183] D. S. Burns, H. Ooshima, and A. O. Converse, "Surface area of pretreated lignocellulosics as a function of the extent of enzymatic hydrolysis," *Appl Biochem Biotechnol*, vol. 20, no. 1, pp. 79–94, Jan. 1989.

[184] M. Barboza, J. Pinzon, S. Wickramasinghe, J. W. Froehlich, I. Moeller, J. T. Smilowitz, L. R. Ruhaak, J. Huang, B. Lönnerdal, J. B. German, J. F. Medrano, B. C. Weimer, and C. B. Lebrilla, "Glycosylation of human milk lactoferrin exhibits dynamic changes during early lactation enhancing its role in pathogenic bacteria-host interactions.," *Mol. Cell Proteomics*, vol. 11, no. 6, pp. M111.015248–M111.015248, Jun. 2012.

[185] D. M. Heithoff, W. R. Shimp, J. K. House, Y. Xie, B. C. Weimer, R. L. Sinsheimer, and M. J. Mahan, "Intraspecies variation in the emergence of hyperinfectious

bacterial strains in nature.," *PLoS Pathog.*, vol. 8, no. 4, p. e1002647, 2012.

[186] Y. Chai, H. C. Wikle, Z. Wang, S. Horikawa, S. Best, Z. Cheng, D. F. Dyer, and B. A. Chin, "Design of a surface-scanning coil detector for direct bacteria detection on food surfaces using a magnetoelastic biosensor," *J. Appl. Phys.*, vol. 114, no. 10, p. 104504, Sep. 2013.

[187] W. Shen, S. Li, M.-K. Park, Z. Zhang, Z. Cheng, V. A. Petrenko, and B. A. Chin, "Blocking Agent Optimization for Nonspecific Binding on Phage Based Magnetoelastic Biosensors," *J. Electrochem. Soc.*, vol. 159, no. 10, pp. B818–B823, 2012.

[188] "Outbreaks Involving Salmonella | CDC," *cdc.gov*. [Online]. Available: https://www.cdc.gov/salmonella/outbreaks.html. [Accessed: 20-Mar-2020].

[189] F. Wang, S. Horikawa, Y. Chai, J. Hu, S. Du, Y. Liu, H. C. Wikle, and B. A. Chin, "Detection of Multiple Pathogens on Fresh Produce Using a Surface-Scanning Coil," presented at the Meeting Abstracts, 2015, no. 46, pp. 1839–1839.

[190] Y. Liu, S. Du, S. Horikawa, I.-H. Chen, J. Xi, T.-S. Huang, and B. A. Chin, "Rapid Pathogen Detection by Surface Swab Sampling and Wireless Biosensing," *ECS Trans.*, vol. 80, no. 10, pp. 1531–1539, Oct. 2017.

[191] Y. Zhang, C.-Q. Xu, T. Guo, and L. Hong, "An automated bacterial concentration and recovery system for pre-enrichment required in rapid Escherichia coli detection," *SCIENTIFIC REPORTS*, vol. 8, no. 1, pp. 1–8, Dec. 2018.

[192] N. Thet, "Modified tethered bilayer lipid membranes for detection of pathogenic bacterial toxins and characterization of ion channels."

[193] W. W. Ye, J. Y. Shi, C. Y. Chan, Y. Zhang, and M. Yang, "A nanoporous

membrane based impedance sensing platform for DNA sensing with gold nanoparticle amplification," *Sensors and Actuators B: Chemical*, vol. 193, pp. 877–882, Mar. 2014.

[194] R. Guntupalli, J. Hu, R. S. Lakshmanan, T. S. Huang, J. M. Barbaree, and B. A. Chin, "A magnetoelastic resonance biosensor immobilized with polyclonal antibody for the detection of *Salmonella* typhimurium.," *Biosensors and Bioelectronic*, vol. 22, no. 7, pp. 1474–1479, Feb. 2007.

[195] S. Nambi, S. Nyalamadugu, S. M. Wentworth, and B. A. Chin, "Radio Frequency Identification Sensors for Food Safety," presented at the Wireless Communications Systems and Circuits Design in the th World Multi-Conference on Systemics, Cybernetics, and Informatics. Orlando, Florida, pp. 386–390.

[196] Y. Liu, S. Horikawa, I.-H. Chen, S. Du, H. C. Wikle, S.-J. Suh, and B. A. Chin, "Highly sensitive surface-scanning detector for the direct bacterial detection using magnetoelastic (ME) biosensors," presented at the SPIE Commercial+ Scientific Sensing and Imaging, 2017, vol. 10217, p. 1021703.

[197] S. Horikawa, S. Du, Y. Liu, I.-H. Chen, Y. Chai, H. C. Wikle, and B. A. Chin, "The Bathtub Method for Detecting Small Quantities of Specific Pathogens," *ECS Trans.*, vol. 75, no. 16, pp. 183–192, Aug. 2016.

[198] R. M. Amaguaña, T. S. Hammack, and W. H. Andrews, "Methods for the Recovery of Salmonella spp. from Carboxymethylcellulose Gum, Gum Ghatti, and Gelatin," *Journal of AOAC International*, vol. 81, no. 4, pp. 721–726, Jan. 1998.

[199] S. J. Blissett, K. J. Bolton, C. E. R. Dodd, G. W. Gould, and W. M. Waites, "Survival of Salmonella senftenberg and Salmonella typhimurium in glassy and

rubbery states of gelatin," *Journal of Applied Microbiology*, vol. 76, no. 4, pp. 345–349, Apr. 1994.

[200] P. Ramu, L. A. Lobo, M. Kukkonen, E. Bjur, M. Suomalainen, H. Raukola, M. Miettinen, I. Julkunen, O. Holst, M. Rhen, T. K. Korhonen, and K. Lähteenmäki, "Activation of pro-matrix metalloproteinase-9 and degradation of gelatin by the surface protease PgtE of *Salmonella* enterica serovar Typhimurium," *International Journal of Medical Microbiology*, vol. 298, no. 3, pp. 263–278, Apr. 2008.

[201] T. Brocklehurst, "The effect of transient temperatures on the growth of Salmonella typhimurium LT2 in gelatin gel," *International Journal of Food Microbiology*, vol. 27, no. 1, pp. 45–60, Sep. 1995.

[202] M. M. BRASHEARS, A. AMEZQUITA, and J. STRATTON, "Validation of Methods Used To Recover Escherichia coli O157:H7 and Salmonella spp. Subjected to Stress Conditions†," *j food prot*, vol. 64, no. 10, pp. 1466–1471, Oct. 2001.

[203] M. Glicksman, *Gum Technology in the Food Industry (Food Science & Technological Monograph)*. Academic Pr.